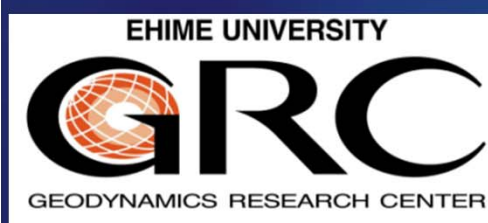


High-pressure physics of the Earth and beyond

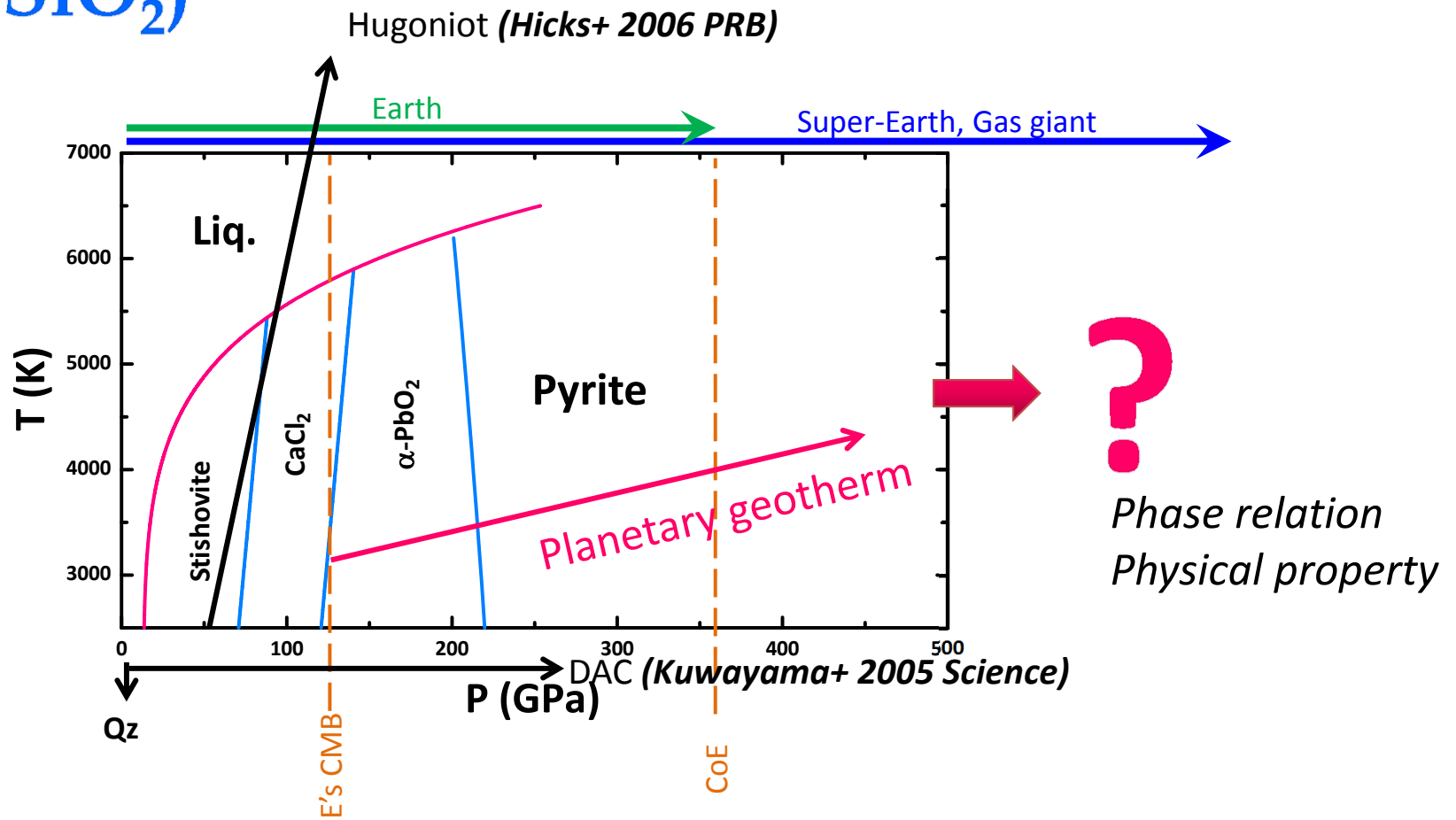


Taku Tsuchiya

Geodynamics Research Center
Ehime University
Japan



High- P,T phase relation of Earth materials (ex. SiO_2)



- Experimental investigations currently almost impossible
 - *Ab initio* theoretical computation method

Ab Initio (first principles) Earth and Planetary Sciences

(i) Structural exploration

--- *Molecular dynamics*

(ii) Vibrational, thermodynamic property

--- *Lattice dynamics*

(iii) Elastic property

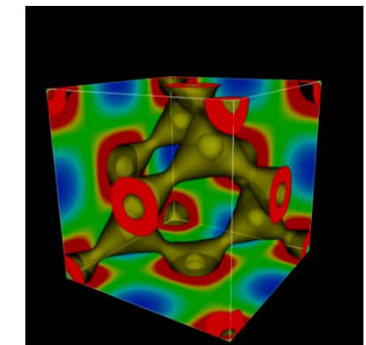
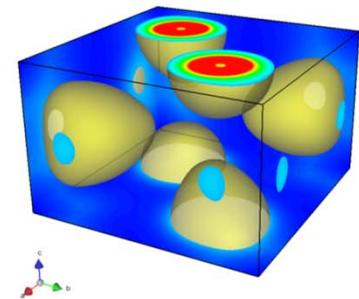
--- *Stress-strain theory*

(iv) Transport property

--- *Atomic, thermal, electrical conductivity*

(v) Mechanical property

--- *Shear response*

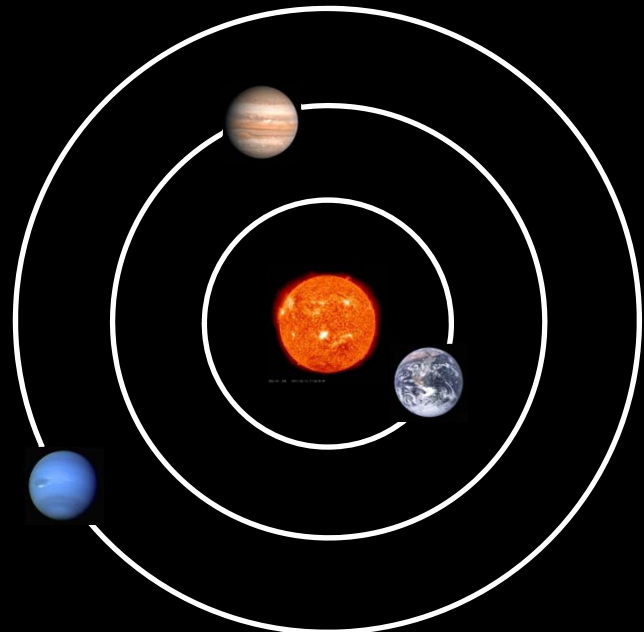


1. Fundamental methodologies of the ab initio electronic structure calculation method

2. Applications to high-pressure mineral physics and Earth & planetary interiors

- Phase relations including melting
- Electronic property
- Transport property

A.U. (Astronomical Unit)

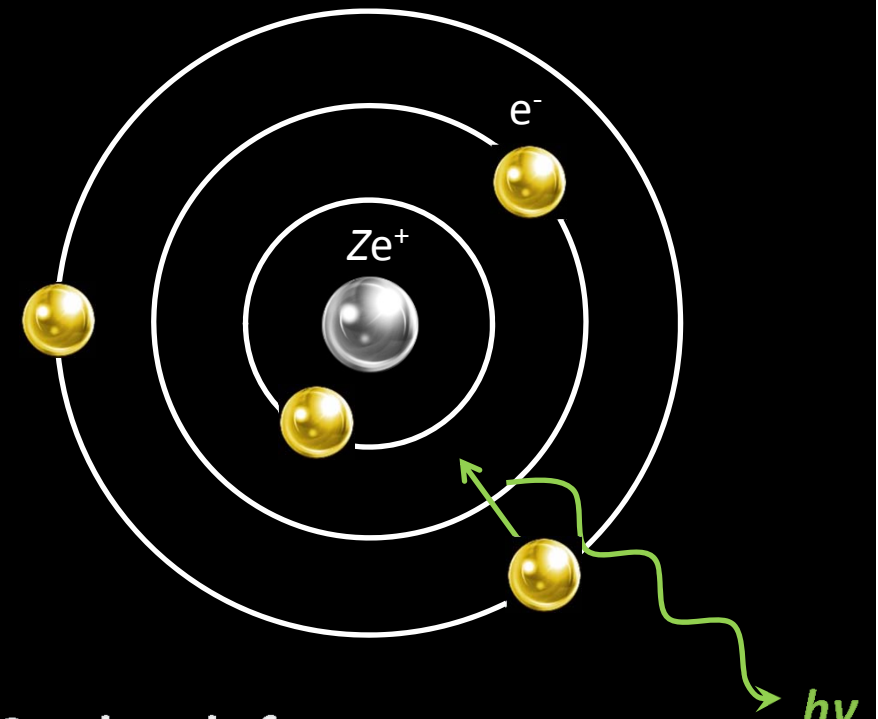


Gravity force:

$$\mathbf{F}(\mathbf{r}) = -\frac{Gm_1m_2}{r^2}\frac{\mathbf{r}}{|\mathbf{r}|}$$

Central force

a.u. (Atomic Unit)



Coulomb force:

$$\mathbf{F}(\mathbf{r}) = -\frac{1}{4\pi\epsilon_0}\frac{q_1q_2}{r^2}\frac{\mathbf{r}}{|\mathbf{r}|}$$

Schrödinger equation

$$\hat{H}(\mathbf{r}_1, \mathbf{r}_2, \dots) \Psi(\mathbf{r}_1, \mathbf{r}_2, \dots) = E \Psi(\mathbf{r}_1, \mathbf{r}_2, \dots)$$

\hat{H} : Hamilton operator (Hamiltonian)

Ψ : Wave function (Eigen vector)

E : Total energy (Eigen value)

Eigenvalue problem

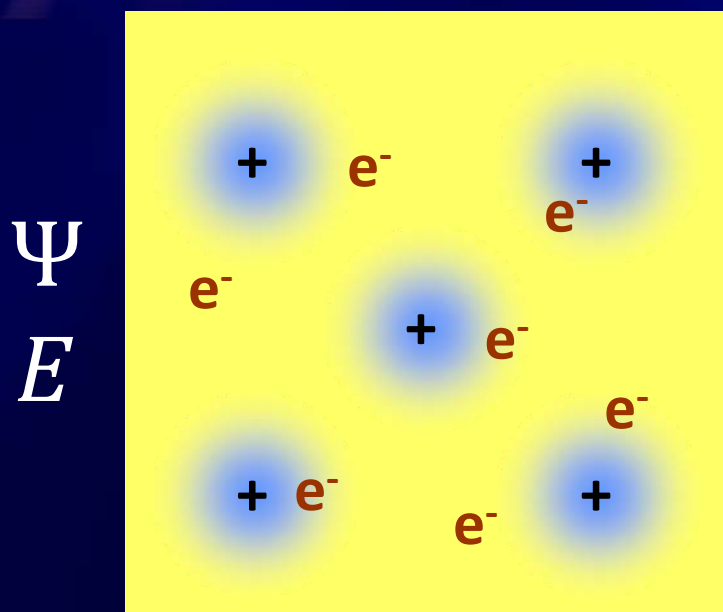
Quantization

$$\hat{p} = -i\hbar\nabla \quad (\text{Momentum})$$

$$\hat{E} = i\hbar\partial/\partial t \quad (\text{Energy})$$

Many-electron system

Interacting electrons



One electron in an effective potential



$$\left[-\frac{\hbar^2}{2m} \Delta + V_n[n(\mathbf{r})] + V_H[n(\mathbf{r})] + V_{XC}[n(\mathbf{r})] \right] \phi_i(\mathbf{r}) = \epsilon_i \phi_i(\mathbf{r}),$$

$$n(\mathbf{r}) = \sum_i |\phi_i(\mathbf{r})|^2$$

Kohn-Sham equations (DFT)
(Hohenberg & Kohn, 1964; Kohn & Sham, 1965)

Density Functional Theory (DFT)

One-electron Hamiltonian

$$\hat{h}_i = -\frac{\hbar}{2m}\Delta + V_n[n(\mathbf{r})] + V_H[n(\mathbf{r})] + V_{XC}[n(\mathbf{r})]$$

↑

Kinetic
energy

↑

Coulomb
potential
between
electrons
and nuclei

↑

Coulomb
potential
between
electrons

↑

Quantum
many-body
effects
II
Exchange-
correlation
potential

Charge density

$$n(\mathbf{r}) = \sum_i |\phi_i(\mathbf{r})|^2$$

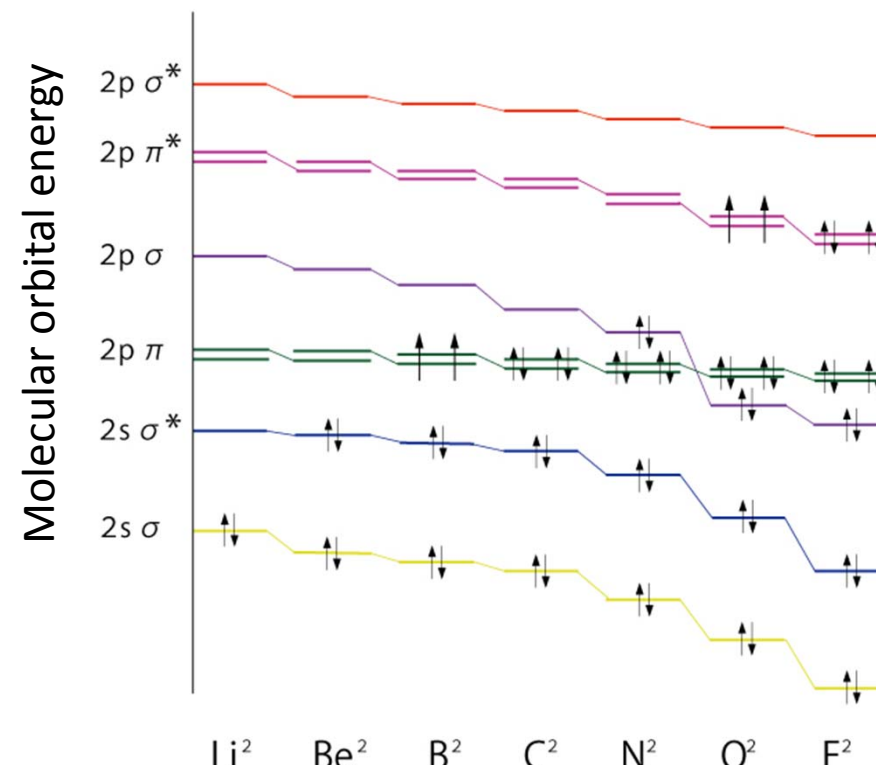
Angular component of a wavefunction in a central force field
 (Coulomb potential) $\propto 1/r$

= Spherical harmonics $\Phi_{l,m}$

l: angular momentum quantum number (*s*, p, d, f)

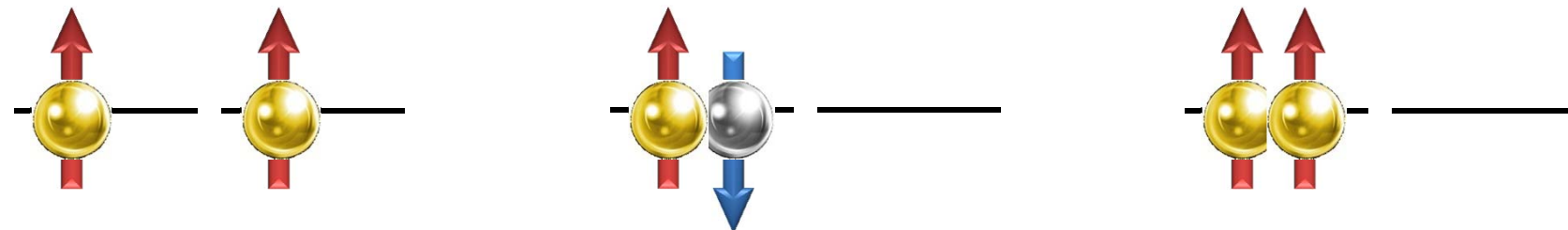
m: magnetic quantum number

+ spin quantum number (up or down)



XC (exchange-correlation) potential (V_{xc})

Electron (fermion) → Quantum many-body effects



Hund's rule

Pauli's exclusion principle

Local density approximation (LDA)

V_{xc} determined for the homogeneous electron gas, which can be calculated precisely, is applied also to general systems.



Quantum Monte-Carlo

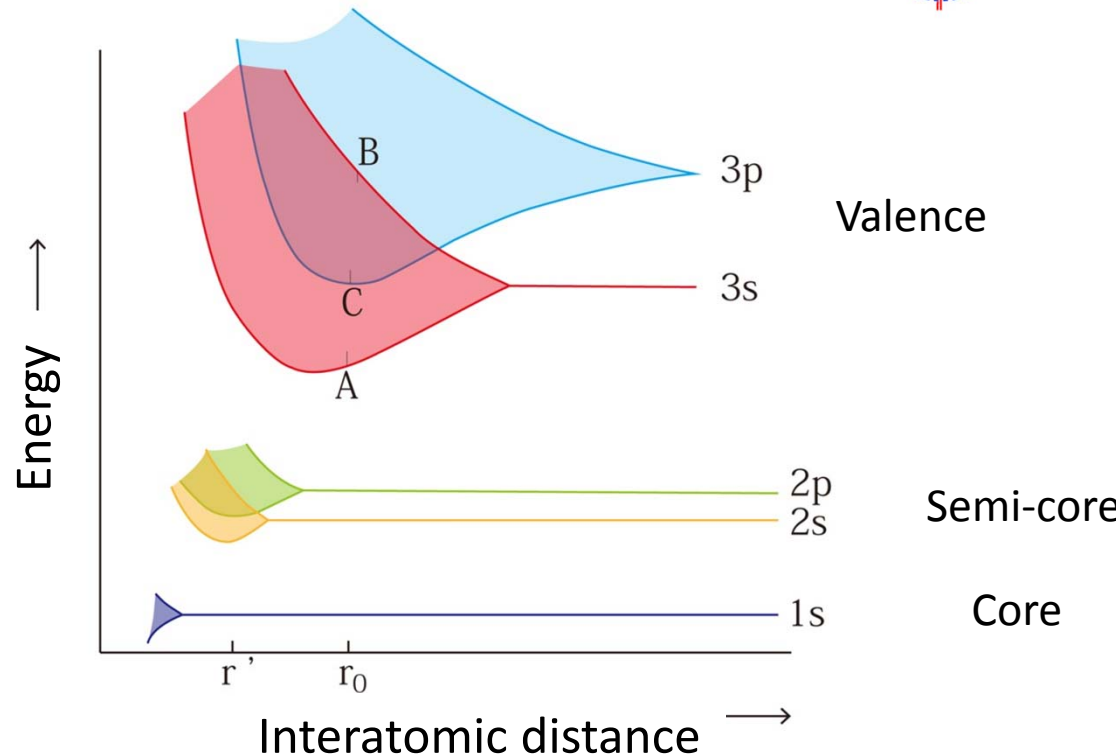
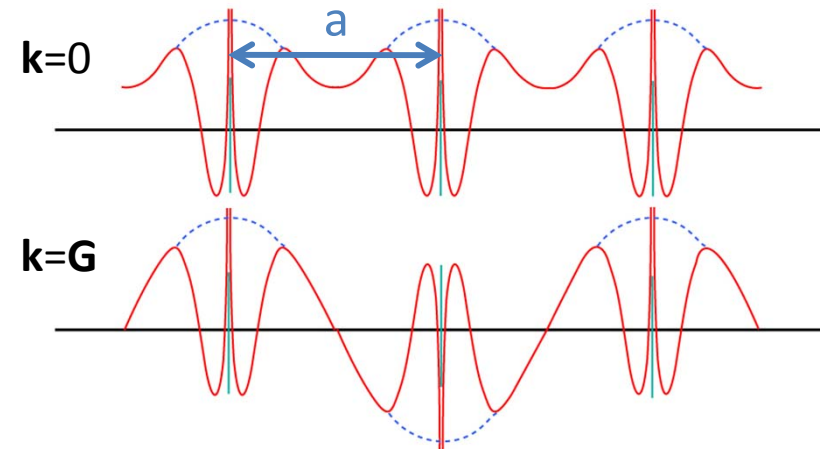
Energy level to energy band

Bloch theorem

(Periodic boundary condition)

$$\psi_{\mathbf{k}}(\mathbf{r}) = a(\mathbf{r})e^{i\mathbf{k}\cdot\mathbf{r}}$$

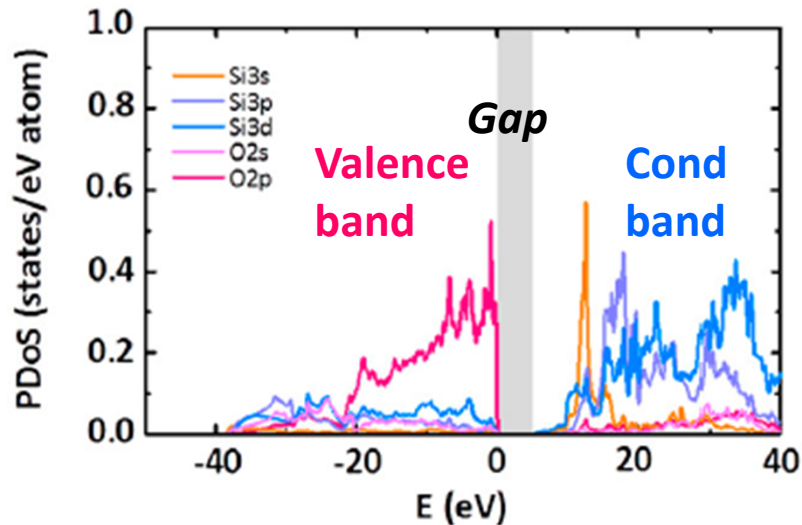
\mathbf{k} -dependency of the energy level
= Energy band



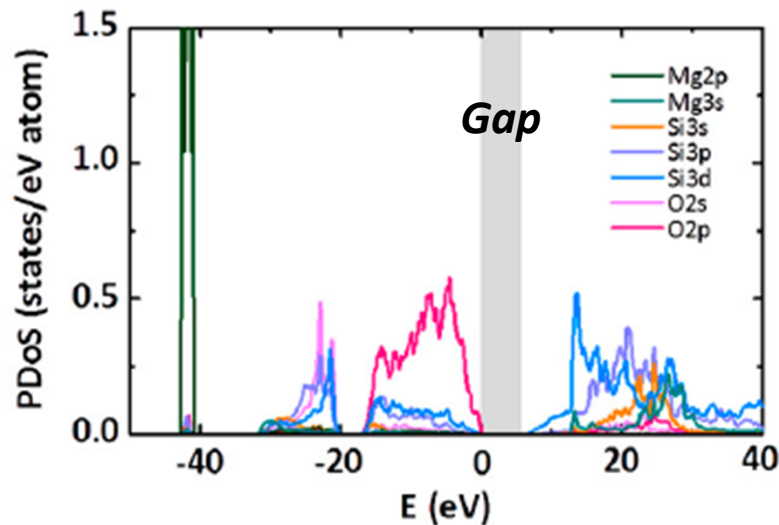
Electronic density of states

T Tsuchiya, 9th ISPS, 25 June 2012
Tsuchiya & Tsuchiya (2011) PNAS

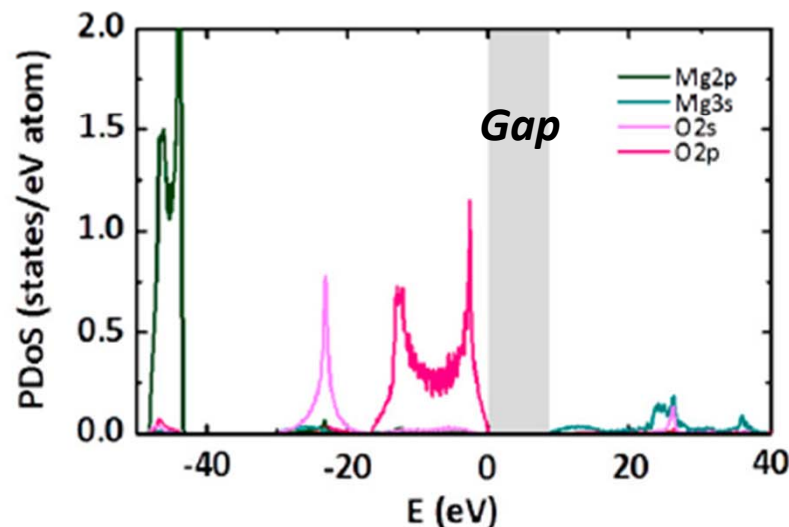
Fe₂P-SiO₂ 1.5 TPa



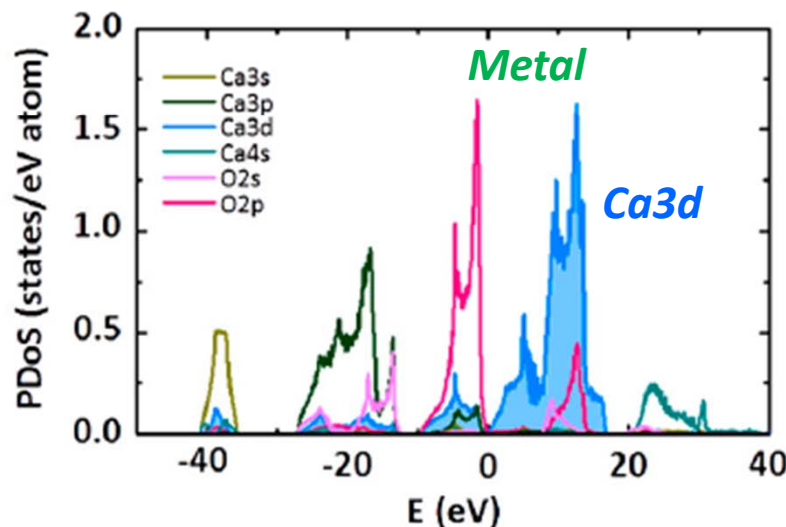
pPv-MgSiO₃ 1.0 TPa



B2-MgO 1.5 TPa

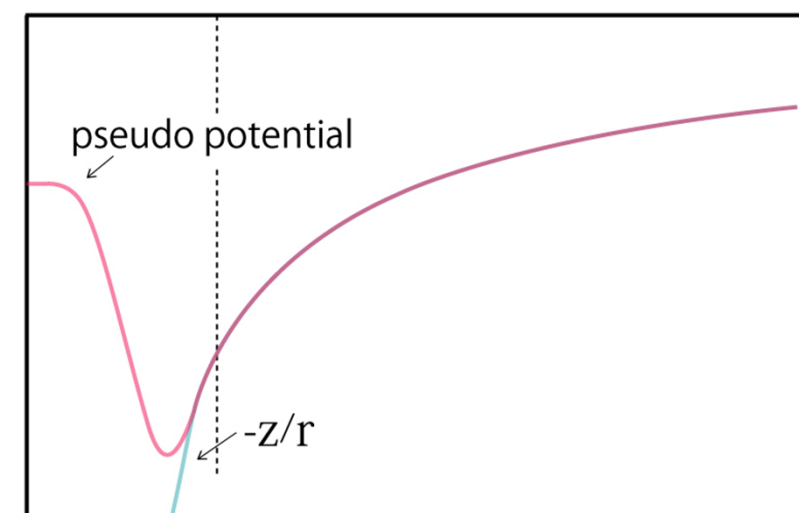
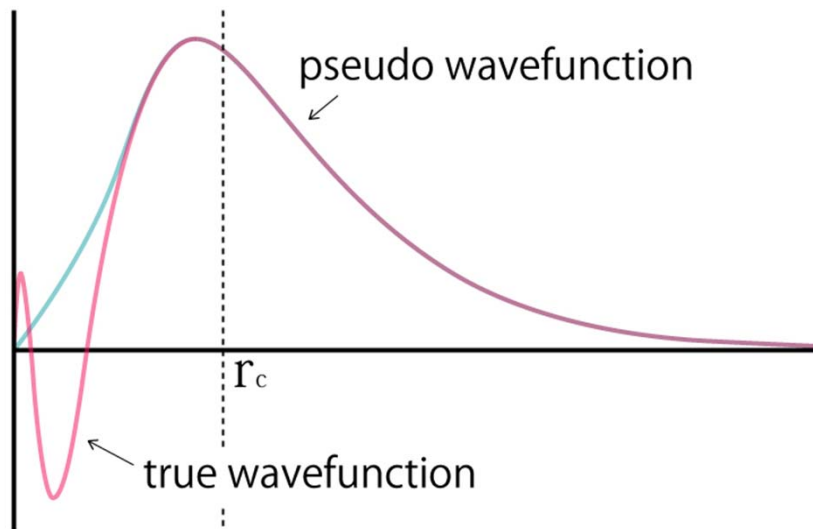


B2-CaO 0.4 TPa



Pseudo-potential approximation

- Valence electrons only contribute chemical bonding.
- Nuclei + Core electrons → Ion potential (with orthogonality of valence and core electrons)



PP is determined nonempirically to reproduce the true wavefunction correctly in the bonding region ($r > r_c$).

Self-Consistent Field (SCF) method

$$\hat{h}_i[n(\mathbf{r})] \phi_i(\mathbf{r}) = \varepsilon_i \phi_i(\mathbf{r})$$

ϕ_i depends on the Hamiltonian $\hat{h}_i[n(\mathbf{r})]$.

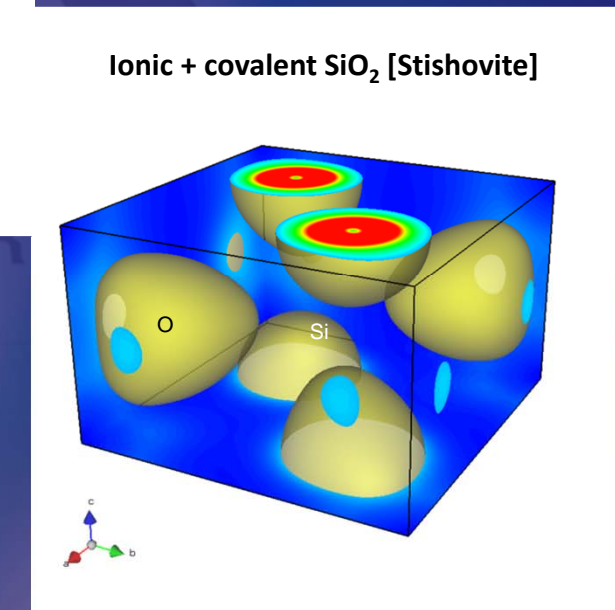
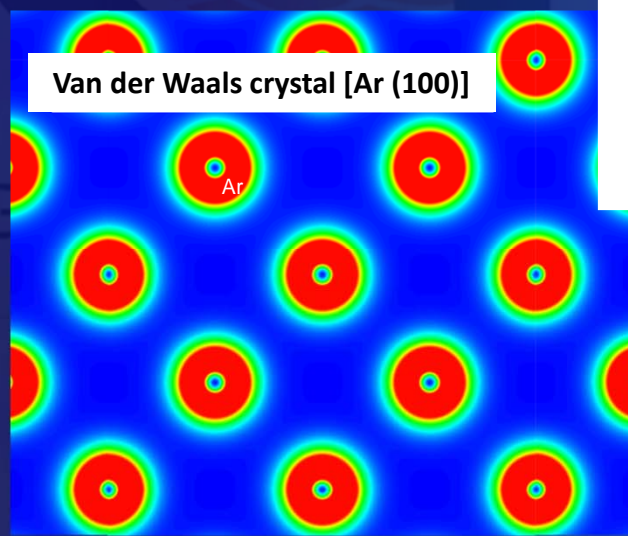
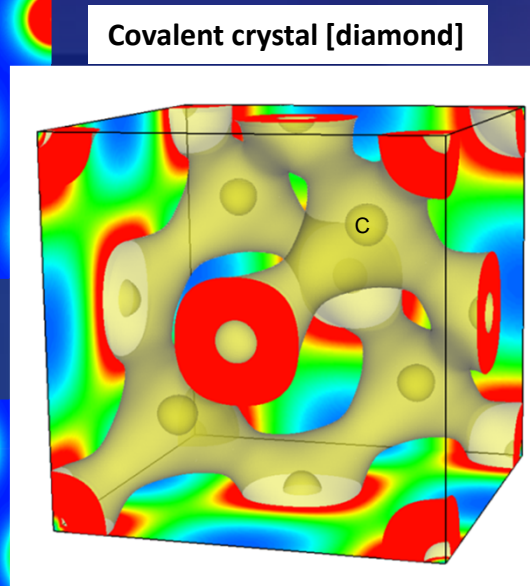
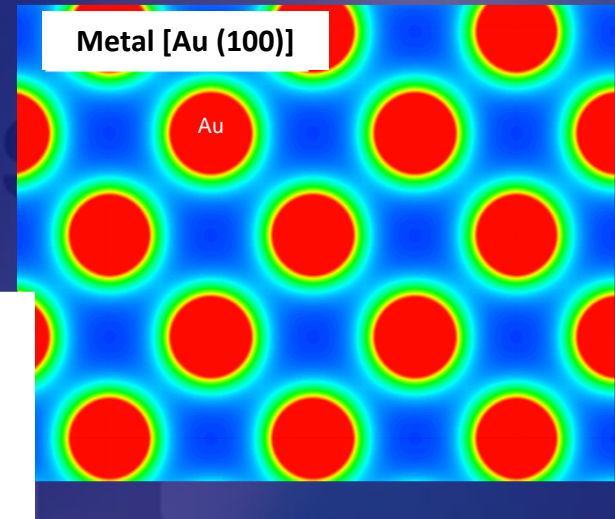
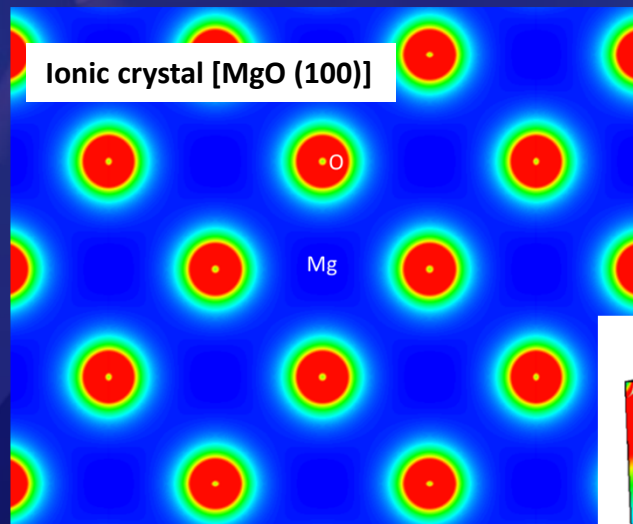
$\hat{h}_i[n(\mathbf{r})]$ depends on the total charge density $n(\mathbf{r})$.

$n(\mathbf{r})$ depends on the wave functions ϕ_i .

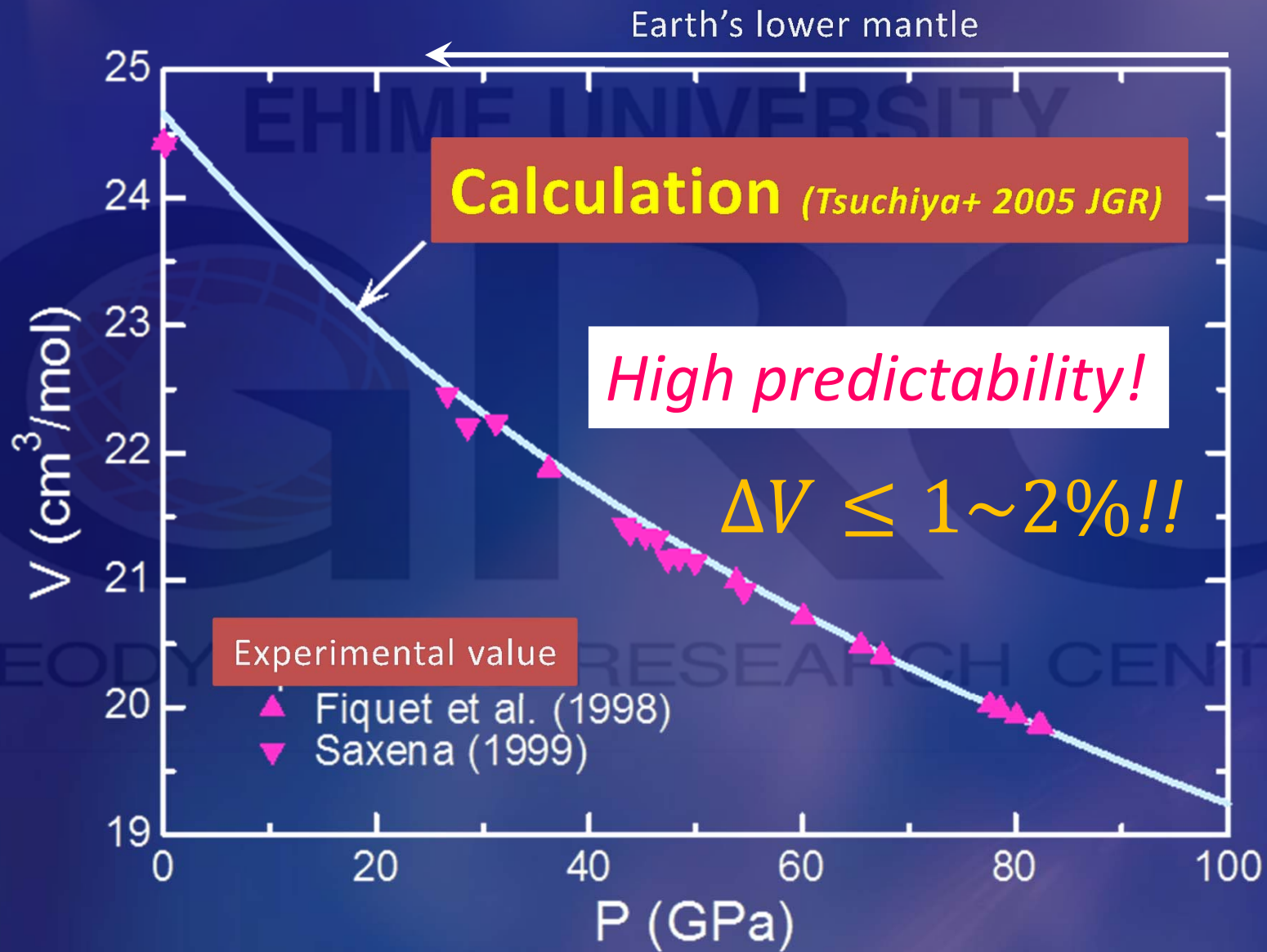


The equation is solved iteratively.

Valence charge density of some representative bond types



Compression curve of MgSiO_3 perovskite (A lower mantle constituent phase)



Large scale computation

GRC-SRFC parallel clusters



理研計算科学研究所@神戸



<http://jp.fujitsu.com>



Atomic dynamics and temperature effects

DFT → Total energy of many-electrons system (E_{tot})

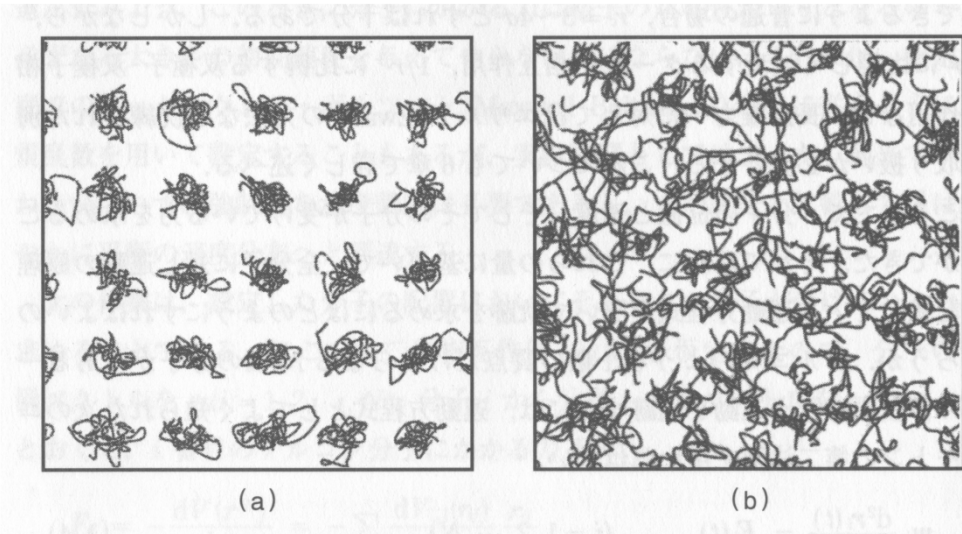
+ Hellman-Feynman theorem (perturbation theory)

$\frac{\partial E_{tot}}{\partial \mathbf{r}_i}$ (Force) → *Ab initio* molecular dynamics
(MD)

$\frac{\partial^2 E_{tot}}{\partial \mathbf{r}_i \partial \mathbf{r}_j}$ (Force constant) → *Ab initio* lattice dynamics
(LD)

Molecular Dynamics method

A method to investigate dynamical property of many-atom systems



Solid (a)
Liquid (b)

Time evolution is calculated by numerically integrating the Newton's equation of motion

$$\mathbf{x}_i(t + \Delta t) = \mathbf{x}_i(t) + \mathbf{v}_i(t)\Delta t + \frac{1}{2}\mathbf{a}_i(t)\Delta t^2$$

$$\mathbf{v}_i(t + \Delta t) = \mathbf{v}_i(t) + \frac{\mathbf{a}_i(t) + \mathbf{a}_i(t + \Delta t)}{2}\Delta t$$

Velocity-Verlet
algorithm

$$\mathbf{a}_i(t) = \mathbf{F}_i(t)/m_i$$

Hellman-Feynman theorem

$$\frac{dE}{d\lambda} = \left\langle \psi(\lambda) \left| \frac{d\hat{H}}{d\lambda} \right| \psi(\lambda) \right\rangle$$

Force acting on an atom can be calculated directly from the SCF charge density.



Force



Stress tensor (*Nielsen & Martin, PRB 1985*)

Macroscopic thermodynamic quantities

Temperature (Energy equipartition principle)

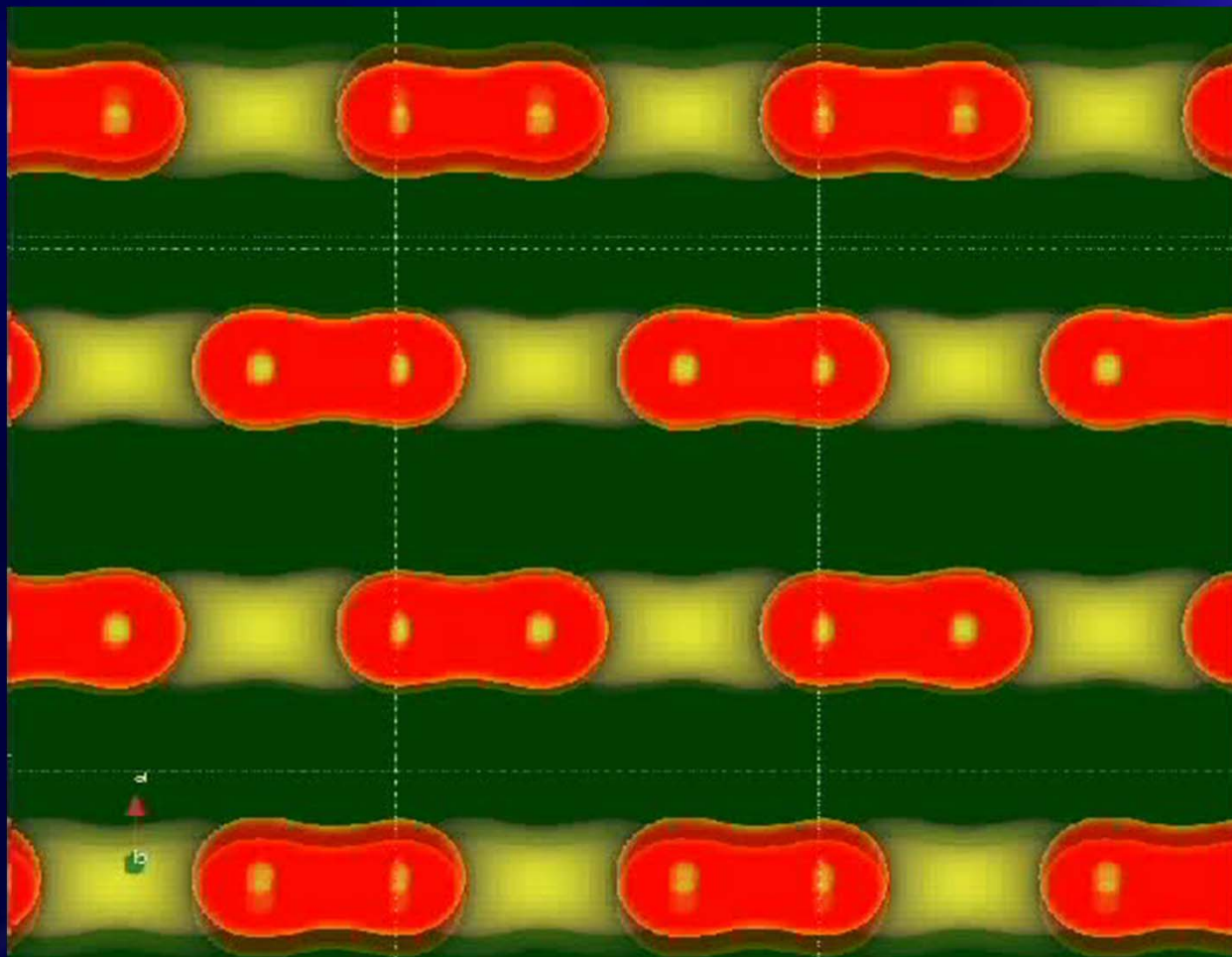
$$T = \frac{1}{3Nk_B} \sum_j m_j v_j^2$$

Pressure (Virial theorem)

$$P = P_{static} + \frac{Nk_B T}{V} - \frac{1}{3V} \sum_{i>j} \mathbf{F}_{ij} \otimes \mathbf{r}_{ij}$$

But not temperature dependence of heat capacity due to the classical Newton's dynamics (Dulong-Petit law)

Graphite

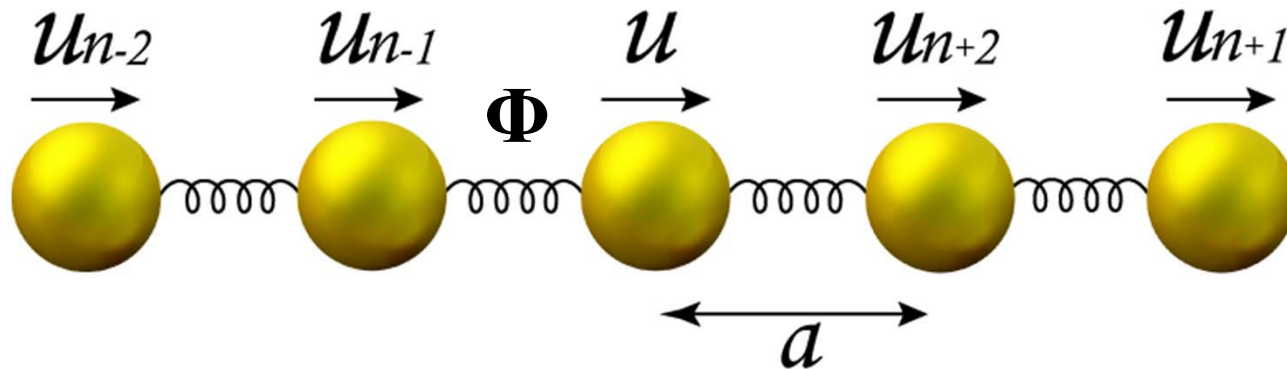


Graphite
 sp^2



(Hexa-)Diamond
 sp^3

Lattice Dynamics Method



Harmonic approximation

$$E^{harm} = \frac{1}{2} \sum_{ll', nn', \alpha\beta} \Phi_{nn'}^{\alpha\beta}(l, l') u_n^\alpha(l) u_{n'}^\beta(l')$$

Force (spring) constant matrix
↓
 $(\alpha, \beta = x, y, z)$

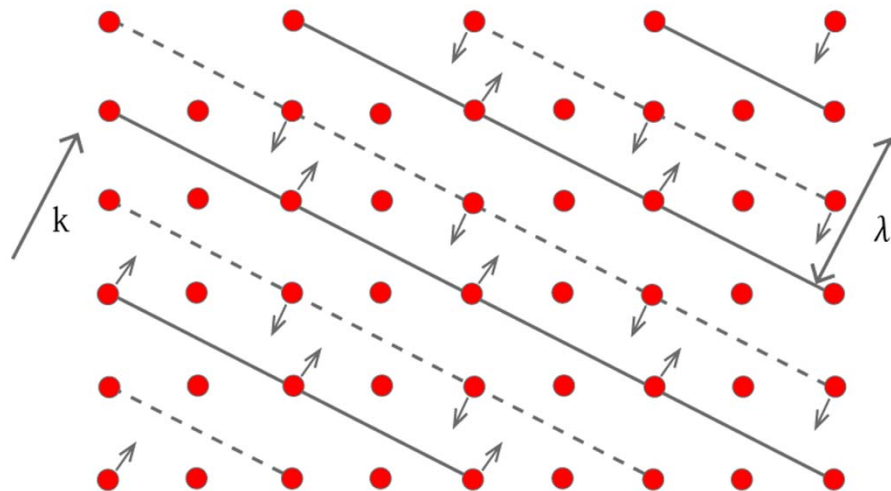
Equation of motion

$$F^\alpha[\mathbf{r}_n(l)] = -\frac{\partial E^{harm}}{\partial u_n^\alpha(l)} = - \sum_{l', ll', \alpha\beta} \Phi_{nn'}^{\alpha\beta}(l, l') u_{n'}^\beta(l')$$

Solution

$$u_n^\alpha(l) = u_n^\alpha(\mathbf{q}) \exp[i\mathbf{q} \cdot \mathbf{r}(l) - i\omega t]$$

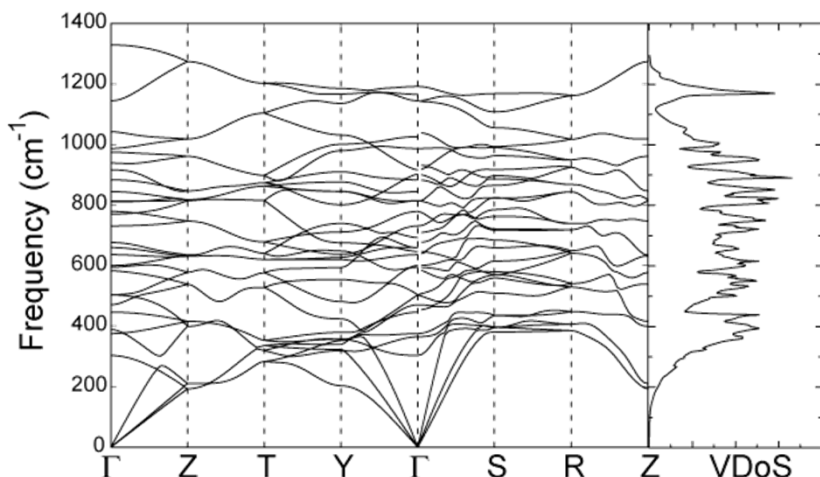
Dynamical matrix $\mathbf{D}_{nn'}^{\alpha\beta}(\mathbf{q}) = \frac{1}{\sqrt{m_n m_{n'}}} \sum_l \Phi_{nn'}^{\alpha\beta}(0, l) \exp[i\mathbf{q} \cdot (\mathbf{r}_0 - \mathbf{r}_l)]$



$$\omega^2 u_n^\alpha(\mathbf{q}) = \sum_{n',\beta} \frac{\mathbf{D}_{nn'}^{\alpha\beta}(\mathbf{q})}{\sqrt{m_n m_{n'}}} u_{n'}^\beta(\mathbf{q})$$

Density Functional Perturbation Theory (DFPT)

(Baroni+ PRB 1987; RMP 2001)



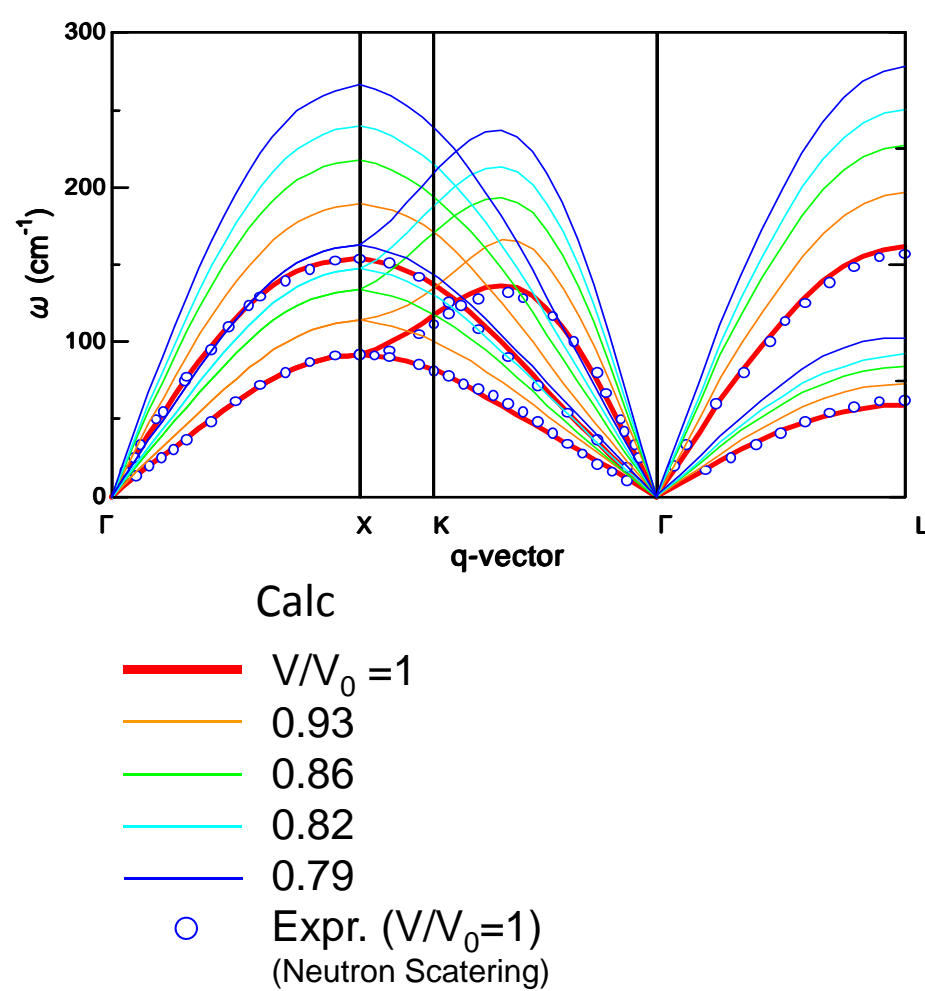
Phonon dispersion of MgSiO_3 pPv ($P=120\text{GPa}$)

Calculate the dynamical matrix based on the quantum perturbation theory



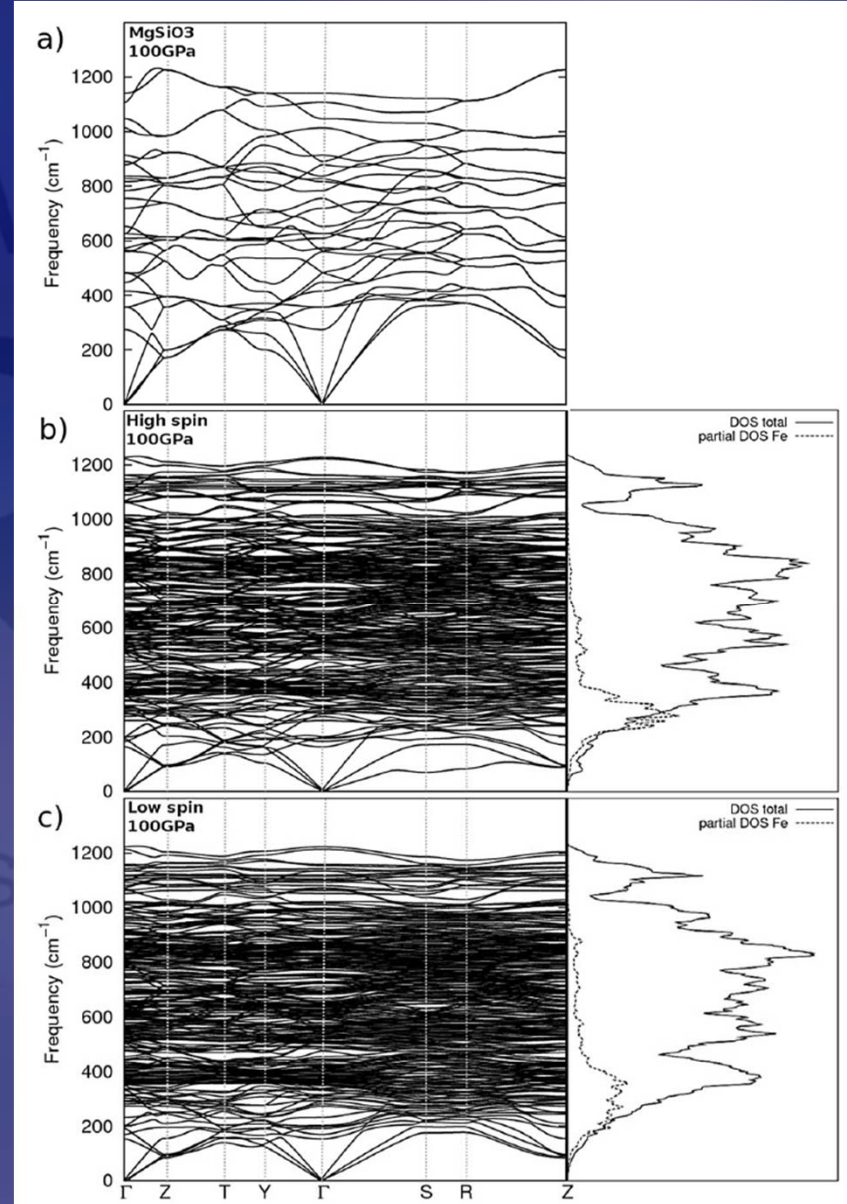
Phonon (quantized lattice vibration) dispersion relation

gold (Au)



Tsuchiya (2003) JGR

Silicates and solid solutions

 $(\text{Mg},\text{Fe})\text{SiO}_3$ Metsue & Tsuchiya (2011,2012)

Quasi-Harmonic Approximation (QHA)

Phonon Helmholtz free energy

$$F_{ph}(V, T) = \frac{1}{2} \sum_{\mathbf{q}, j} h\omega_j(\mathbf{q}, V) + k_B T \sum_{\mathbf{q}, j} \ln \left[1 - \exp \left\{ -\frac{h\omega_j(\mathbf{q}, V)}{k_B T} \right\} \right]$$

Total Helmholtz free energy

$$F(V, T) = U_{stat}(V) + F_{ph}(V, T) + F_{el}(V, T) + \dots$$

Pressure

$$P = - \left[\frac{\partial F}{\partial V} \right]_T$$

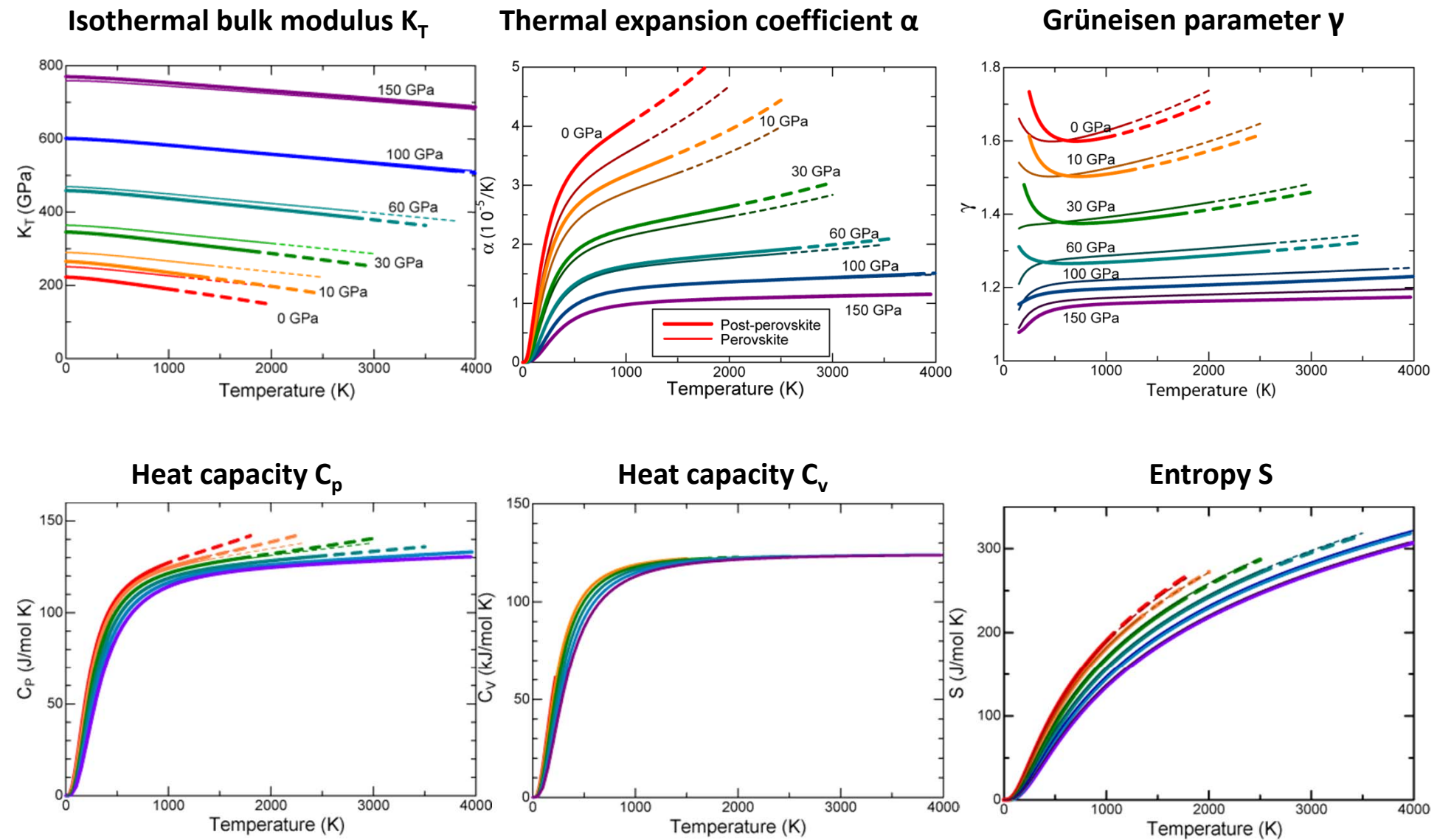
Entropy

$$S = - \left[\frac{\partial F}{\partial T} \right]_V$$

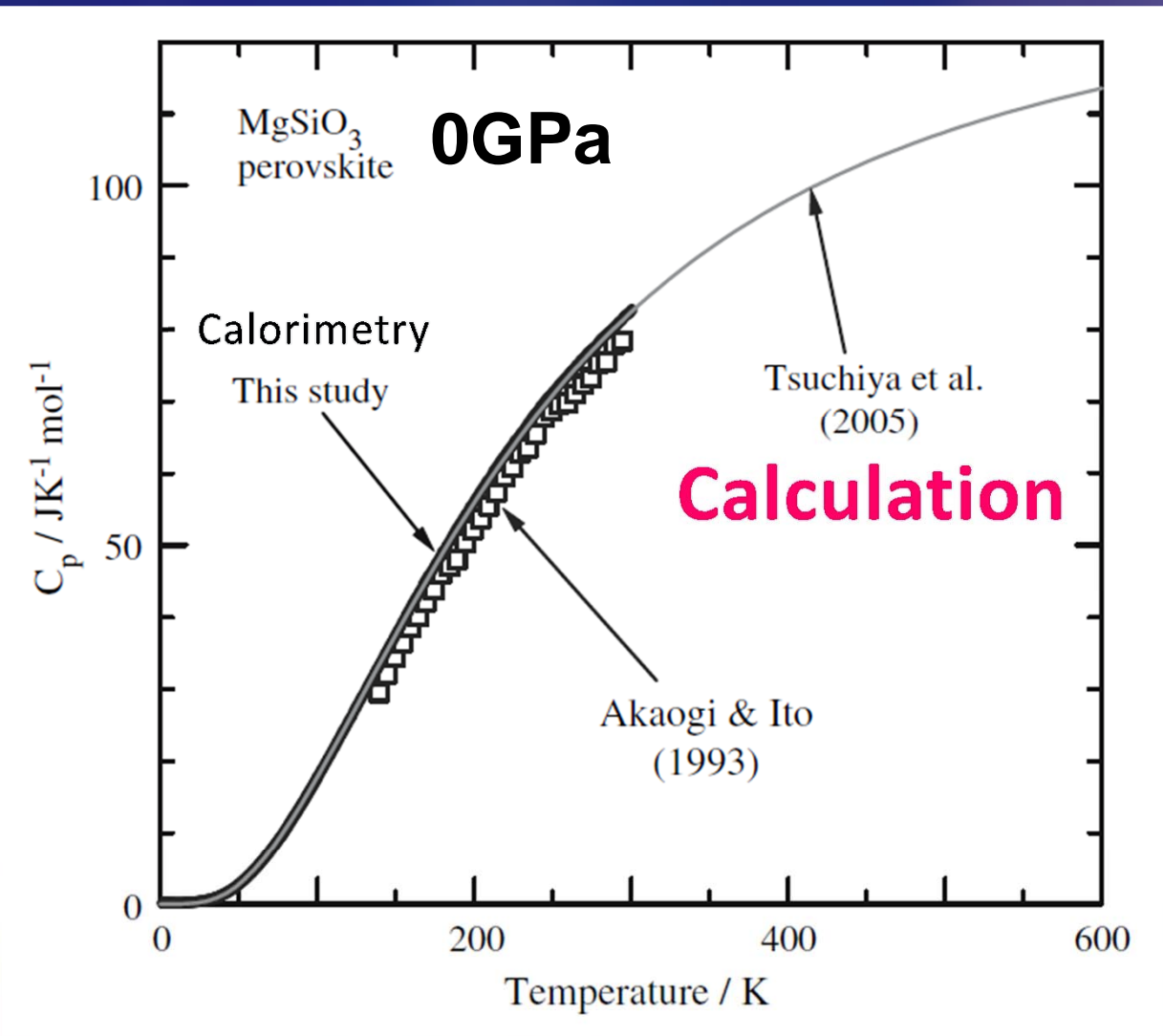
Other thermodynamic functions including

$$G(P, T) = F(V, T) + P(V, T)V$$

Crystal thermodynamics (e.g., MgSiO₃ Pv and PPv)



Akaogi+ (2008) *Phys Chem Miner*

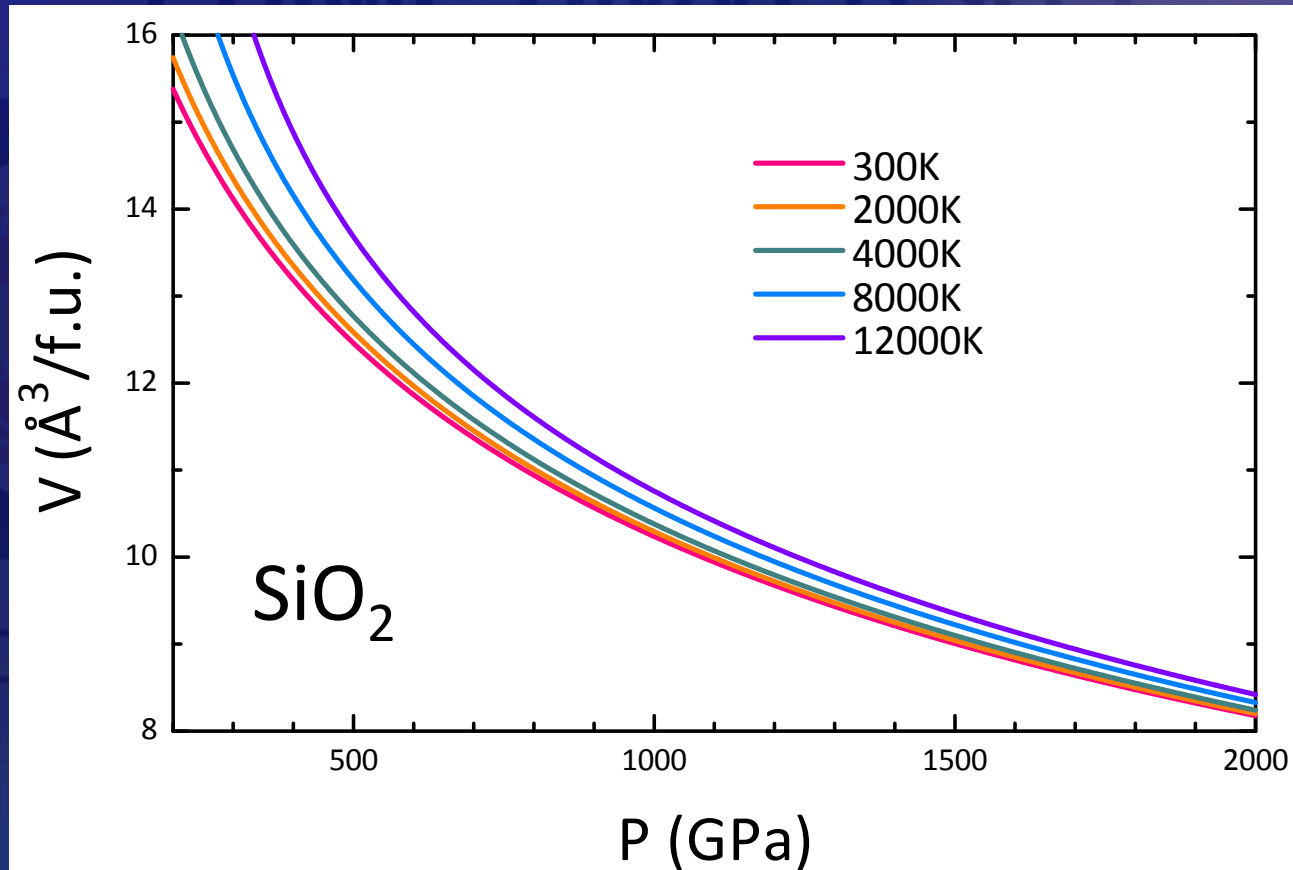


Excellent agreement

P - V - T equation of state up to ultrahigh P, T

$$P(V, T) = P_{static}(V) + P_{thermal}(V, T)$$

$$P_{thermal}(V, T) = P_{ph}(V, T) + P_{el}(V, T) + P_{mag}(V, T)$$

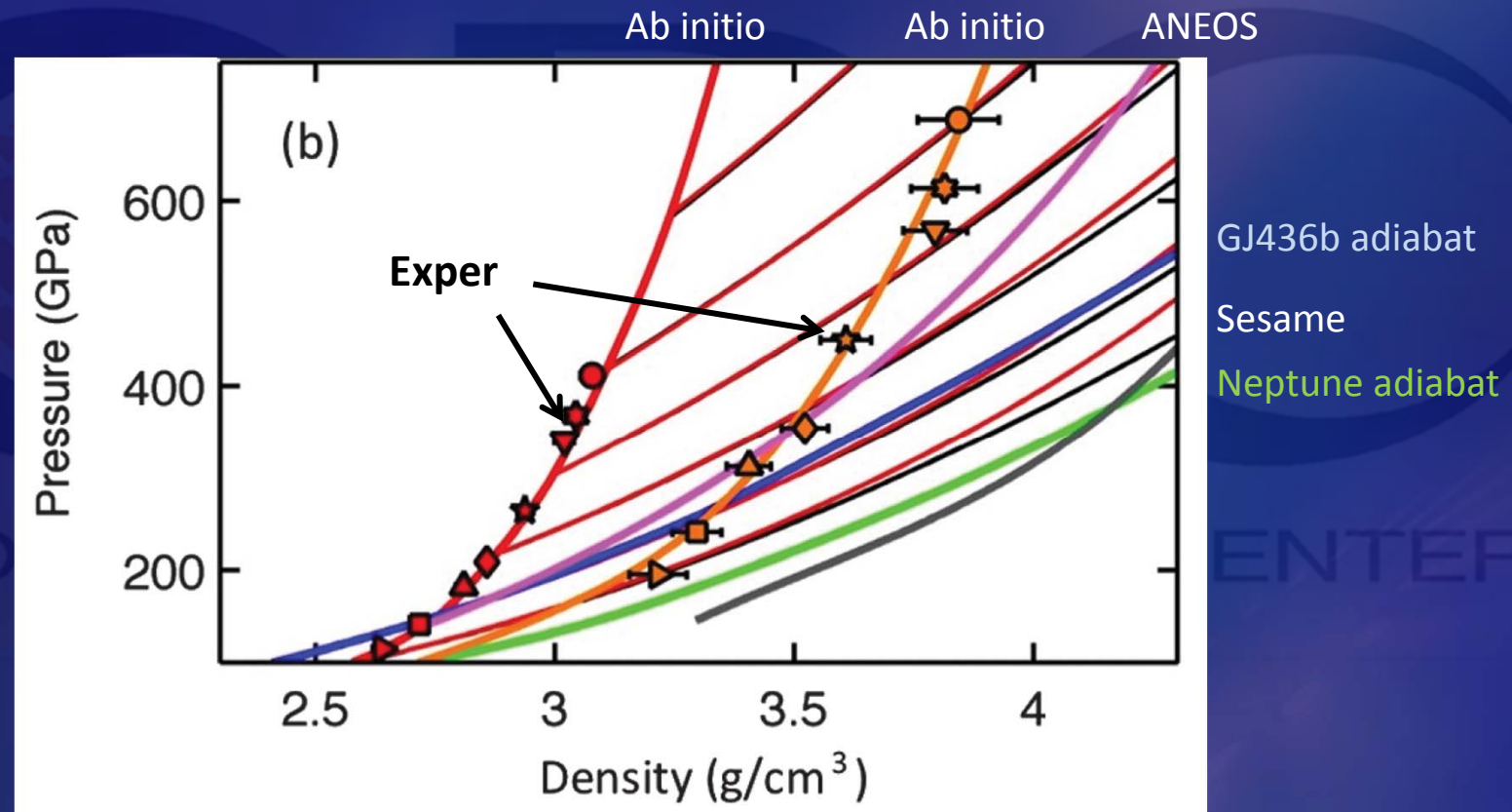


Hugoniot condition

$$H = E - E_0 + 1/2(P + P_0)(V - V_0) = 0$$

How accurate are calculated EoS? e.g., EoS of H_2O

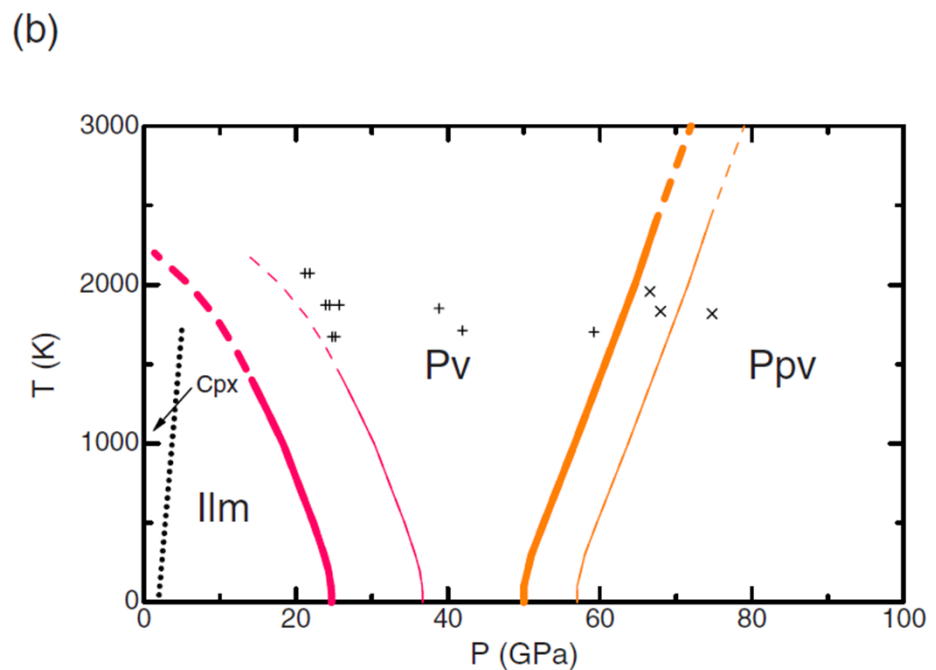
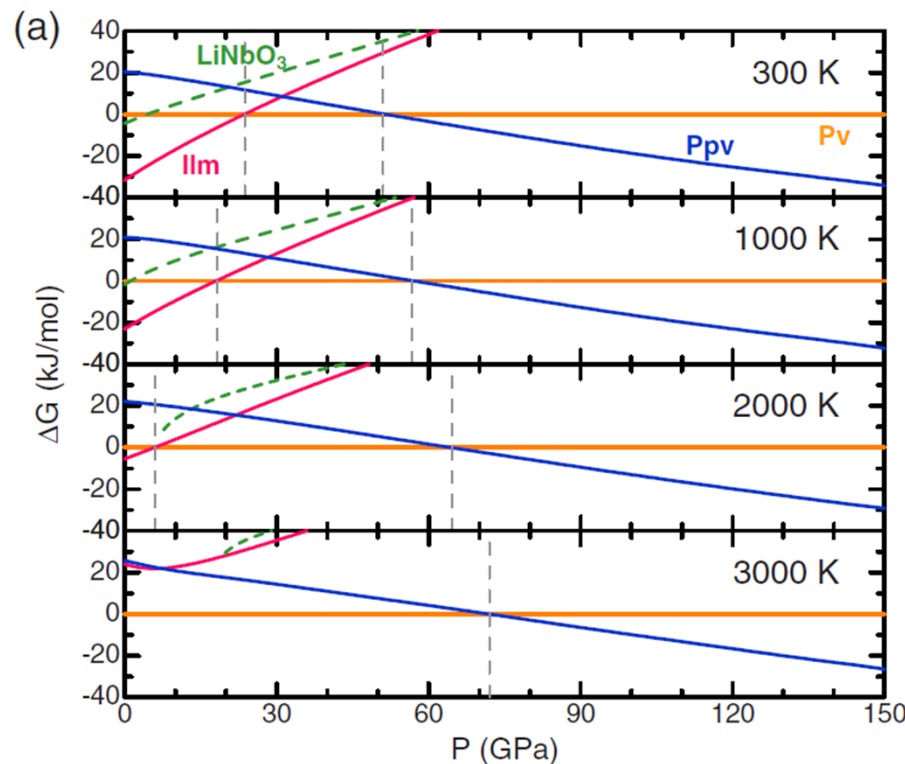
Experimental confirmation in the TPa condition is quite difficult.
Laser or magnetic shock technique seems hopeful.



Thermodynamic phase stability

Gibbs free energy

$$G(P, T) = F(V, T) + P(V, T)V$$



MgGeO₃: Tsuchiya & Tsuchiya (2007) PRB

High- P, T phase boundaries can be determined.

Multicomponent (P - V - T - x) phase equilibrium

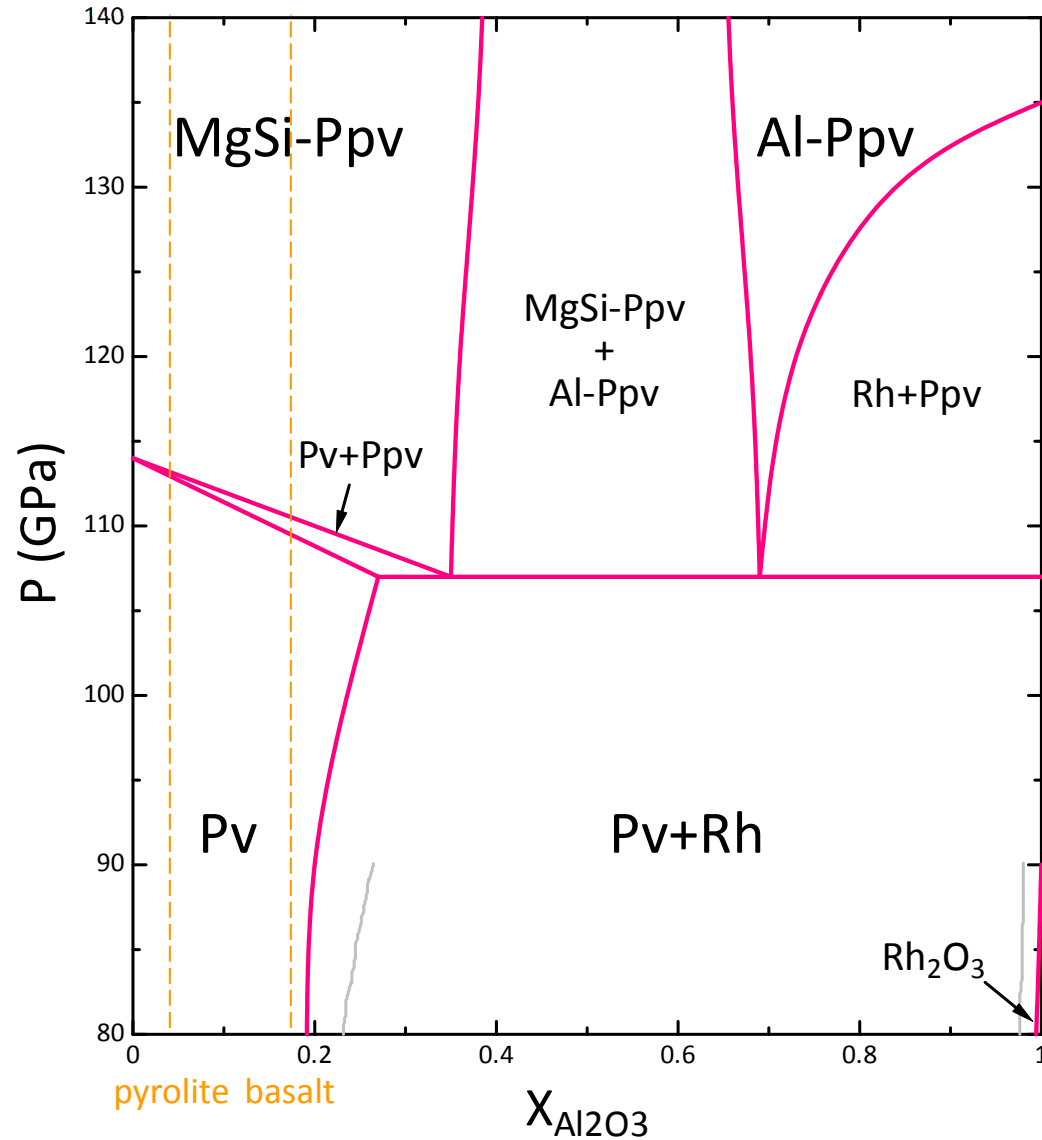
PPv phase equilibrium in
 $\text{MgSiO}_3\text{-Al}_2\text{O}_3$ system

$$\begin{aligned} G(P, T, x) \\ = -k_B T \ln Y(P, T, x) \end{aligned}$$

$Y(P, T, x)$:
 P, T partition function



Multi-configuration sampling
(MCS) technique

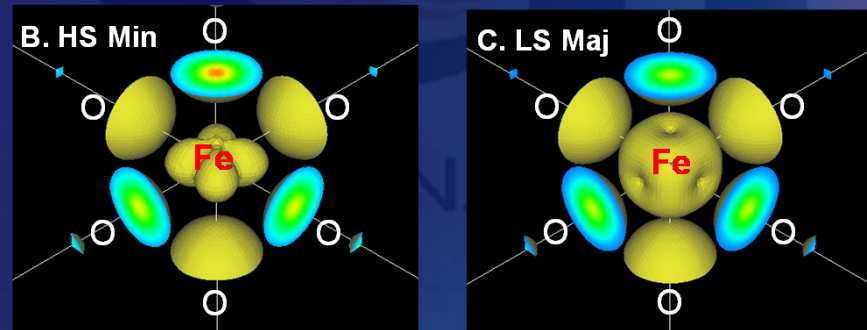


Internally consistent LDA+ U for Fe-bearing system

$$E^{LDA+U}[n(\mathbf{r})] = E^{LDA}[n(\mathbf{r})] + E^{Hub}[\{n_m^{I\sigma}\}] - E^{DC}[\{n^{I\sigma}\}]$$

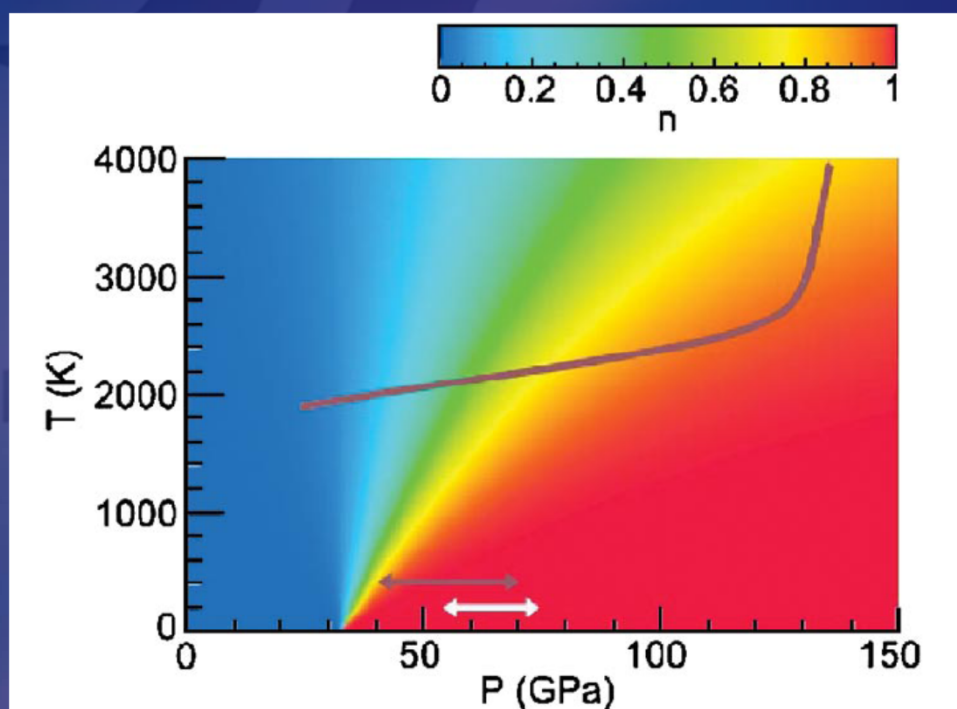
$$E^{Hub}[\{n_{mm'}^{I\sigma}\}] - E^{DC}[\{n^{I\sigma}\}] = \frac{U}{2} \sum_{I,\sigma} \text{Tr}[\mathbf{n}^{I\sigma}(1 - \mathbf{n}^{I\sigma})]$$

On-site Coulomb U parameter
determined non-empirically based
on a linear response formalism



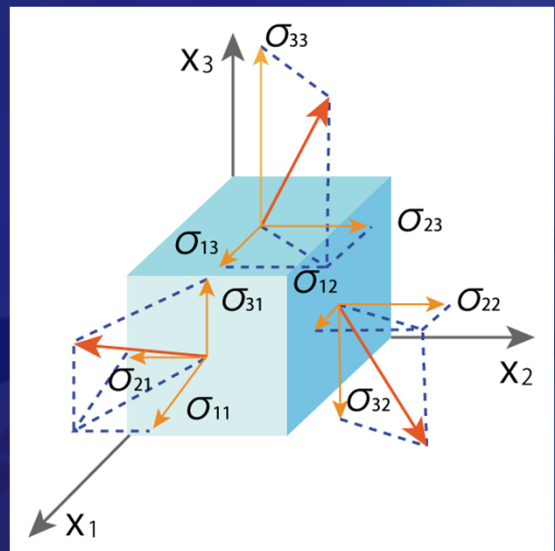
Tsuchiya+ (2006) PRL

Spin transition in ferropericlase (Mg,Fe)O

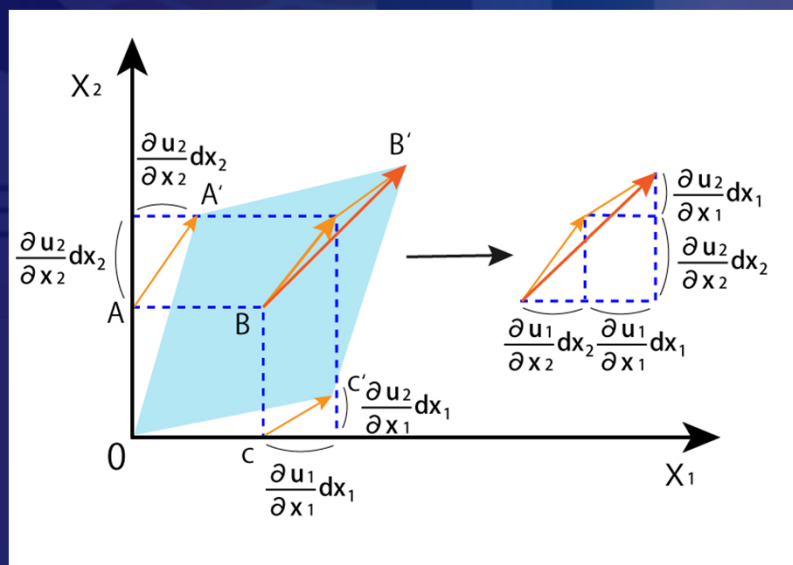


Crystal elasticity

Stress σ_{ij}



Strain ε_{ij}



$$\sigma_{ij} = \begin{pmatrix} \sigma_{11} & \sigma_{12} & \sigma_{13} \\ \sigma_{21} & \sigma_{22} & \sigma_{23} \\ \sigma_{31} & \sigma_{32} & \sigma_{33} \end{pmatrix}$$

$$\varepsilon_{ij} = \begin{pmatrix} \varepsilon_{11} & \varepsilon_{12} & \varepsilon_{13} \\ \varepsilon_{21} & \varepsilon_{22} & \varepsilon_{23} \\ \varepsilon_{31} & \varepsilon_{32} & \varepsilon_{33} \end{pmatrix}$$

$$\varepsilon_{ii} = \frac{\partial u_i}{\partial x_j}, \varepsilon_{ij} = \varepsilon_{ji} = \frac{1}{2} \left(\frac{\partial u_1}{\partial x_2} + \frac{\partial u_2}{\partial x_1} \right)$$

Elastic constant tensor

Linear response between stress and strain (Hooke's law)

$$\sigma_{ij} = \sum_{kl} c_{ijkl} \varepsilon_{kl}$$

or

$$\varepsilon_{ij} = \sum_{kl} s_{ijkl} \sigma_{kl}$$

c_{ijkl} : elastic stiffness tensor

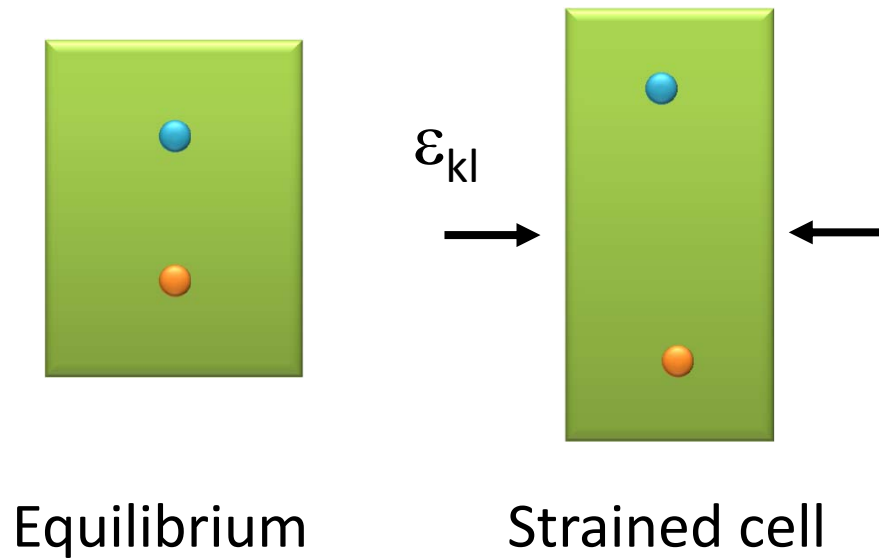
s_{ijkl} : elastic compliance tensor

$$(i, j, k, l = 1 \sim 3)$$

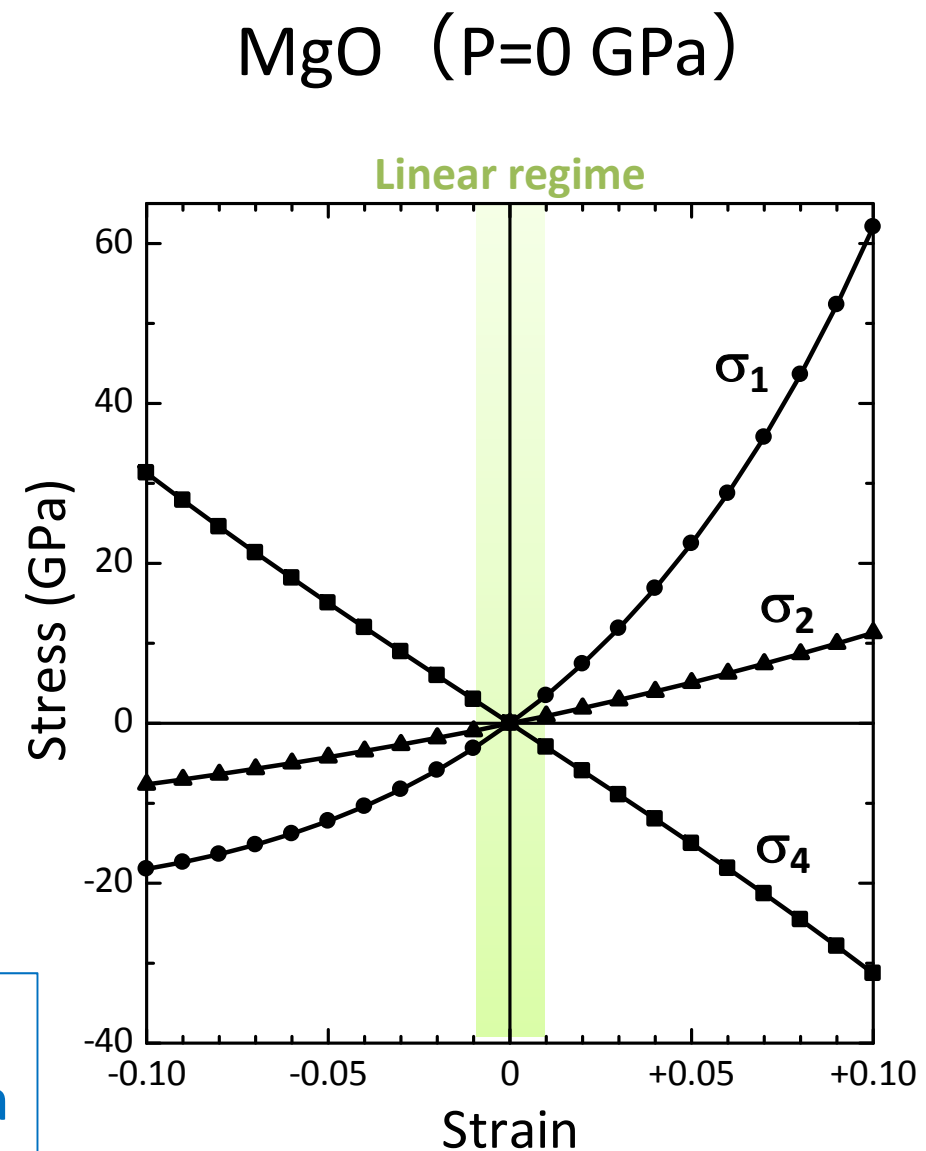
Voigt notation (simplified notation)

$$11 \rightarrow 1, 22 \rightarrow 2, 33 \rightarrow 3, 23 = 32 \rightarrow 4, 31 = 13 \rightarrow 5, 12 = 21 \rightarrow 6$$

$$\text{e.g., } c_{1111} = c_{11}, \quad c_{1122} = c_{12}, \quad c_{2323} = c_{44}$$



Linear regime
typically within
 $|\varepsilon| \leq 0.01$



Acoustic (elastic) wave speed

Equation of motion

$$\begin{aligned}\rho \frac{\partial^2 u_1}{\partial t^2} &= \frac{\partial \sigma_{11}}{\partial x_1} + \frac{\partial \sigma_{12}}{\partial x_1} + \frac{\partial \sigma_{13}}{\partial x_1}, \\ \rho \frac{\partial^2 u_2}{\partial t^2} &= \frac{\partial \sigma_{22}}{\partial x_2} + \frac{\partial \sigma_{23}}{\partial x_2} + \frac{\partial \sigma_{21}}{\partial x_2}, \\ \rho \frac{\partial^2 u_3}{\partial t^2} &= \frac{\partial \sigma_{33}}{\partial x_3} + \frac{\partial \sigma_{31}}{\partial x_3} + \frac{\partial \sigma_{32}}{\partial x_3}\end{aligned}$$

Orientational average
 ⇒ Polycrystalline wave speed

$$V_P = \sqrt{\frac{B_S + 4/3\mu}{\rho}} \quad V_S = \sqrt{\frac{\mu}{\rho}} \quad V_\Phi = \sqrt{\frac{B_S}{\rho}}$$

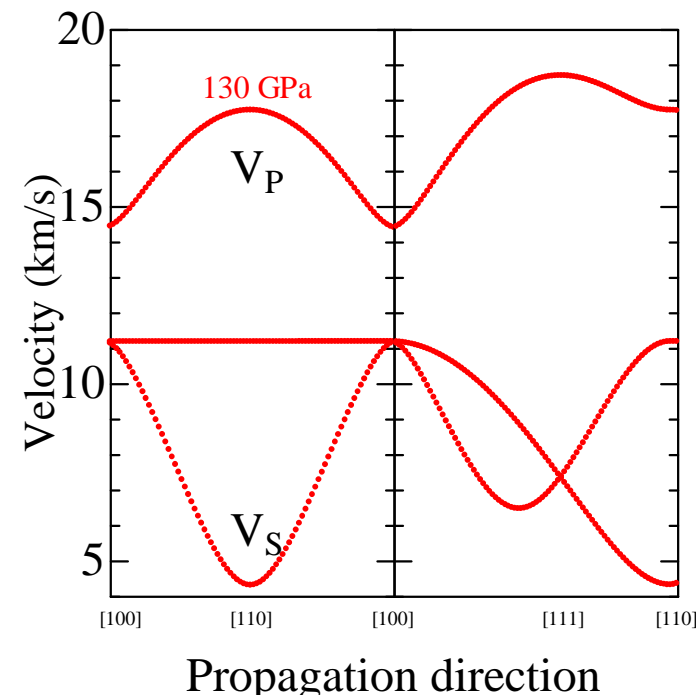
**Direct comparison with
 seismological observations**

Cristoffel's equation

$$|c_{ijkl} \mathbf{n}_j \mathbf{n}_l - \rho V \delta_{ik}| = 0$$

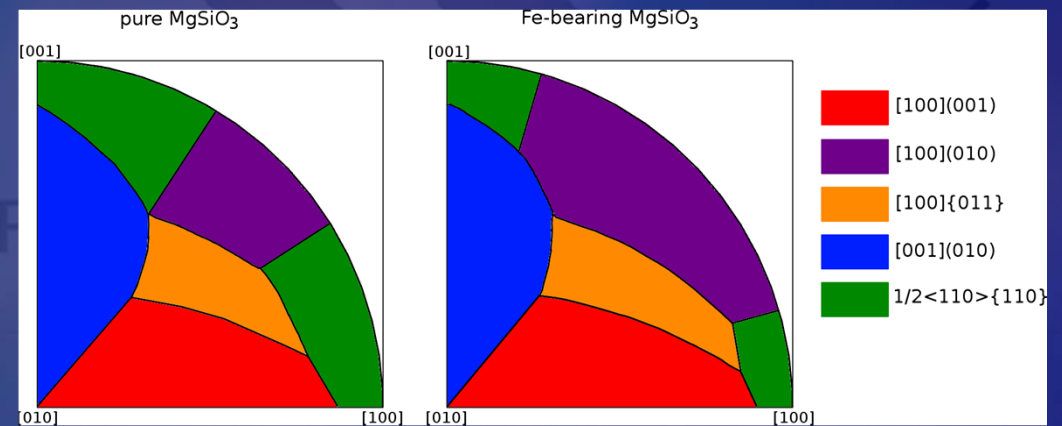
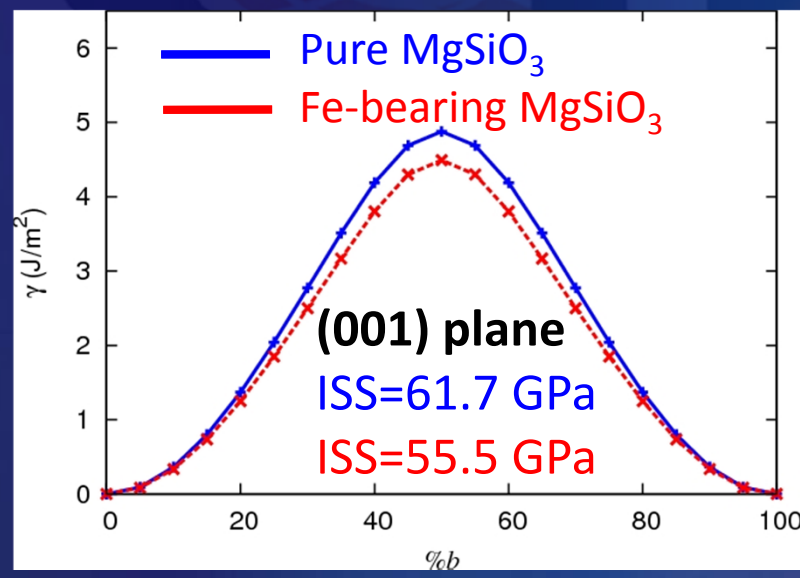
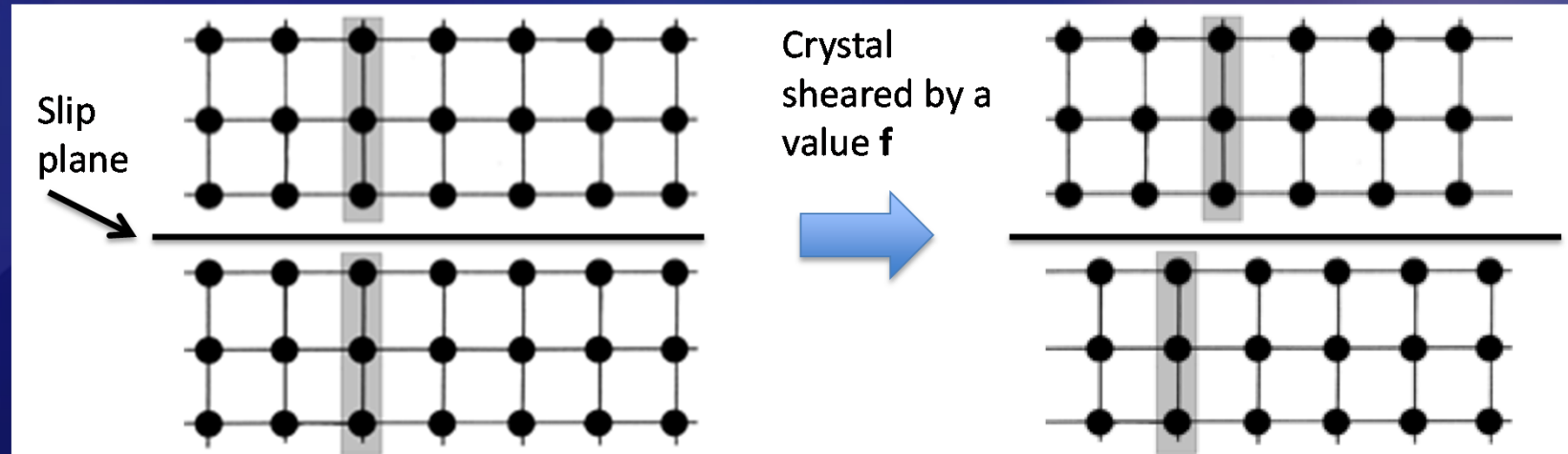
⇒ Single-crystal wave speed

e.g., ice X phase (P=130 GPa)



Shear response of crystals

Generalized Stacking Faults (GSF) Theory (Vitek, 1968; Cordier+ 2004; etc)



Metsue & Tsuchiya, under review

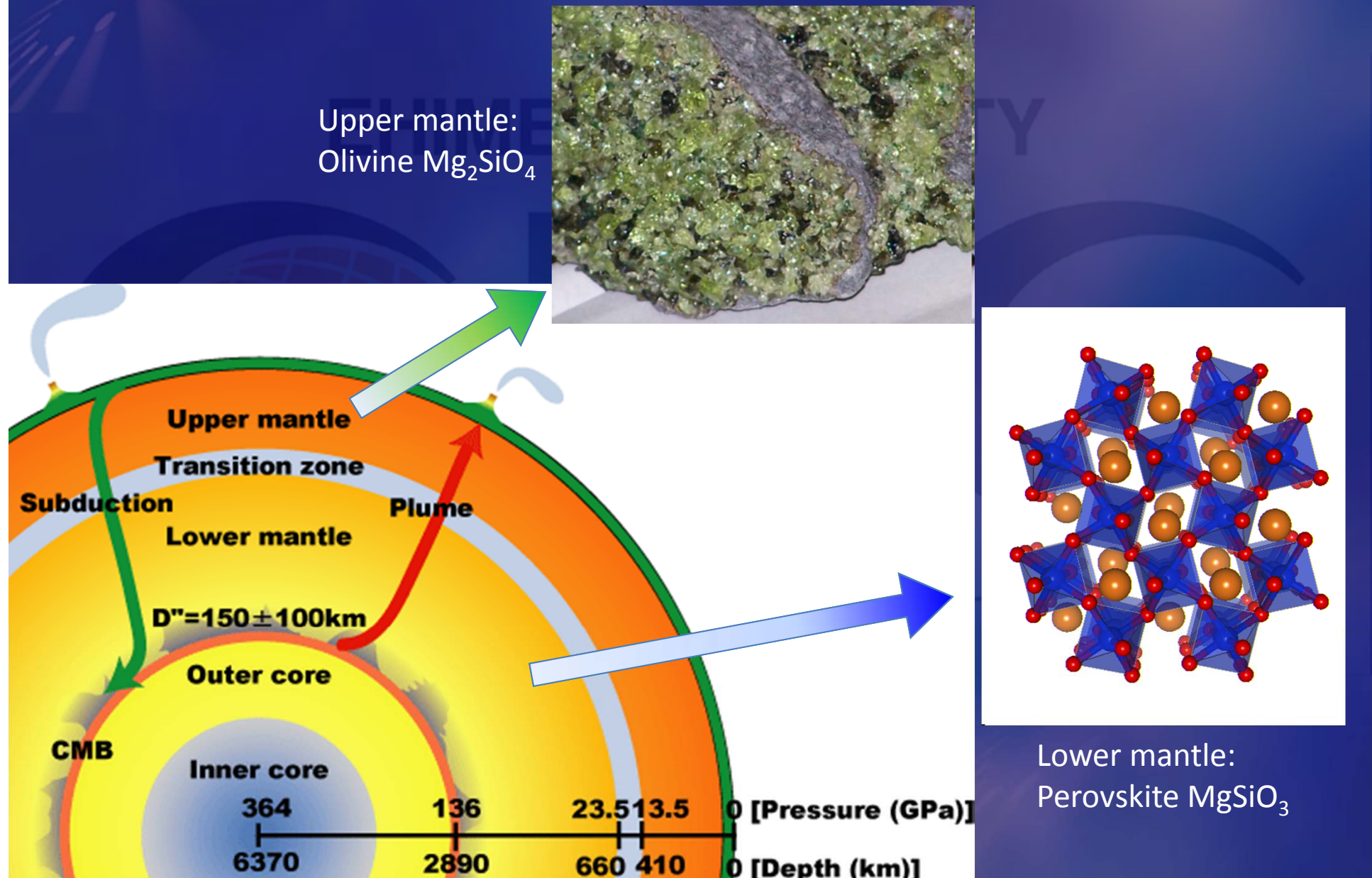
Solid viscosity still uneasy

1. Fundamental methodologies of the ab initio electronic structure calculation method

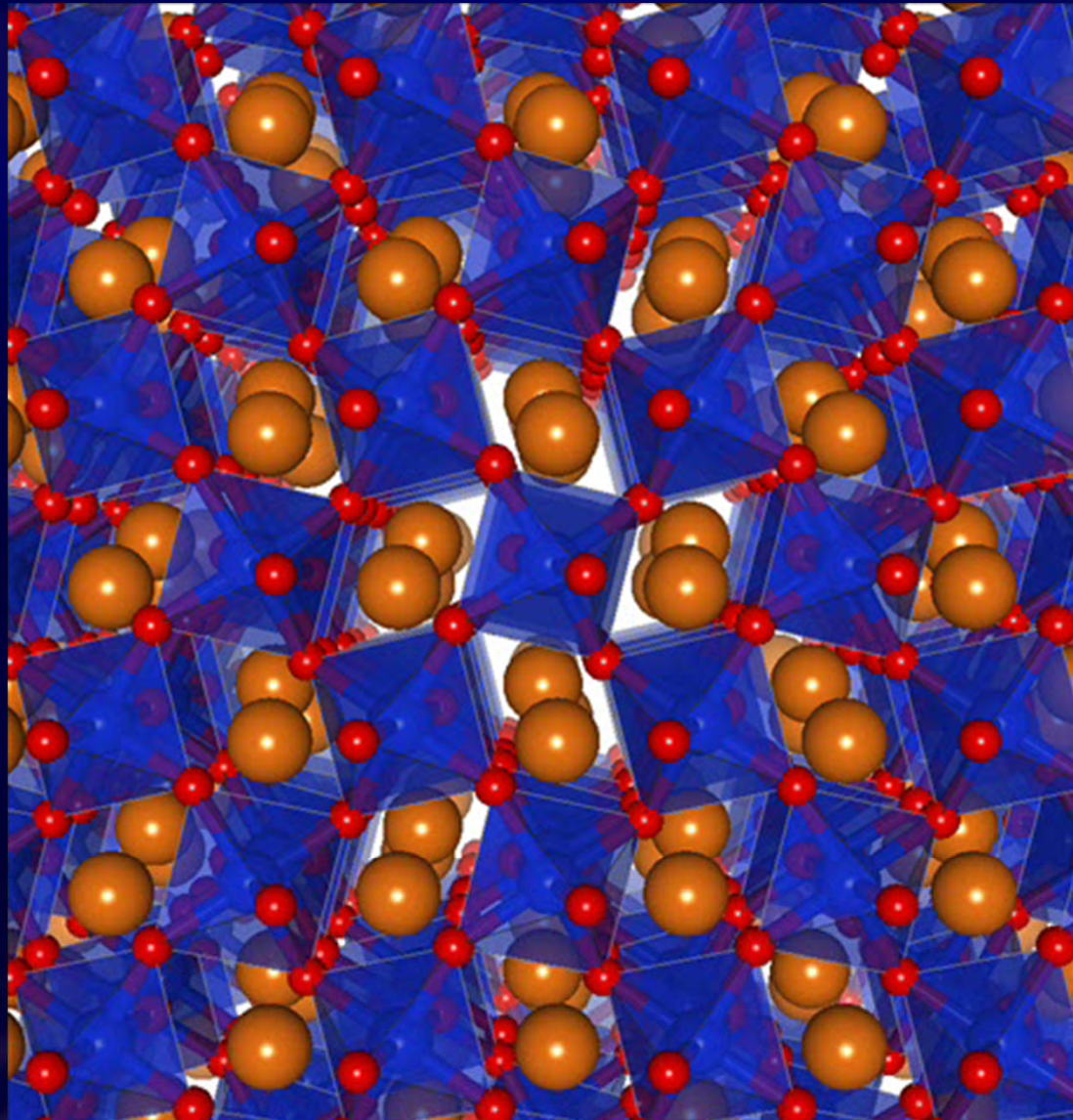
2. Applications to high-pressure mineral physics and Earth & planetary interiors

- Phase relations including melting
- Electronic property
- Transport property

Example: Post-perovskite transition in MgSiO_3

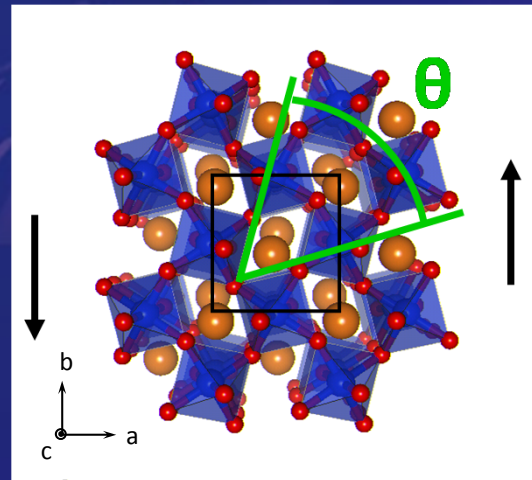


Perovskite to post-perovskite structural change

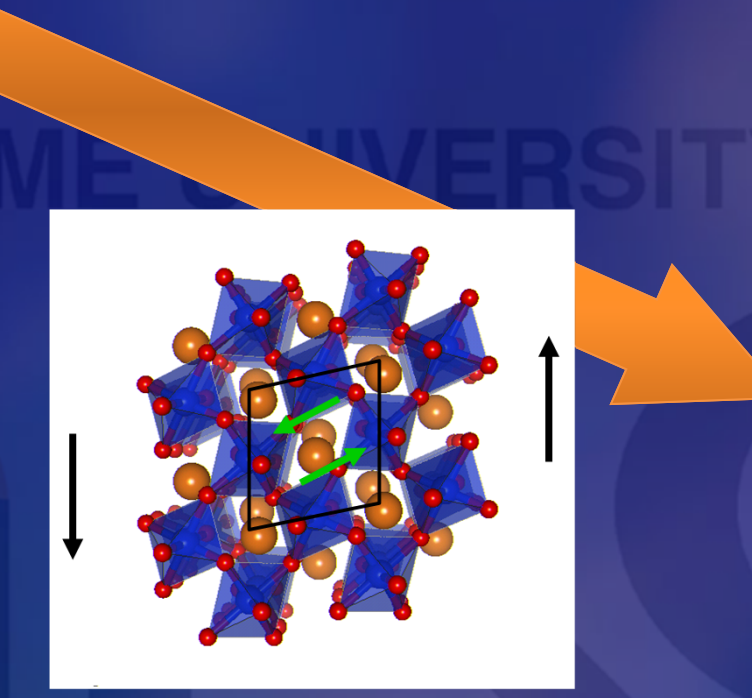


Mg
Si
O

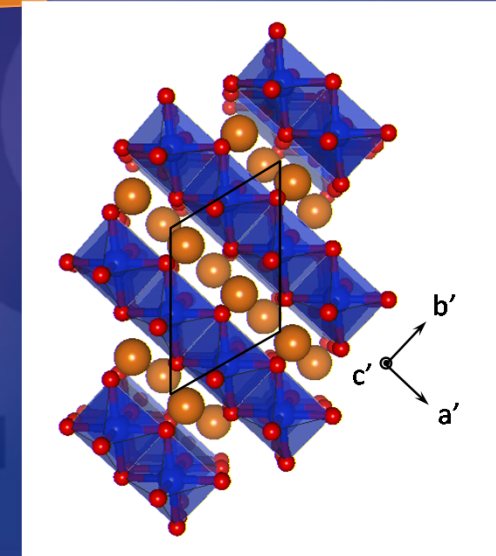
Tsuchiya+ (2004) EPSL



Perovskite
(Lower
mantle)



Shear
deformation
(ε_6)



Post-Perovskite
(D'' layer)

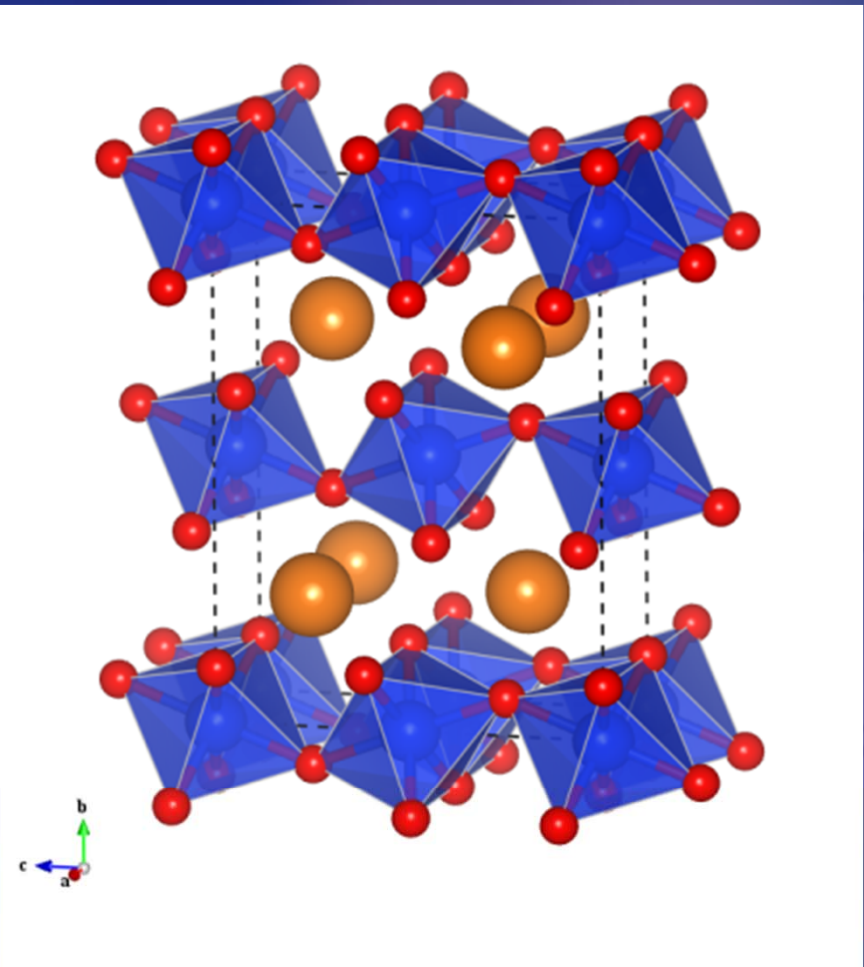
CaIrO₃-type structure

- Orthorhombic cell ($Cmcm$, $Z = 4$) with SiO₆ octahedra.
- Those octahedra are connected with each other by sharing edges along the a direction. This is a major reason for the structure more stable than Pv.

Exper: Murakami+ (2004)

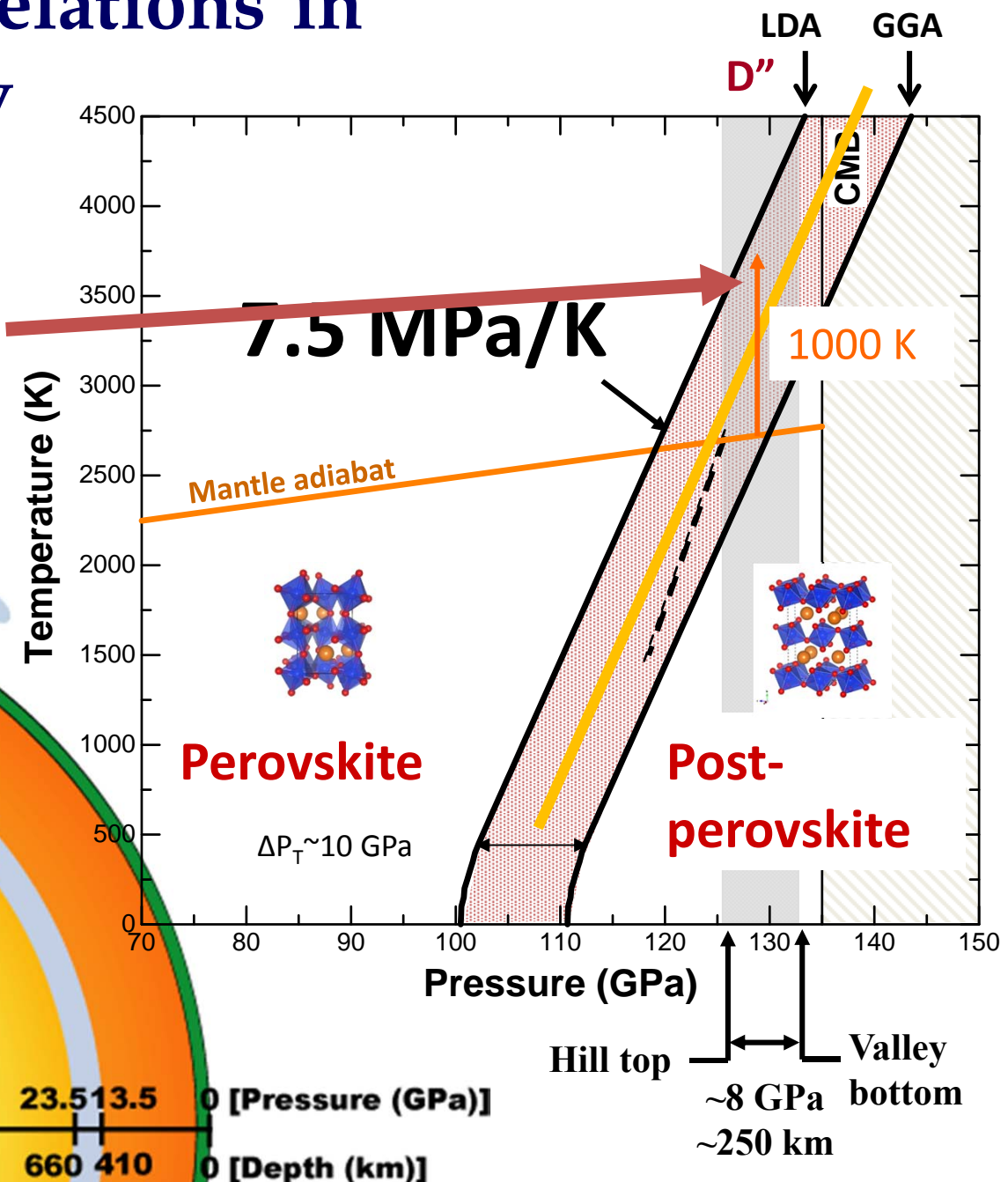
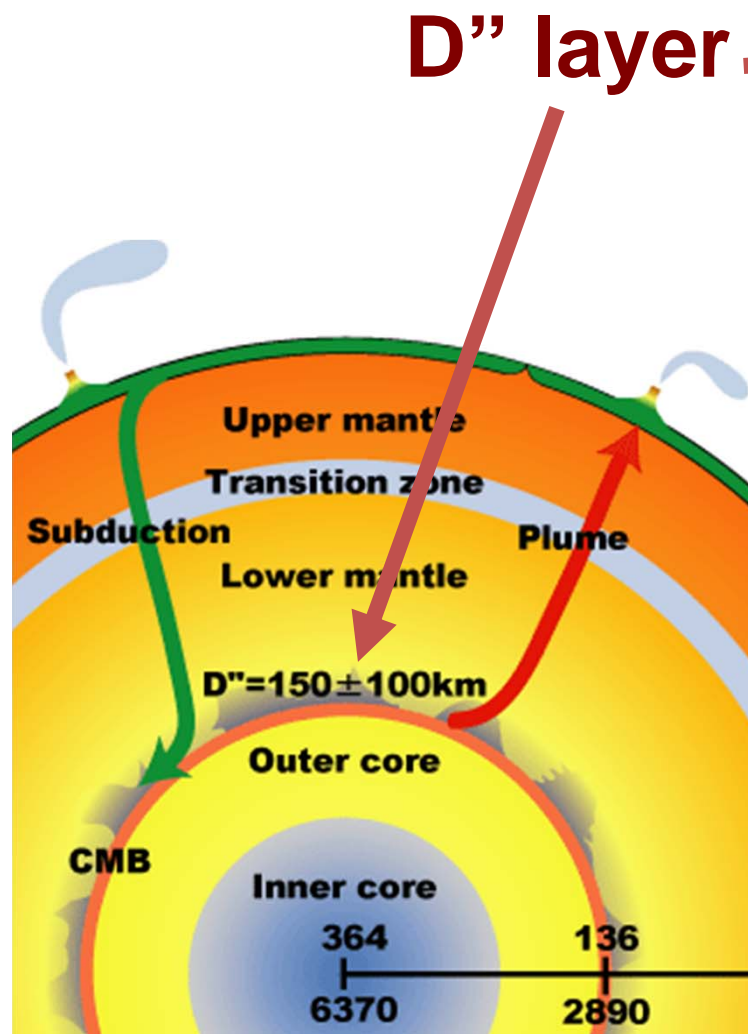
Theor: Tsuchiya+ (2004)

etc

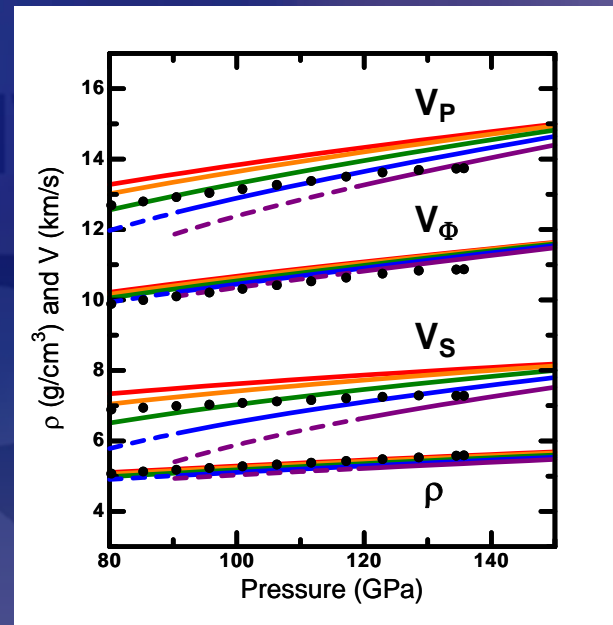
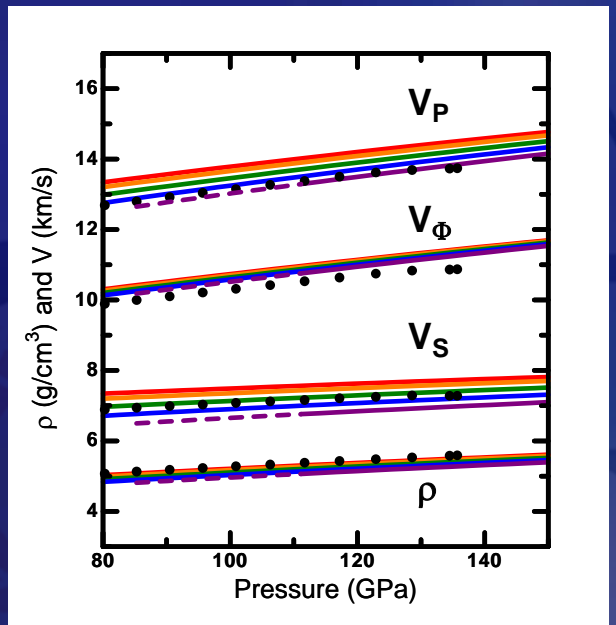
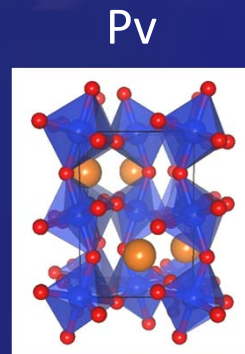


High- P,T phase relations in MgSiO_3 Pv & PPv

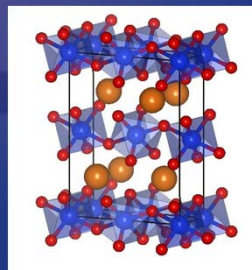
Tsuchiya+ (2004) EPSL



High- P,T elastic wave velocities and density of $\text{MgSiO}_3\text{-Pv}$ and PPv



PPv



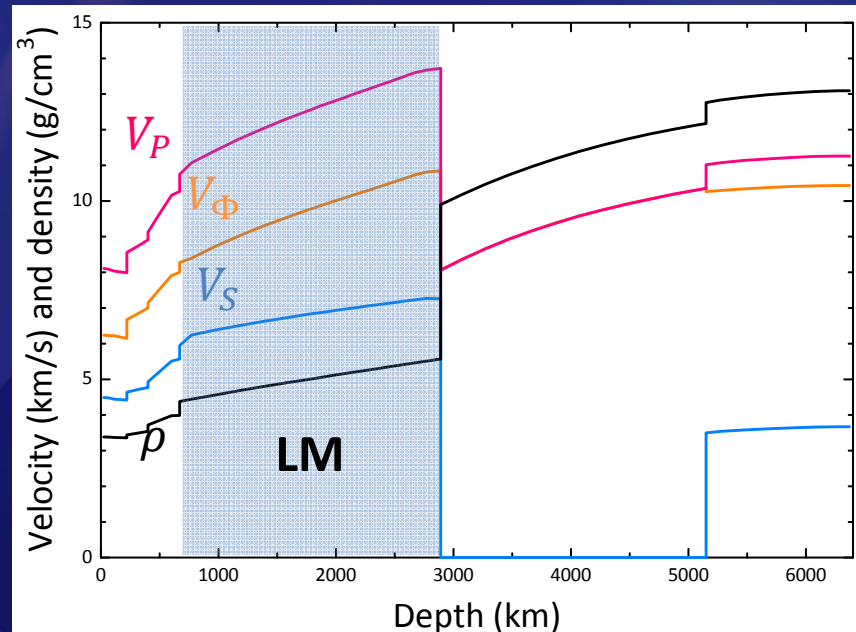
Wentzcovitch, Tsuchiya & Tsuchiya (2006) PNAS

Effects of Fe and Al incorporation

Table 2. Logarithmic Derivatives of Velocities and Density With Respect to Lateral Variations in the Fe and Al Content at 100 GPa

	$\frac{\partial \ln V_p}{\partial X}$		$\frac{\partial \ln V_s}{\partial X}$		$\frac{\partial \ln V_\Phi}{\partial X}$		$\frac{\partial \ln \rho}{\partial X}$	
	Fe	Al	Fe	Al	Fe	Al	Fe	Al
Pv	-0.140	-0.049	-0.220	-0.083	-0.098	-0.026	0.231	0.017
PPv	-0.156	-0.057	-0.236	-0.131	-0.099	-0.012	0.228	0.021

Velocity structure of the Earth



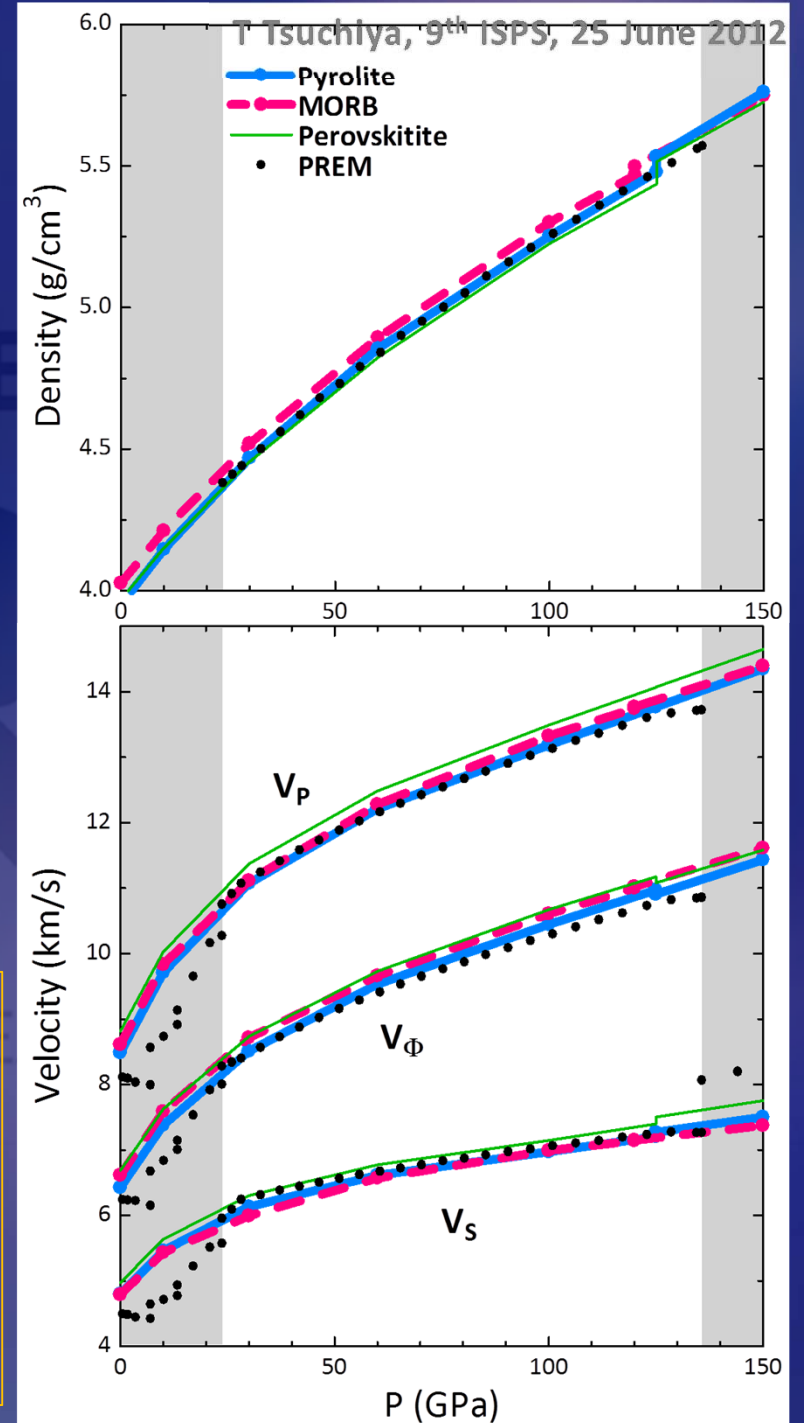
Observations (PREM, *Dziewonski & Anderson, 1981*)

Calculated velocities and density of some model rocks along adiabatic geotherm

(*Tsuchiya PEPI 2011; Tsuchiya & Kawai, under review*)

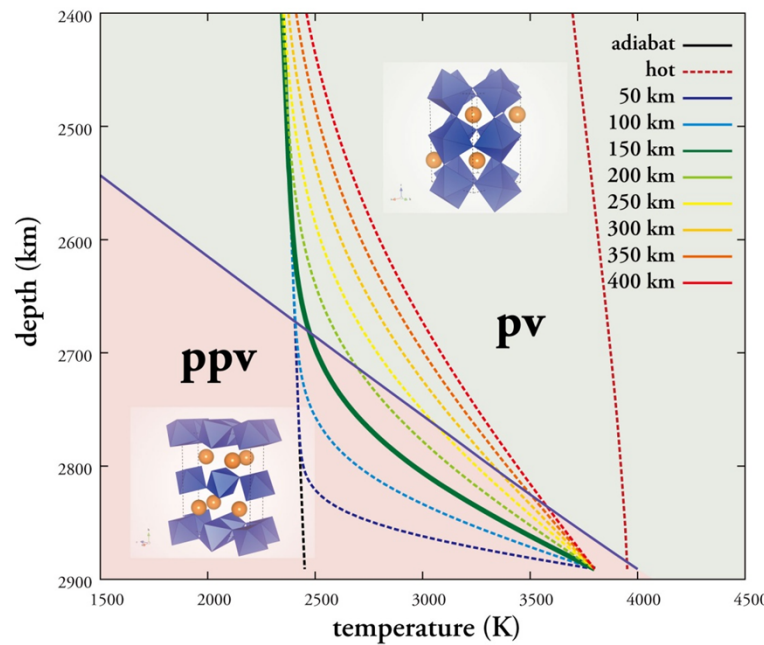
V_S is the most insensitive to the composition among these three models.

(cf, *Murakami+ 2012*)



D'' velocity structure model

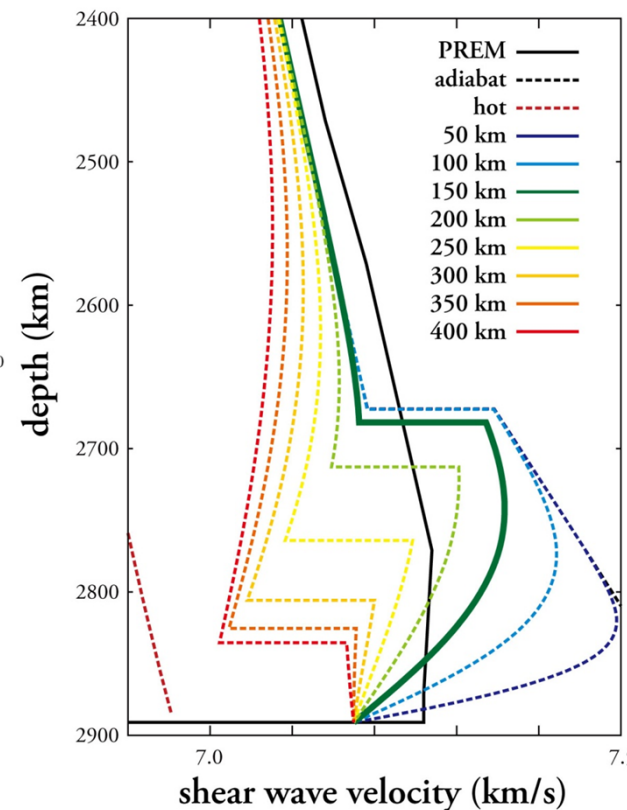
Case: $T_{CMB} = 3800$ K



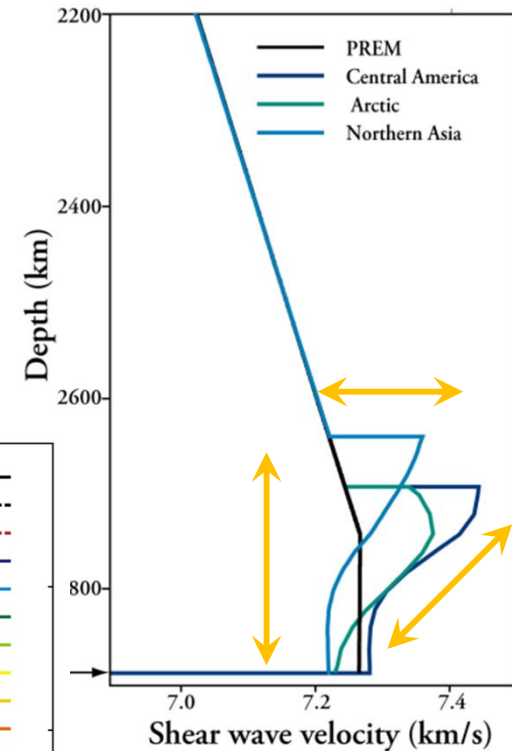
Temperature structure

$$\Delta T_{TBL} = 1200 \text{--} 1300 \text{ K}$$

$$D_{TBL} = 250 \text{ km}$$



Modeled velocity structure



Observations

Kawai & Tsuchiya (2009) PNAS

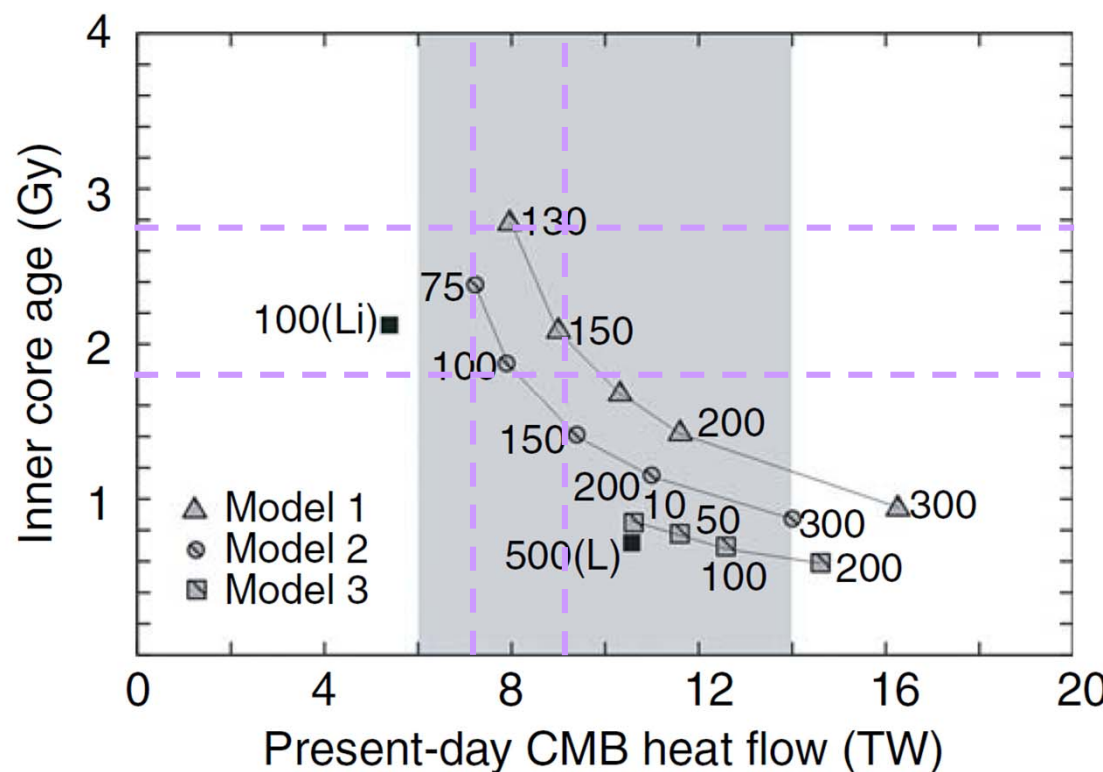
About CMB heat flux

CMB heat flux $q \sim \kappa \frac{\Delta T_{TBL}}{D_{TBL}}$

$$\left. \begin{array}{l} \Delta T_{TBL} = 1200 \sim 1300 \text{ K} \\ D_{TBL} = 250 \text{ km} \\ \kappa = \sim 10 \text{ W K}^{-1}\text{m}^{-1} \end{array} \right\} \text{Kawai \& Tsuchiya (2009)}$$

\leftarrow Representative value

= 7~9 TW

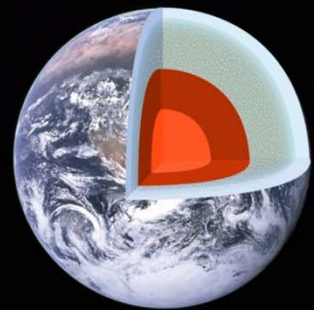


Relationship btwn
CMB heat flow and Inner core age
(Nimmo, ToG, 2007)

Estimated inner core age
= 2~3 Gy

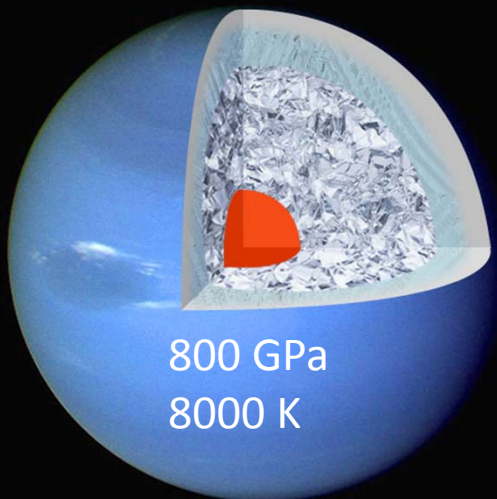
However, **κ (thermal conductivity)** of minerals under pressure still highly unclear

Extend to planetary interiors



360 GPa
6000 K

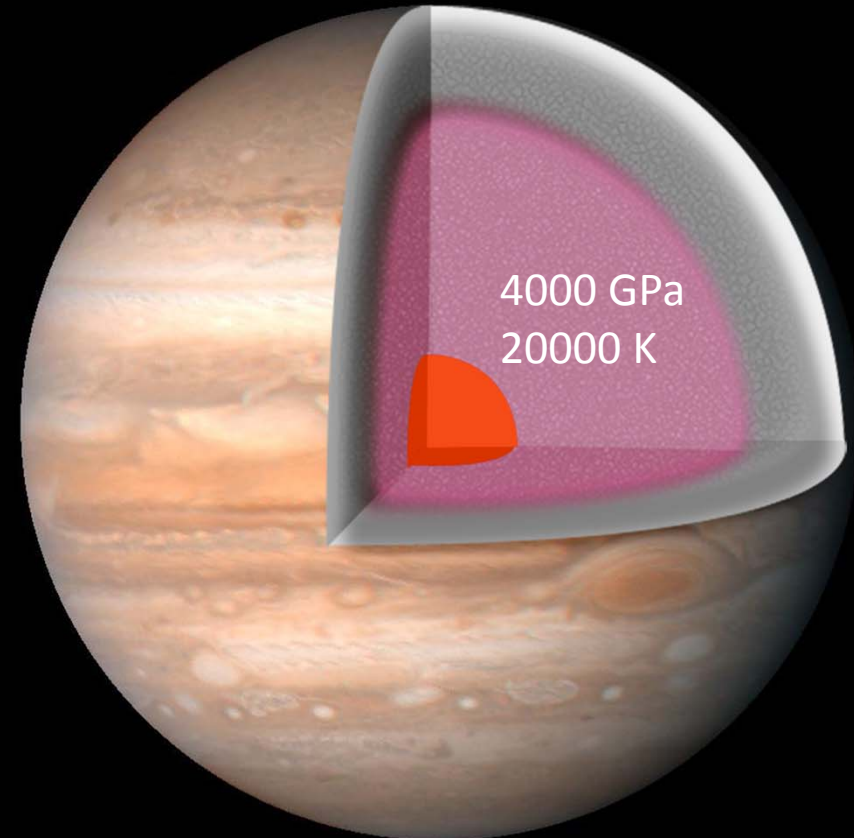
Rocky (silicate) mantle +
iron core



800 GPa
8000 K

Icy ($\text{H}_2\text{O}, \text{CH}_4$ + rocky core)

$\sim 2M_\oplus$



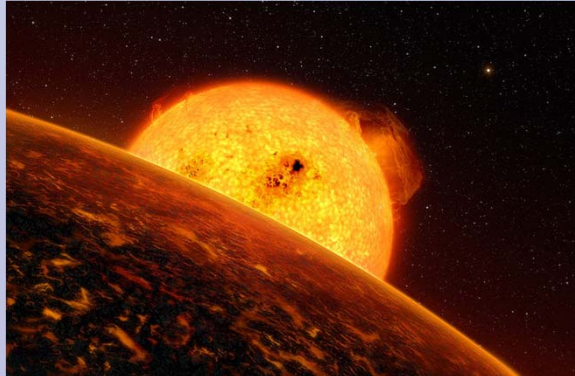
Gassy (H,He + rock+ice core?)

$\sim 10M_\oplus$

e.g., Guillot (1999) Science

Now, more than 700 exoplanets have been found.

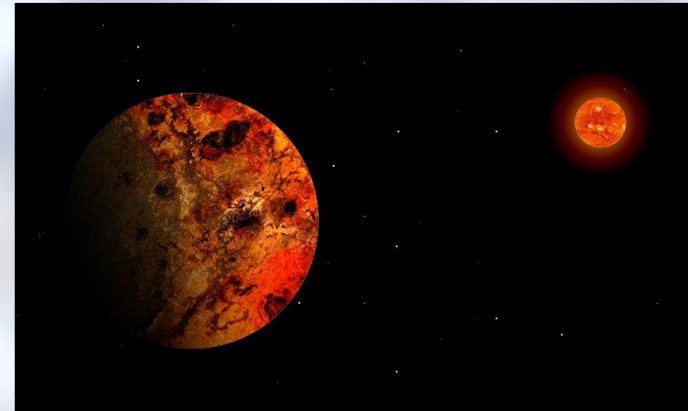
Some of them are terrestrial = **Super-Earths (SE)**.



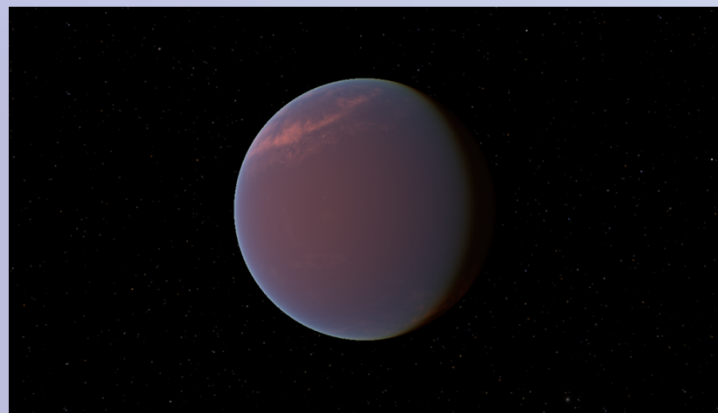
CoRoT-7b ($\sim 4.8M_{\oplus}$)



GJ876d ($\sim 7.5M_{\oplus}$)



HD69830b ($\sim 10M_{\oplus}$)



GJ1214 ($\sim 6.55M_{\oplus}$ rock+H₂O)

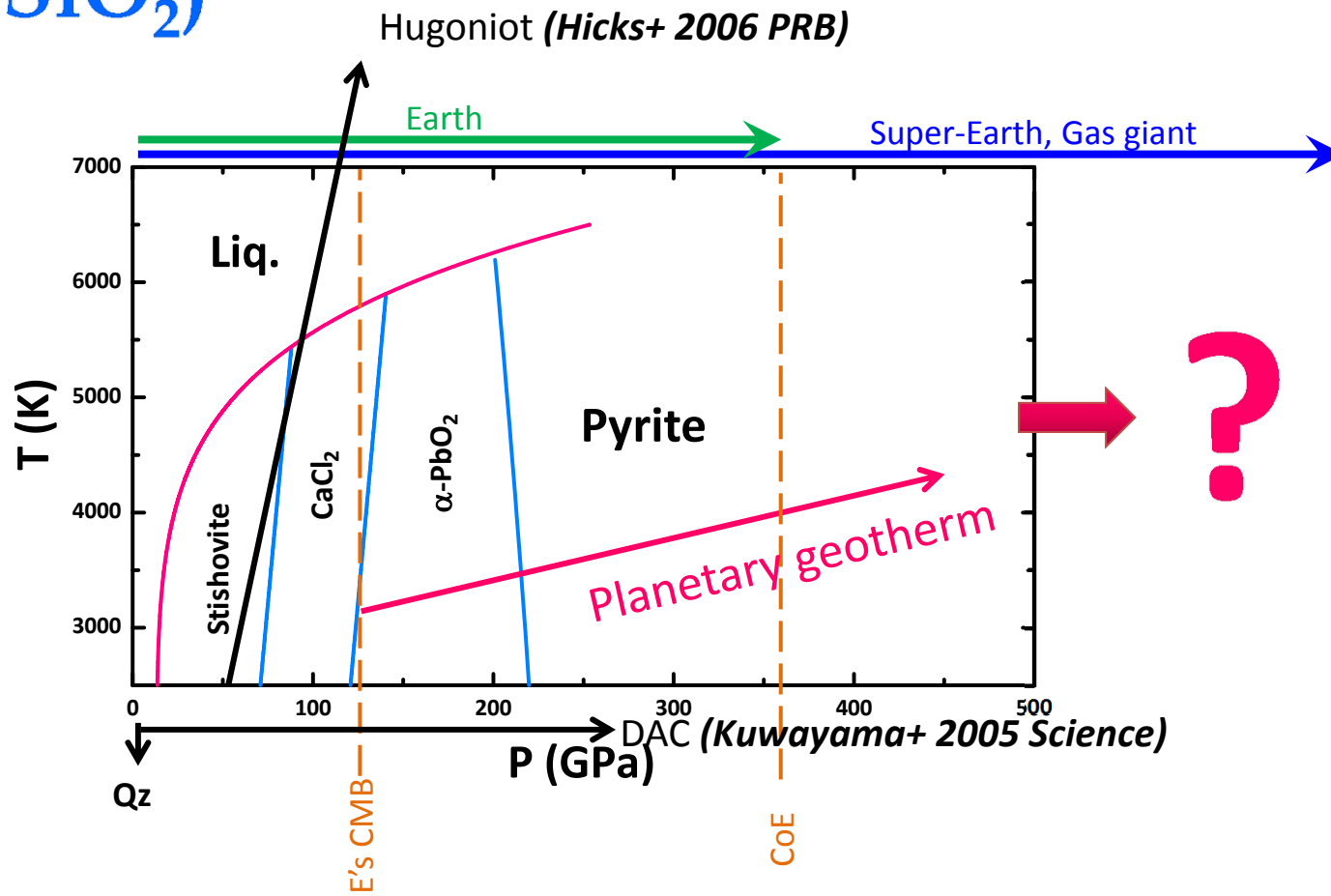


CoRoT space telescope
(France)



Kepler space telescope
(USA)

High- P,T phase relation of Earth materials (ex. SiO_2)



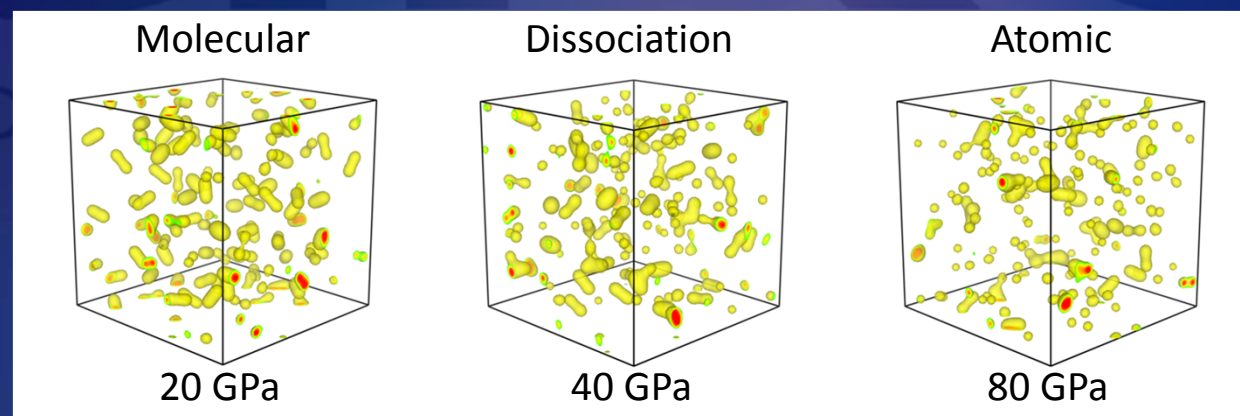
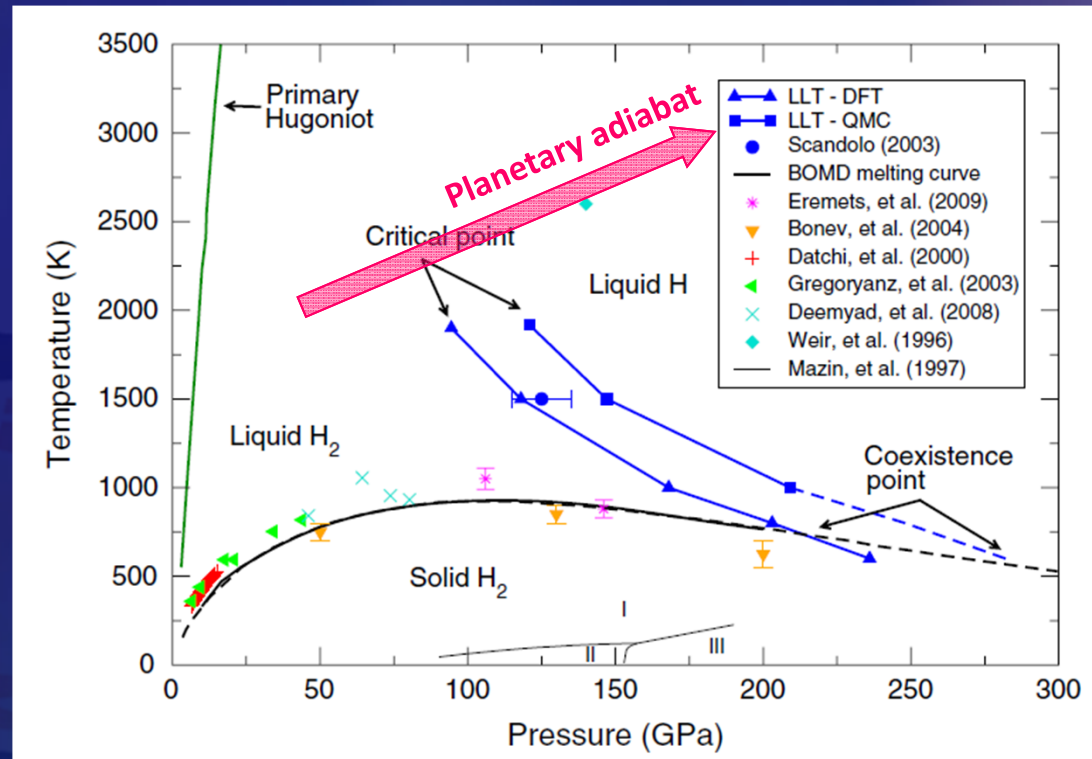
- High- P,T phase relations highly unclear at ultrahigh pressures
- But several important advances made by ab initio calculations

Hydrogen

T Tsuchiya, 9th ISPS, 25 June 2012

Morales+ (2010) PNAS

Ab initio MD

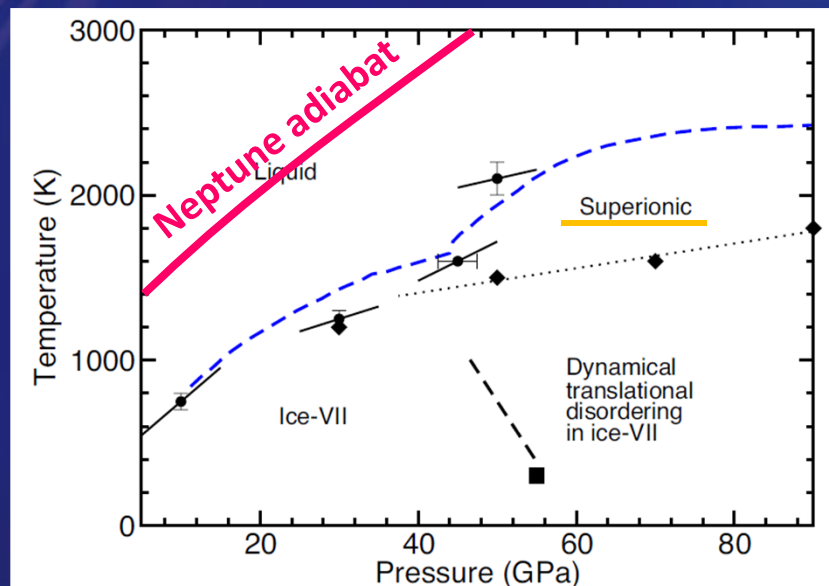


T Tsuchiya, 9th ISPS, 25 June 2012

Water

Schwegler+ (2008) PNAS

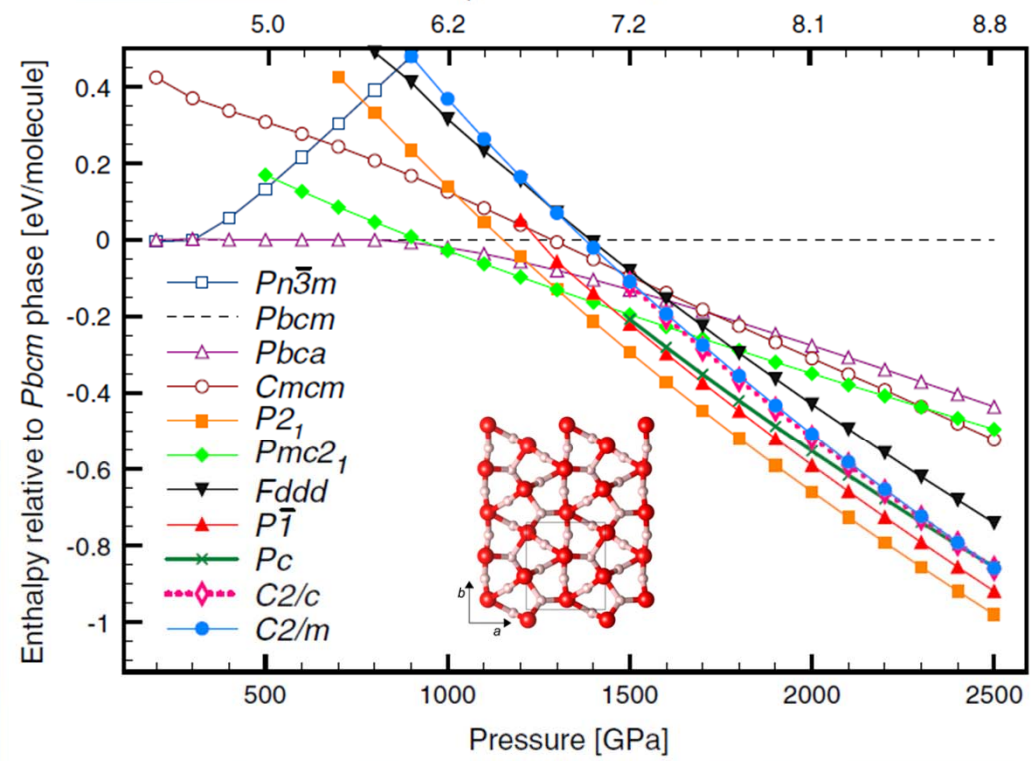
Ab initio melting curve



Ice

Hermann+ (2012) PNAS

Ab initio static phase stability

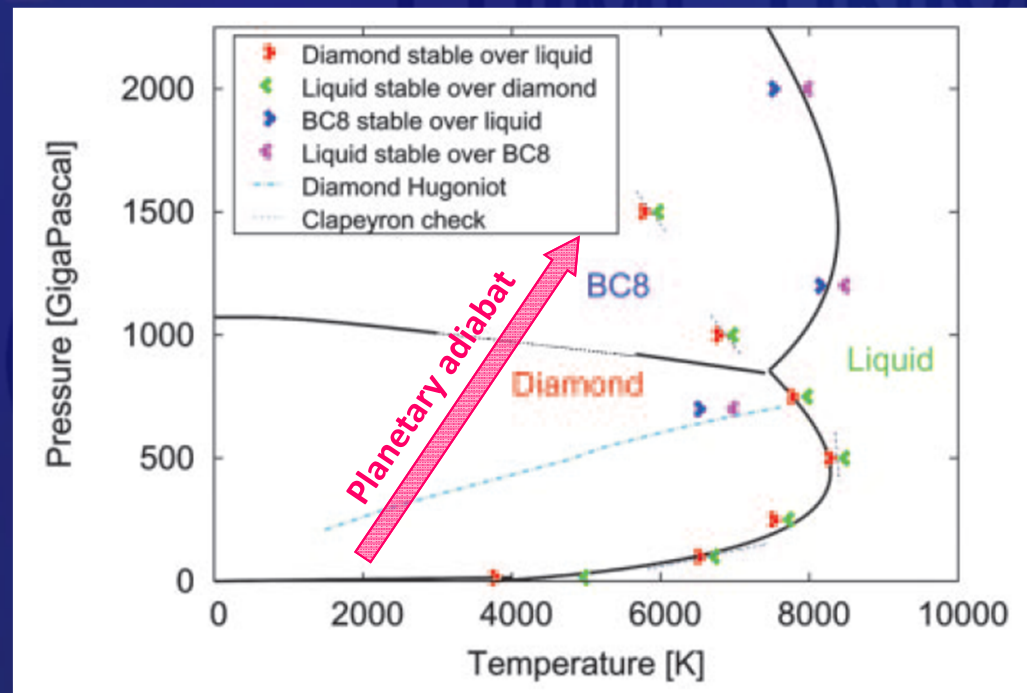


Carbon

"Diamonds in the sky" Ross+ (1981) Nature ?

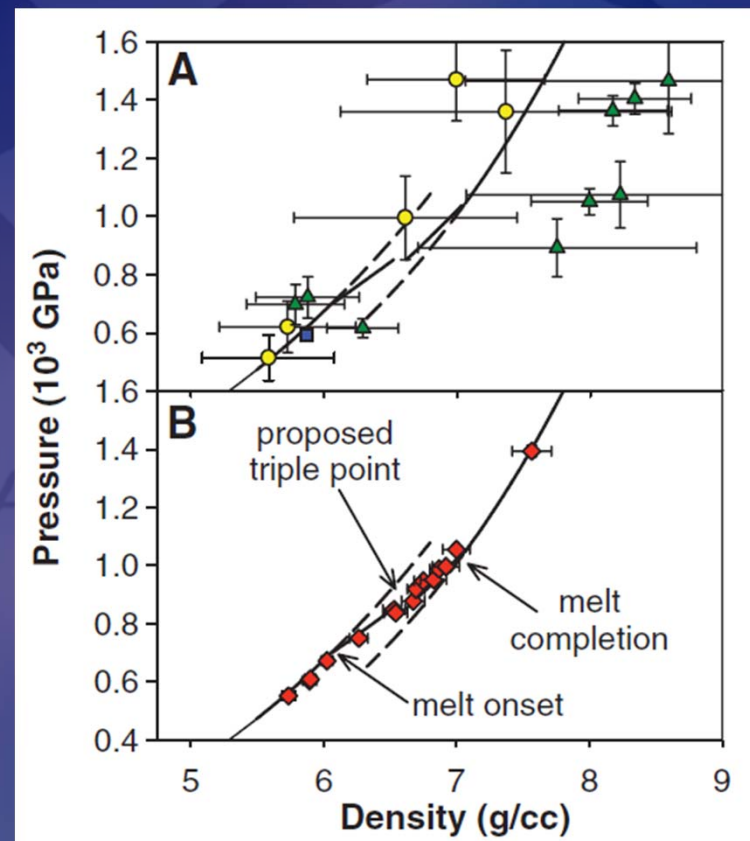
Correa+ (2006) PNAS

Ab initio high-*P,T* phase diagram of C



Knudson+ (2008) Science

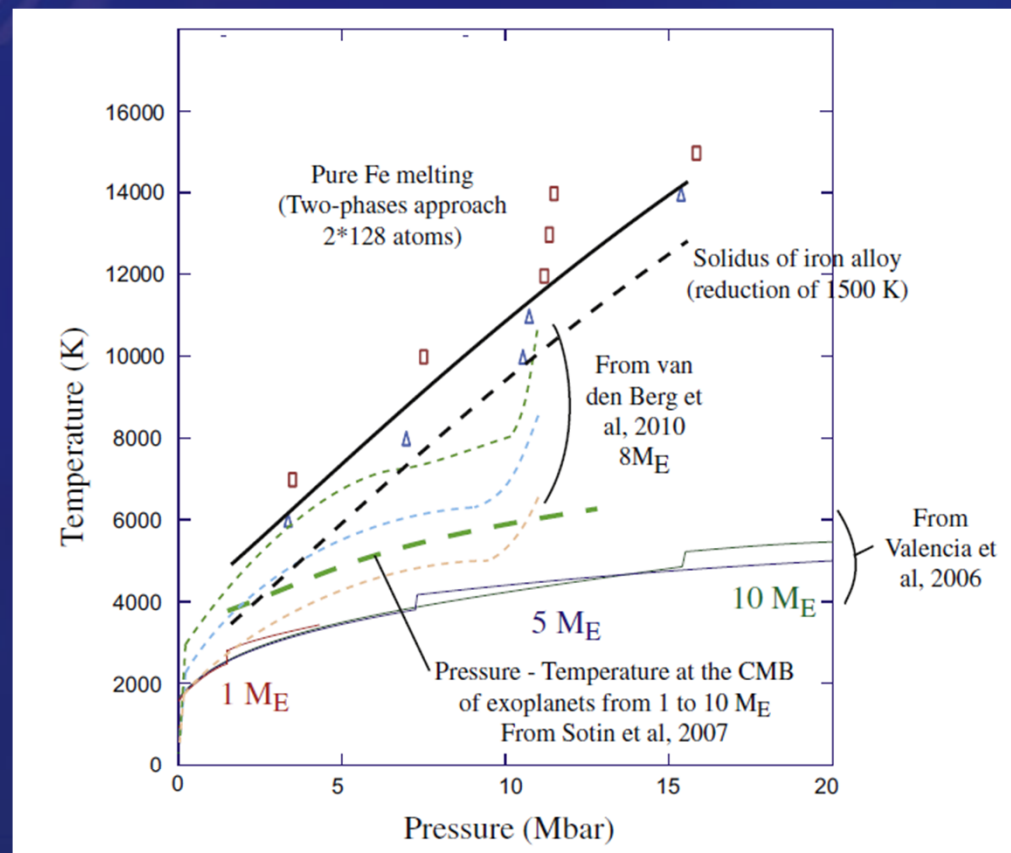
Experimental confirmation of the Dia-BC8-Liq triple point



Iron

Morard+ (2011) HEDP

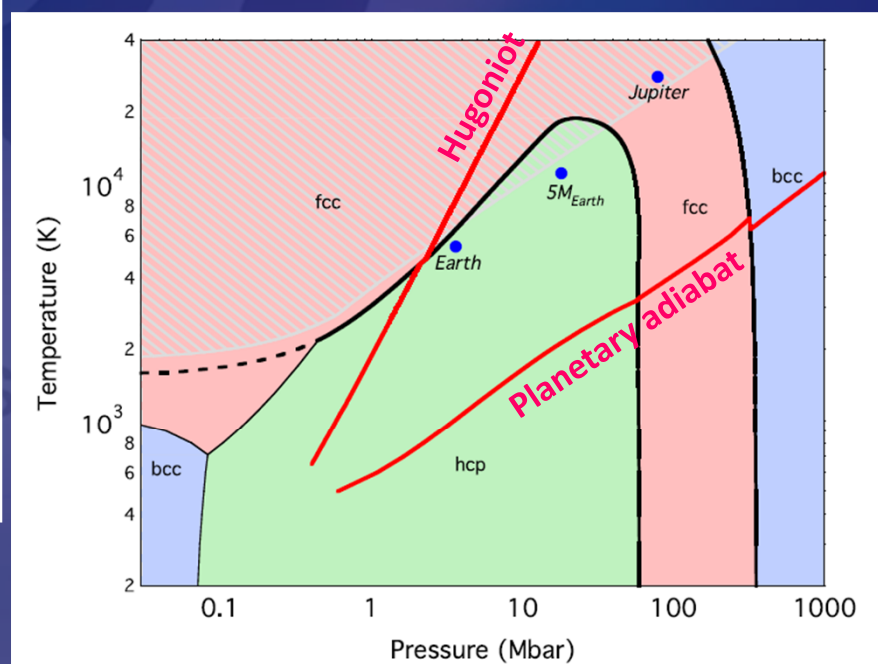
Ab initio melting curve



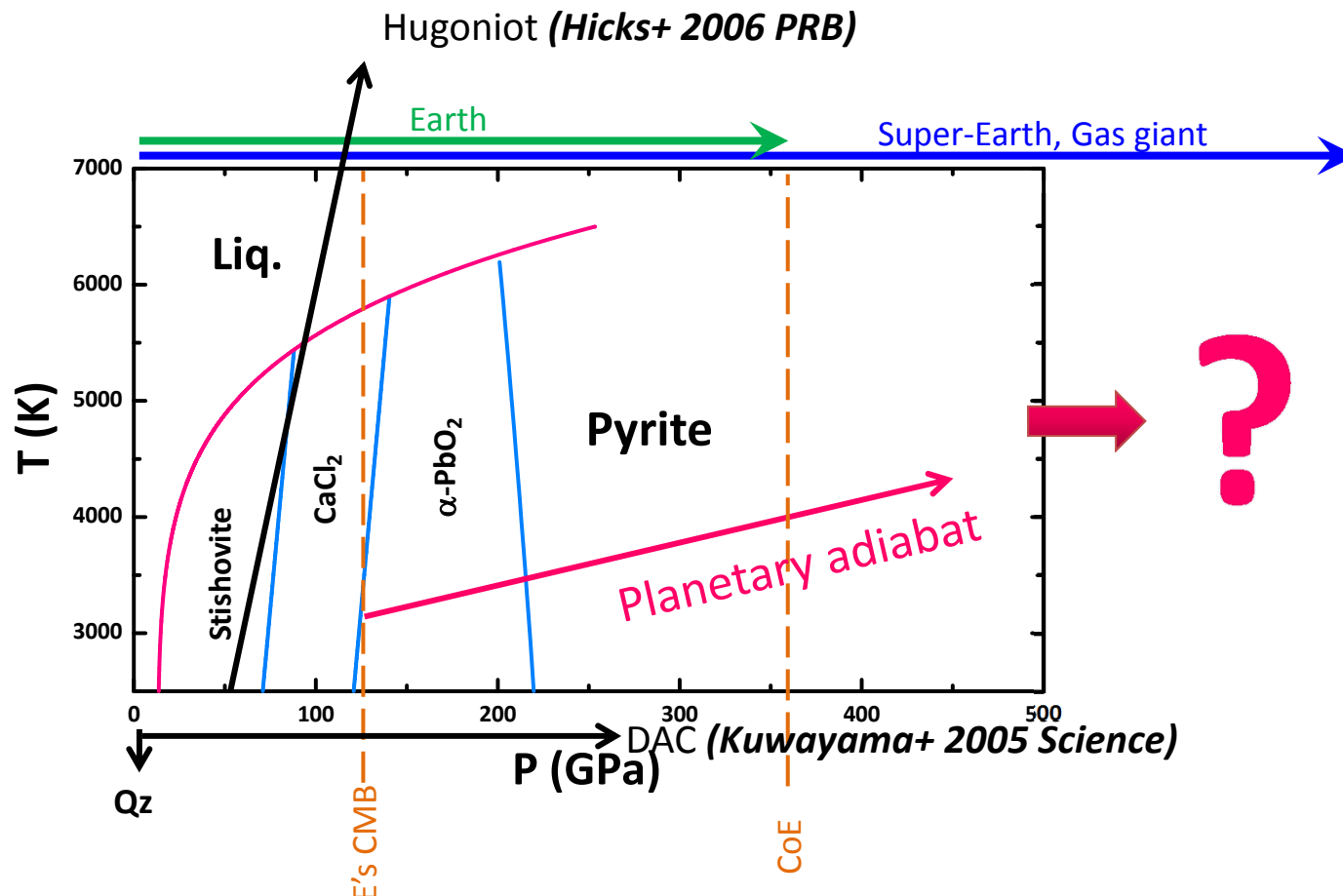
No liquid iron core in giant planets

Stixrude (2012) PRL

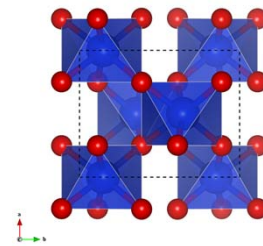
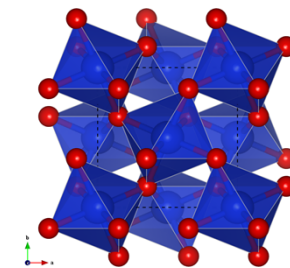
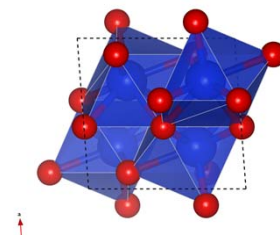
Ab initio High-*P,T* phase diagram



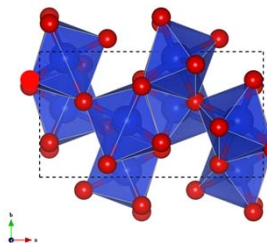
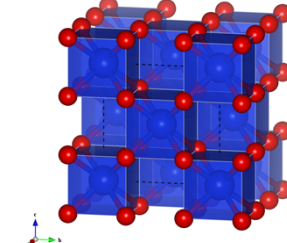
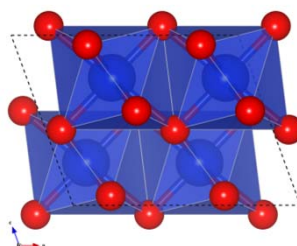
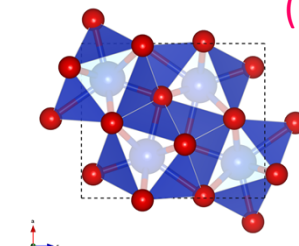
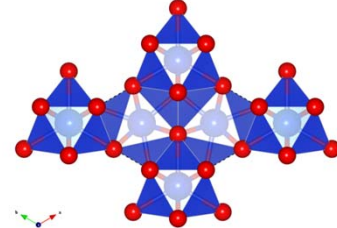
High- P,T phase relation of SiO_2



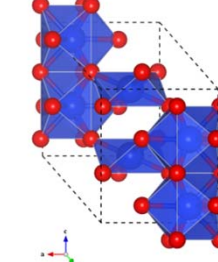
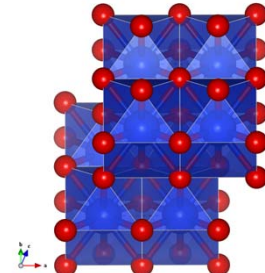
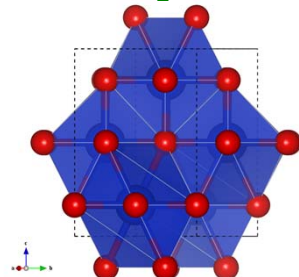
Dense packing structures with AX_2 stoichiometry for initial models (15 in total)

(1) $\alpha\text{-PbO}_2$ (VI)(2) Pyrite (FeS_2) (VI)(3) Baddeleyite (ZrO_2) (VII)

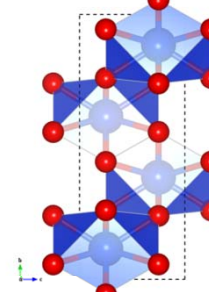
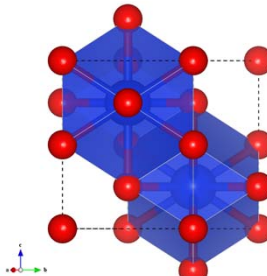
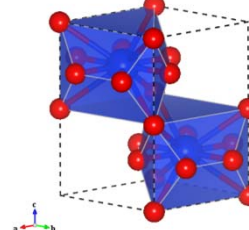
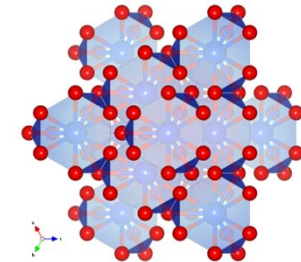
(4) Orthorhombic-I (VII)

(5) Fluorite (CaF_2) (VIII)(6) $P2_1/m$ (VIII)(7) Cotunnite (PbCl_2) (IX)(8) Fe_2P (IX)

(9) P-1 (IX)

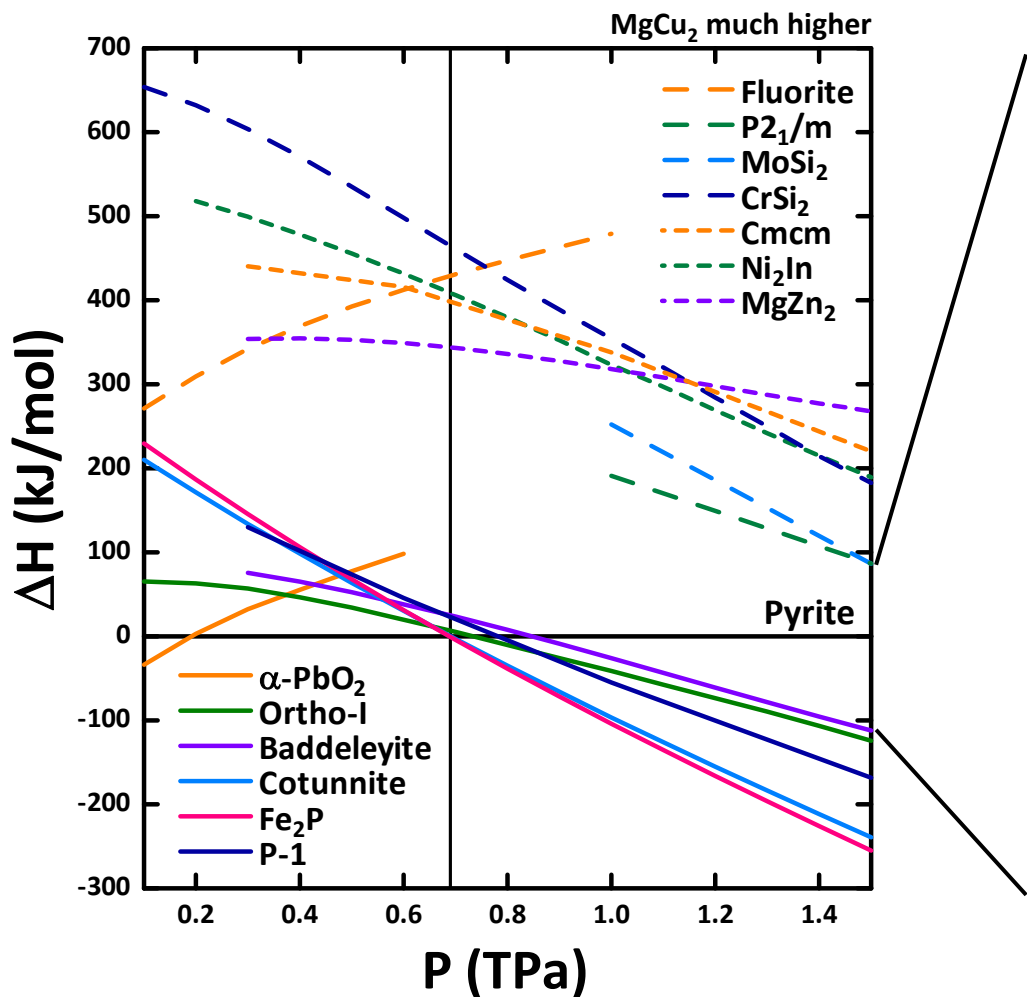
(10) MoSi_2 (X)(11) CrSi_2 (X)

(12) Cmcm (X)

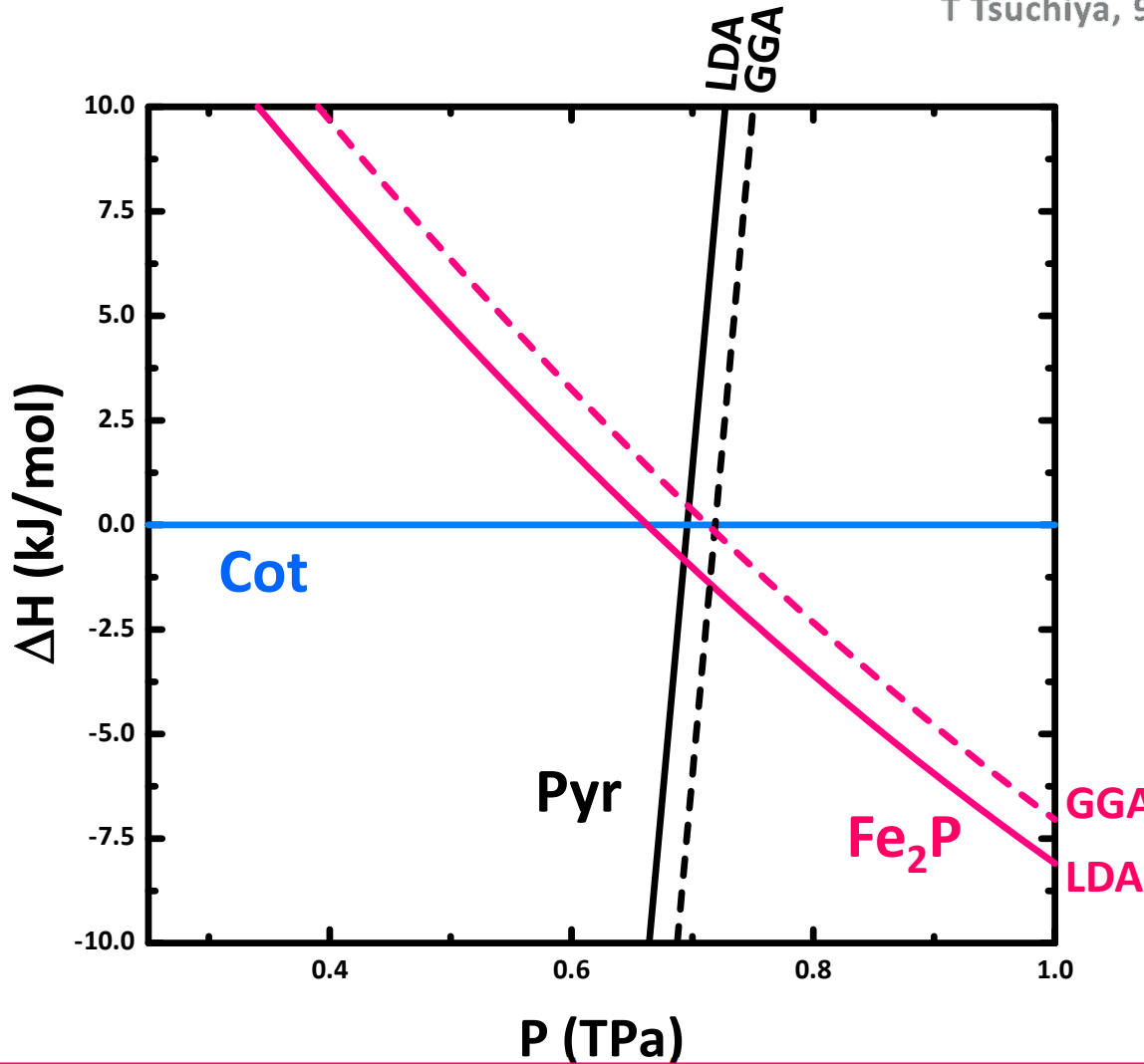
(13) Ni_2In (XI)(14) MgZn_2 (XII)(15) MgCu_2 (XII)

Blue: Si
Red: O

Static enthalpy differences relative to the pyrite phase



$$H(P) = E_{tot}(P) + PV$$



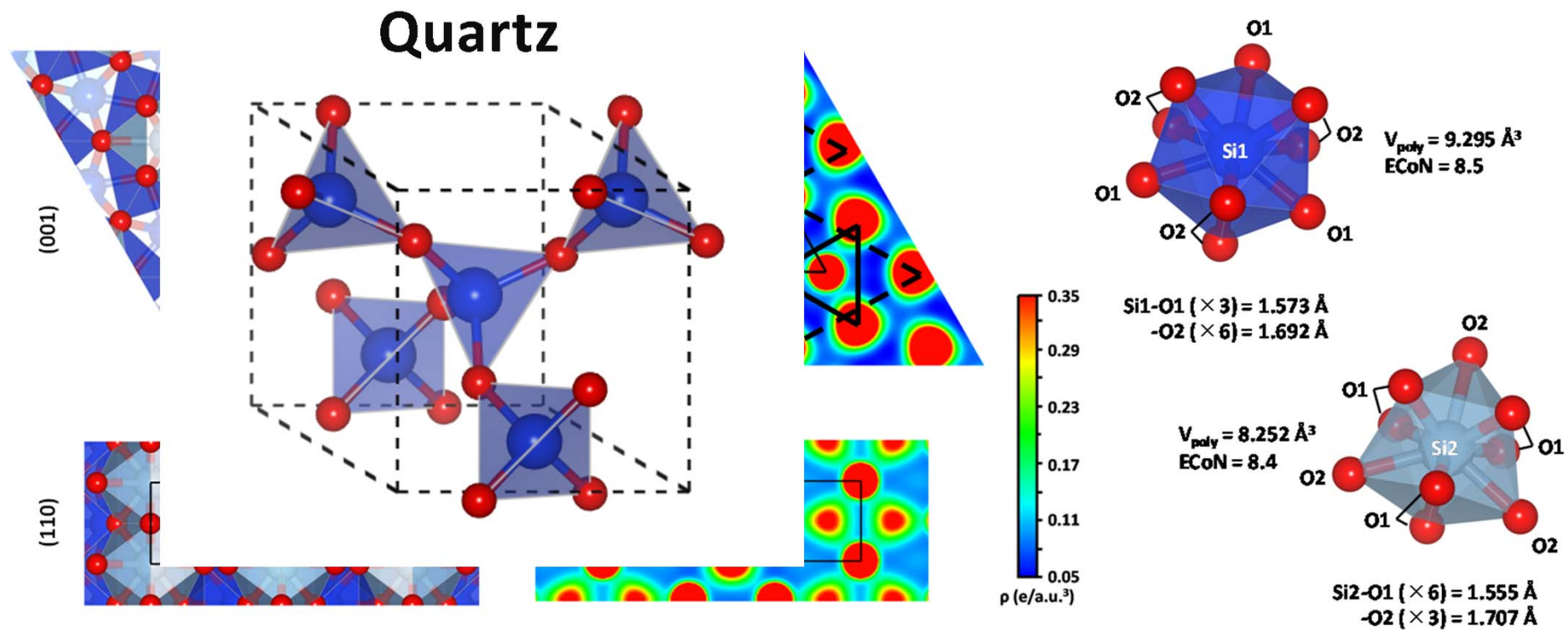
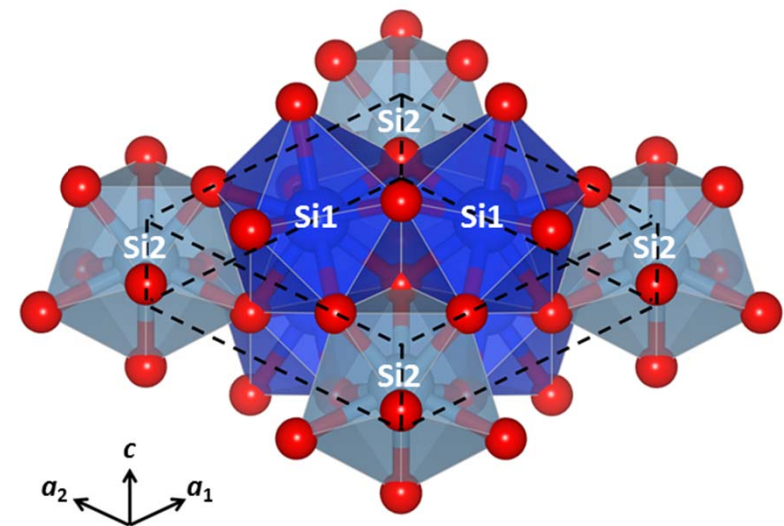
- Pyrite directly transforms to the Fe_2P -type phase (not cotunnite) at ~7 Mbar!

- No other stable structures
- No elemental dissociation of SiO_2 into Si (hcp) plus O_2 (ζ), either

Crystal structure of the Fe₂P-type new high-*P* phase of SiO₂

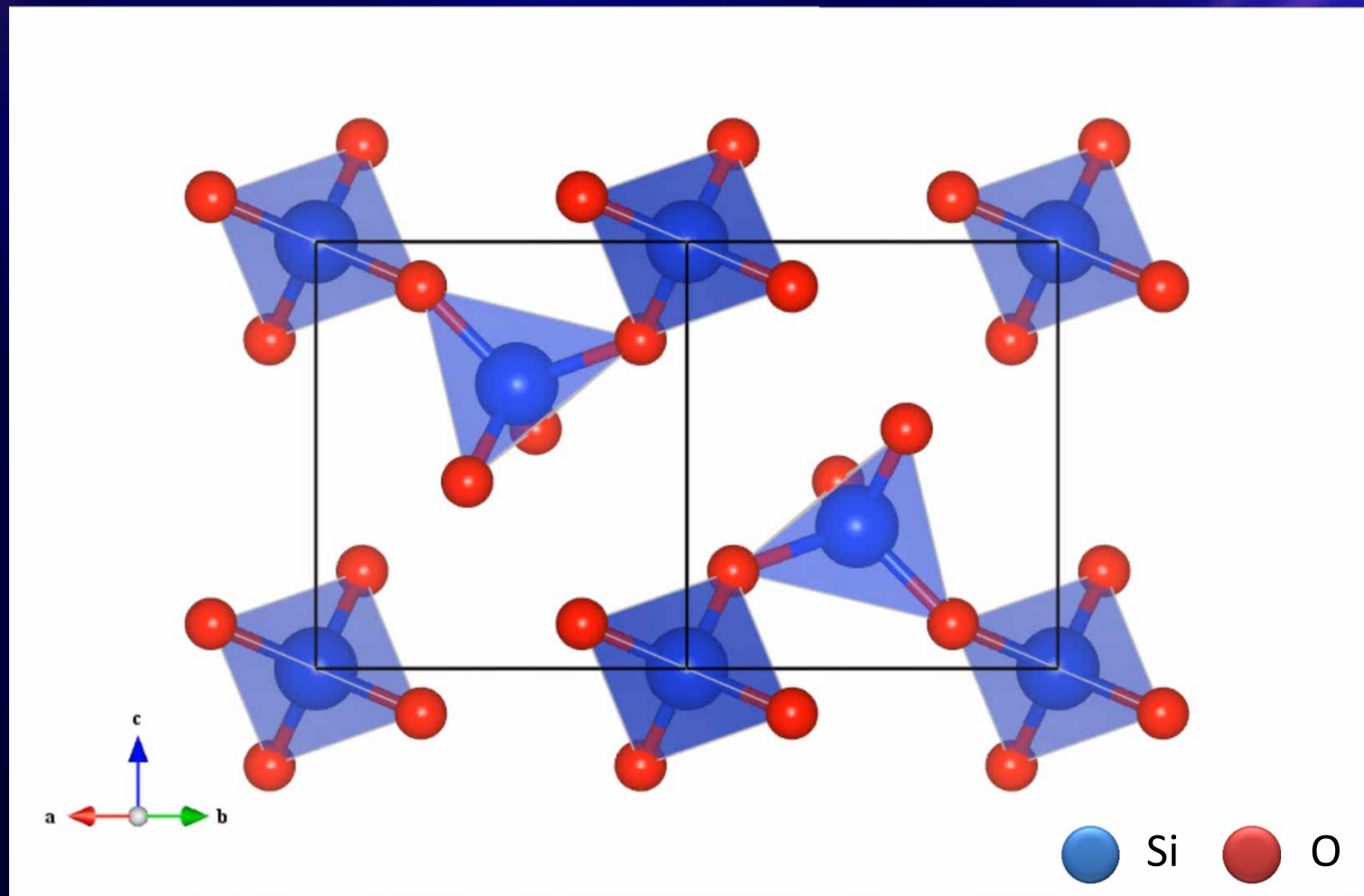
Tsuchiya & Tsuchiya (2011) PNAS

- Hexagonal cell ($P\bar{6}2m$, $Z = 3$) with two different kinds of SiO₉ tricapped trigonal prisms
- Those polyhedra are fairly regular. This makes the structure more stable than Cot.



SiO₂ Quartz

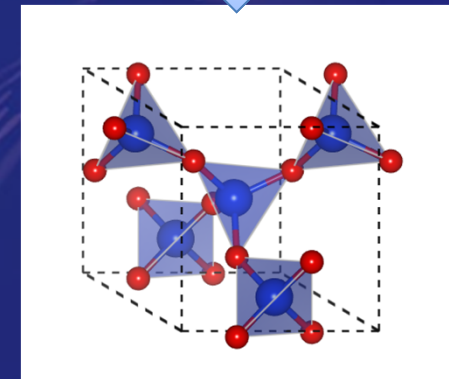
Tsuchiya & Tsuchiya (2011) PNAS



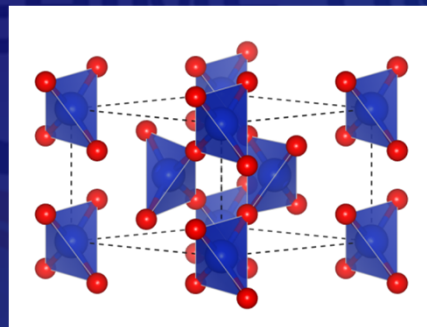
Qz



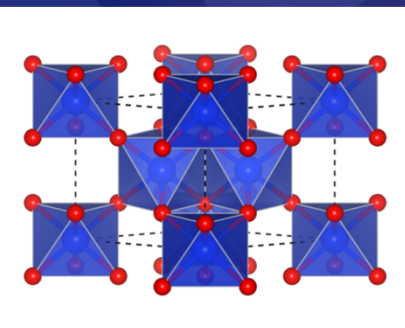
Fe₂P



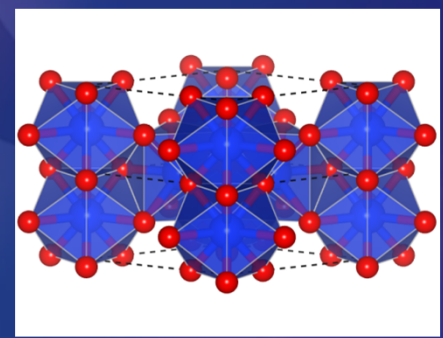
(1) Quartz
 SiO_4



(2) P2
(metastable)
 SiO_{4+6}

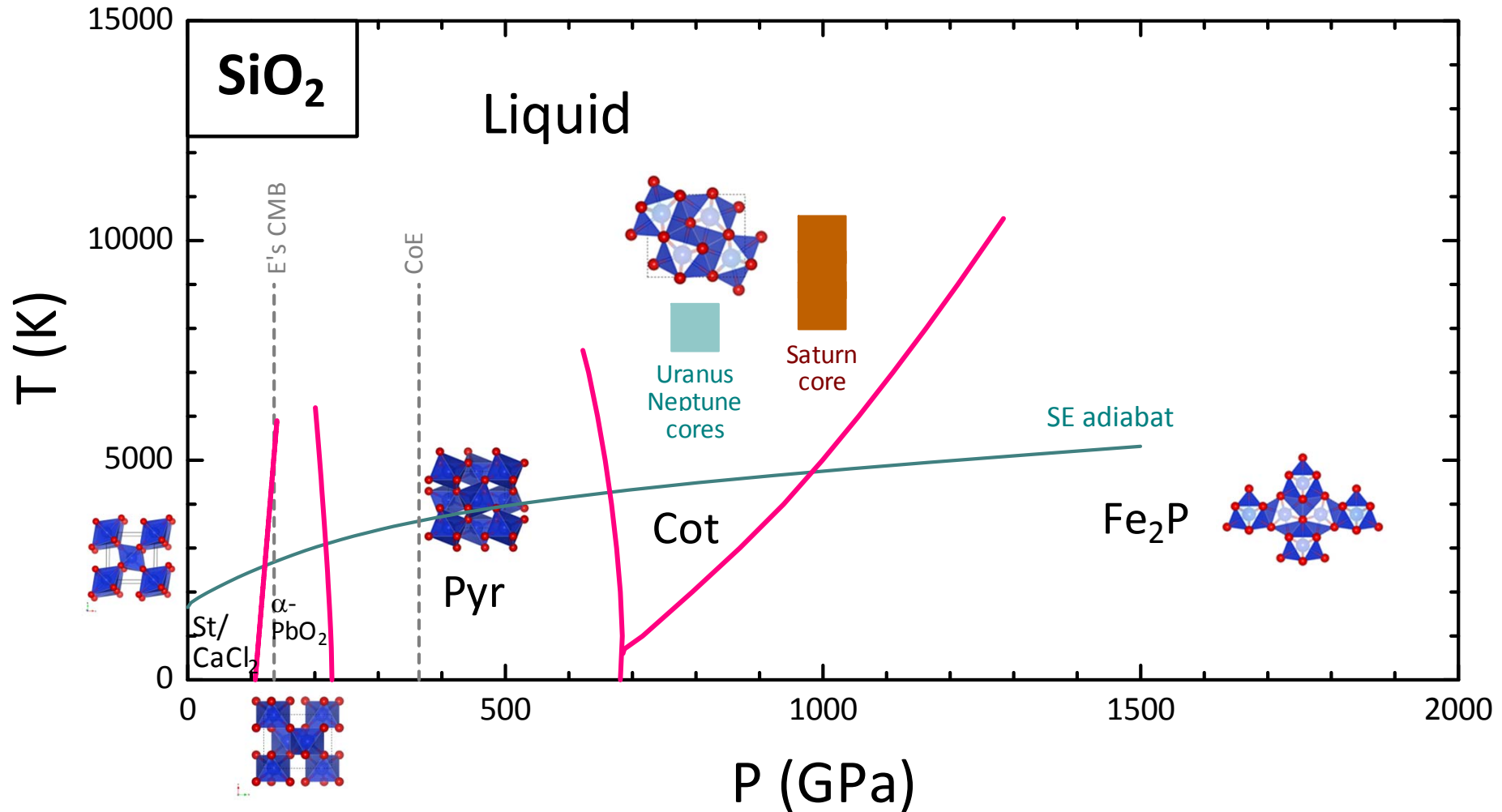


(3) Li₂ZrF₆-type
(metastable)
 SiO_6



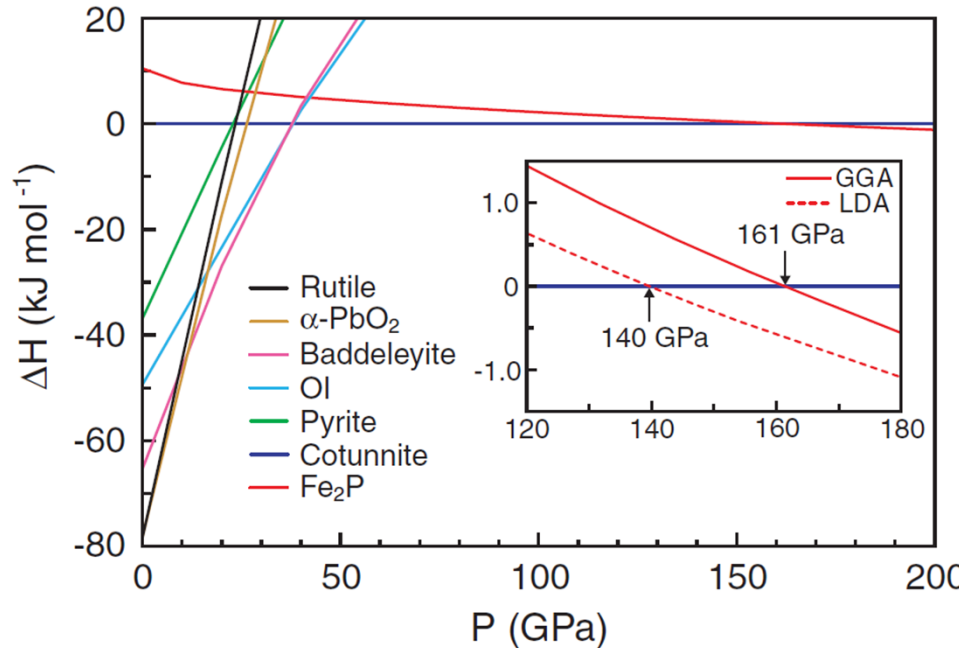
(4) Fe₂P-type
(stable >~700 GPa)
 SiO_9

Ultrahigh- P,T phase relations in SiO_2



Tsuchiya & Tsuchiya (2011) PNAS

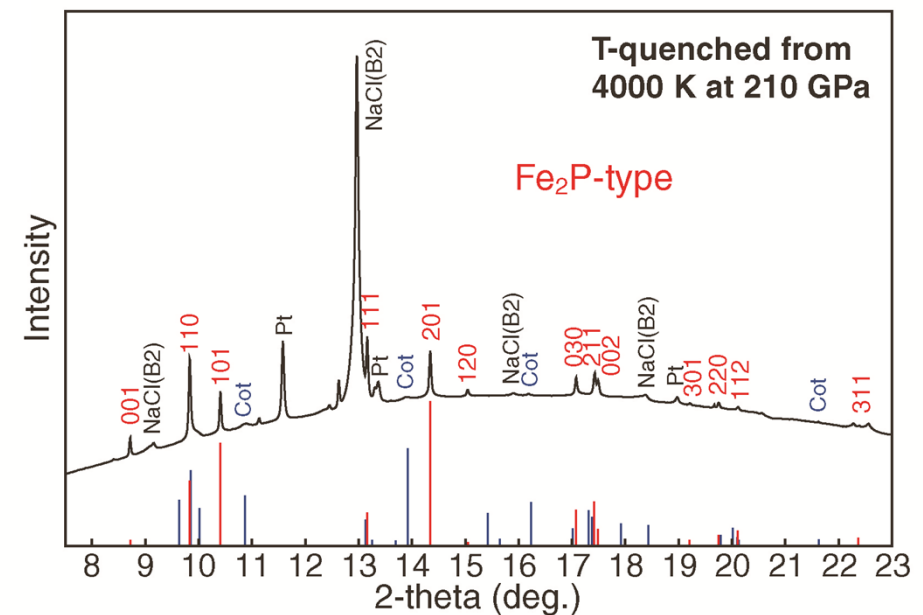
Experimental confirmation using a low- P analog, TiO_2



Successful experimental identification by LH-DAC at SPring-8



Low-transition pressure from cotunnite-type to Fe_2P -type at ~150 GPa and 0 K



Dekura, Tsuchiya+ (2011) PRL

Experimental confirmation

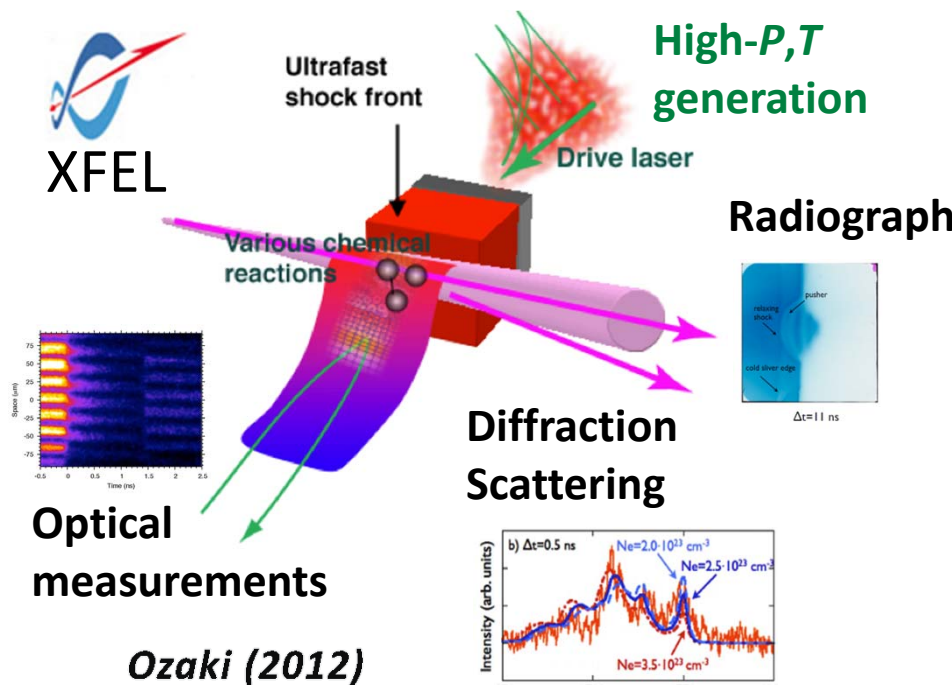
- Laser shock technique
- Magnetic shock (Z-machine)

USA, France, ...

A new project in Japan at Spring-8



XFELとパワーレーザーによる
新極限物質材料の探索



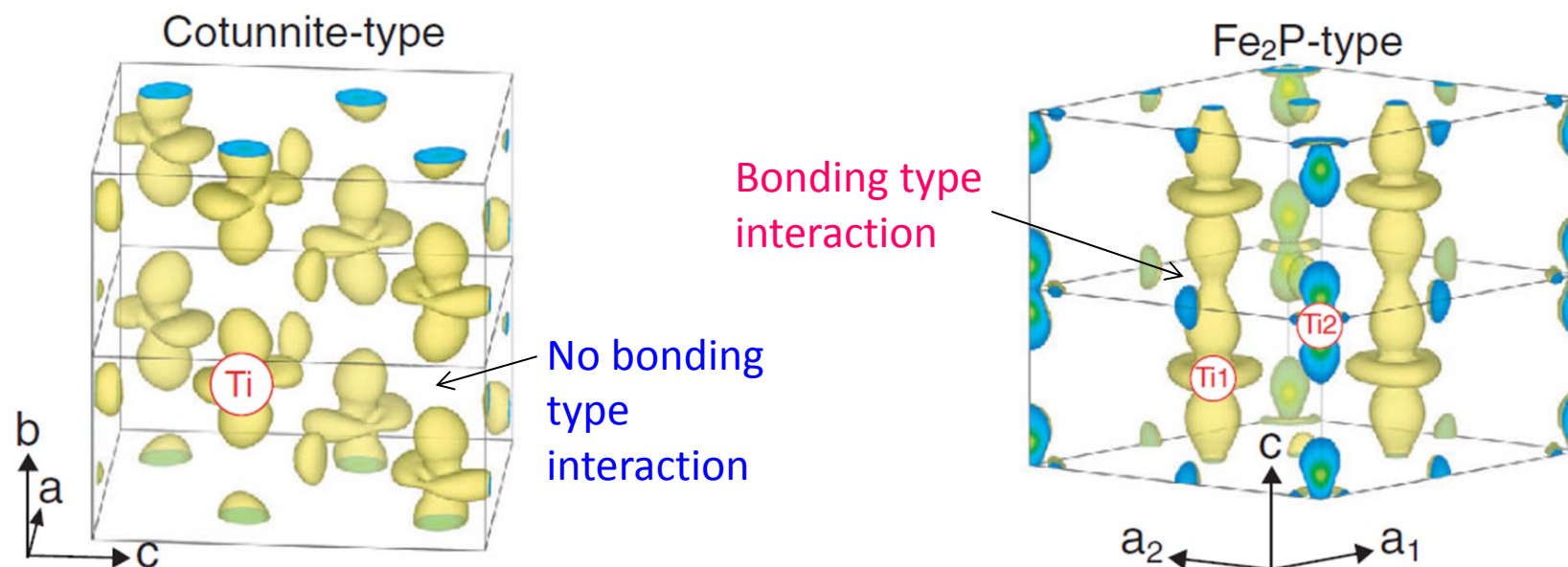
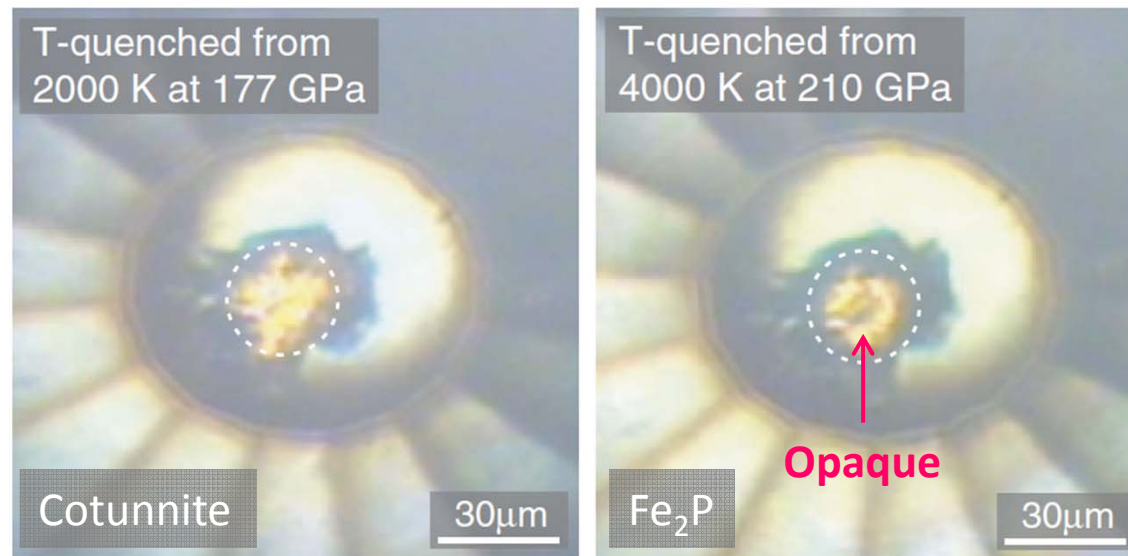
K. Tanaka, N. Ozaki, O. Sakata,
T. Tsuchiya, T. Sano, T. Sekine,
K. Arakawa, ... (>20 people)

Osaka Univ., NIMS, Ehime Univ., Hiroshima
Univ., Shimane Univ., ...

X-ray Free Electron Laser (XFEL)

In situ observation in TPa regime

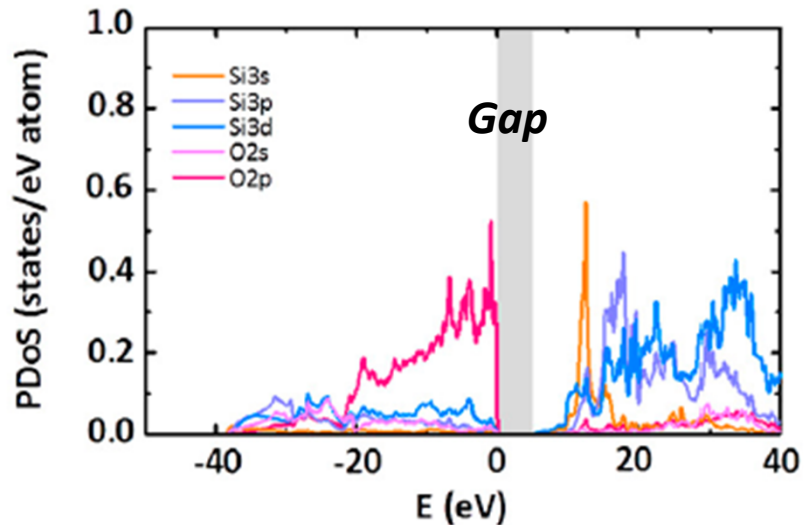
Significant optical absorption of Fe₂P-typ TiO₂



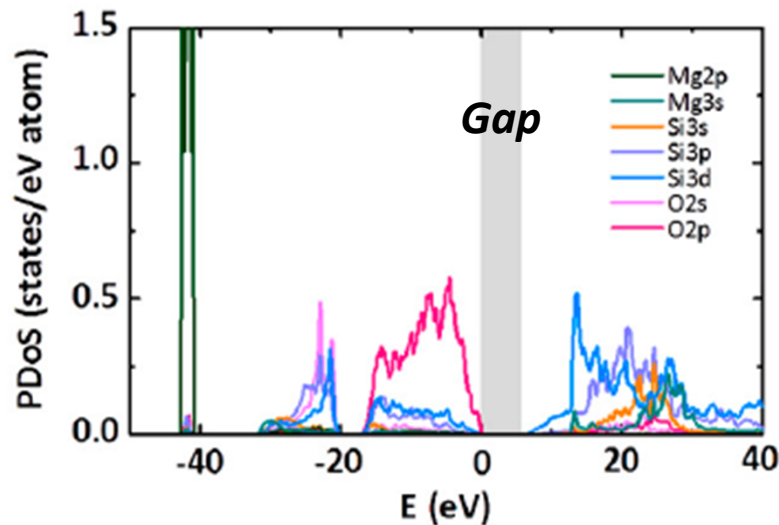
Electronic density of states

T Tsuchiya, 9th ISPS, 25 June 2012
Tsuchiya & Tsuchiya (2011) PNAS

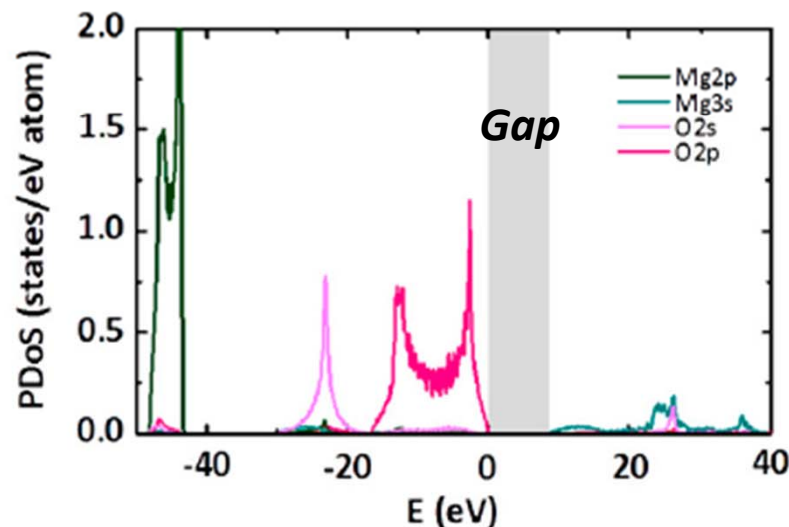
Fe₂P-SiO₂ 1.5 TPa



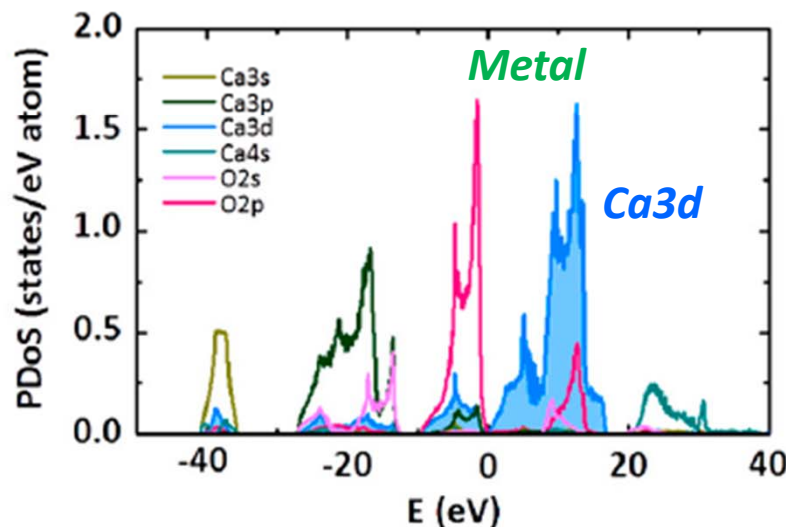
pPv-MgSiO₃ 1.0 TPa

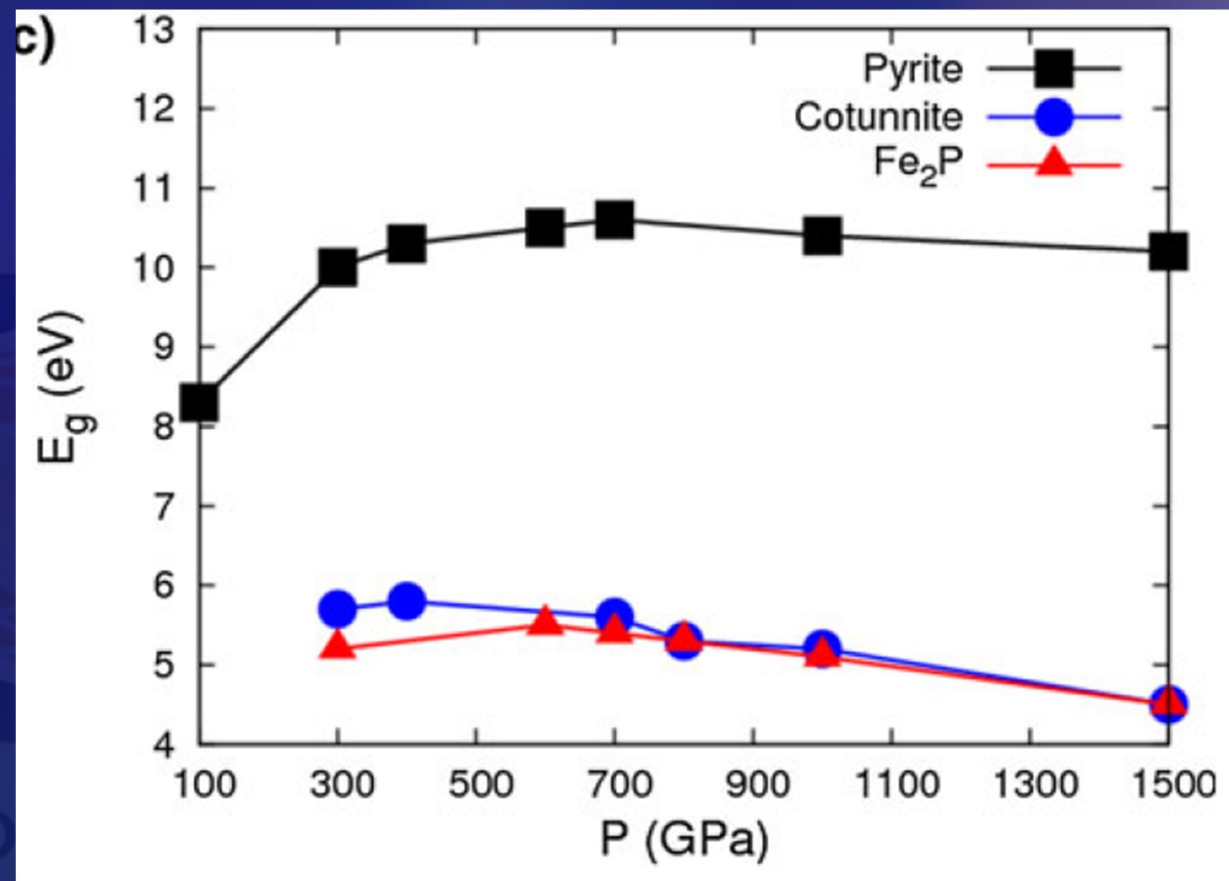


B2-MgO 1.5 TPa



B2-CaO 0.4 TPa

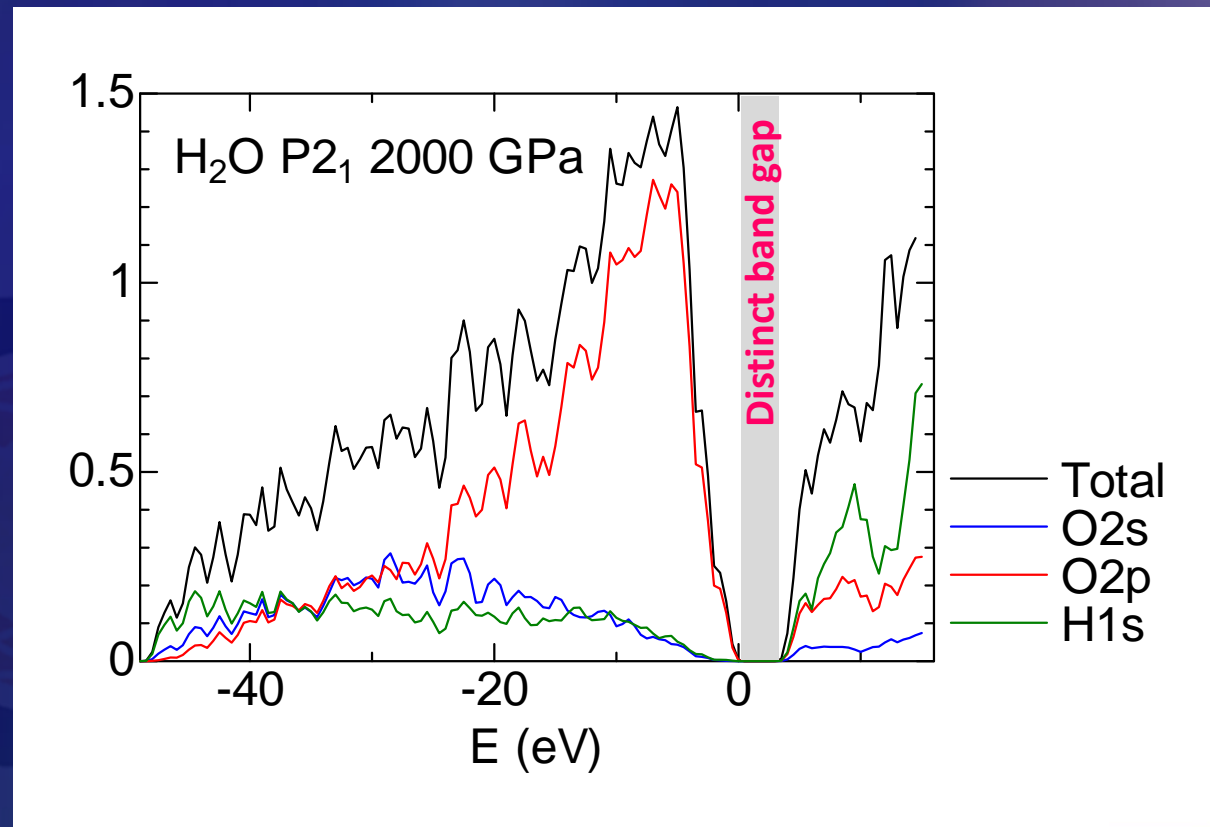


Band gap vs pressure in SiO_2 phases

Metsue & Tsuchiya (2012) Phys Chem Min

Fe_2P -type SiO_2 has much smaller gap than Pyr
but still remains insulating even above 1 TPa.

P2₁-type H₂O ice electronic DoS

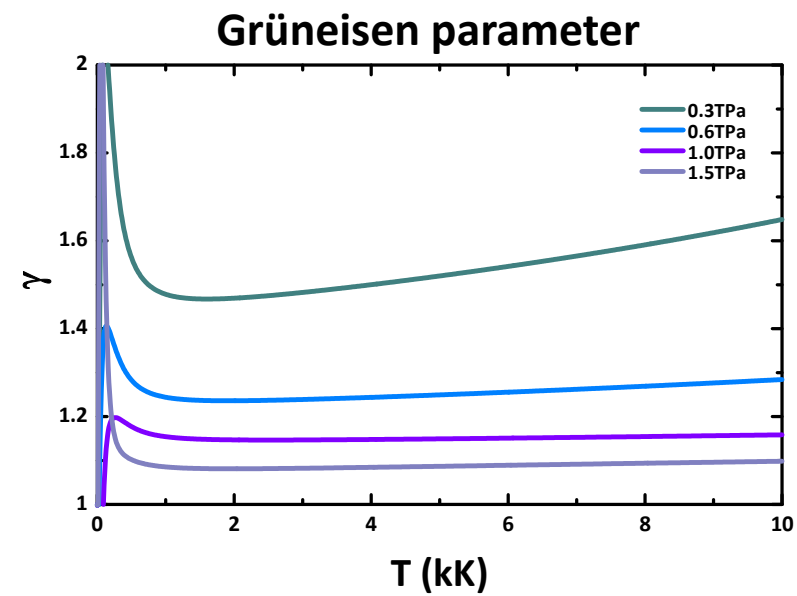
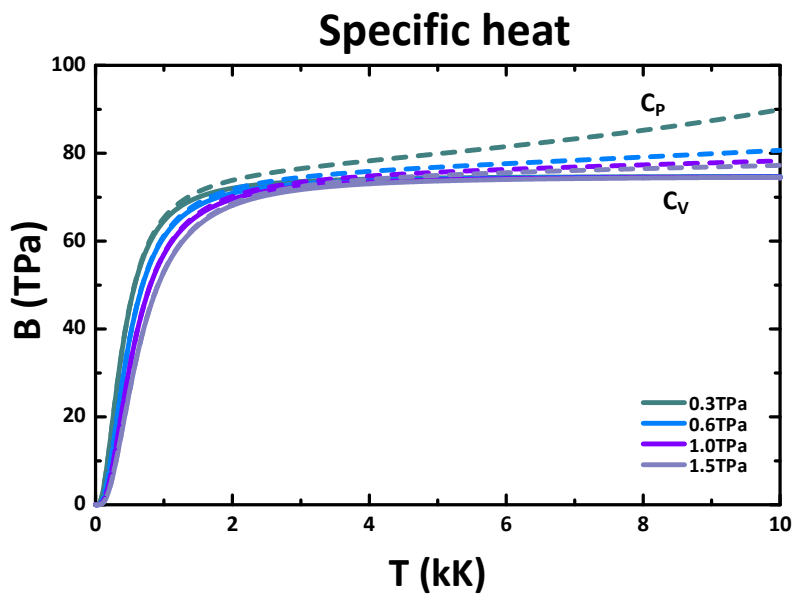
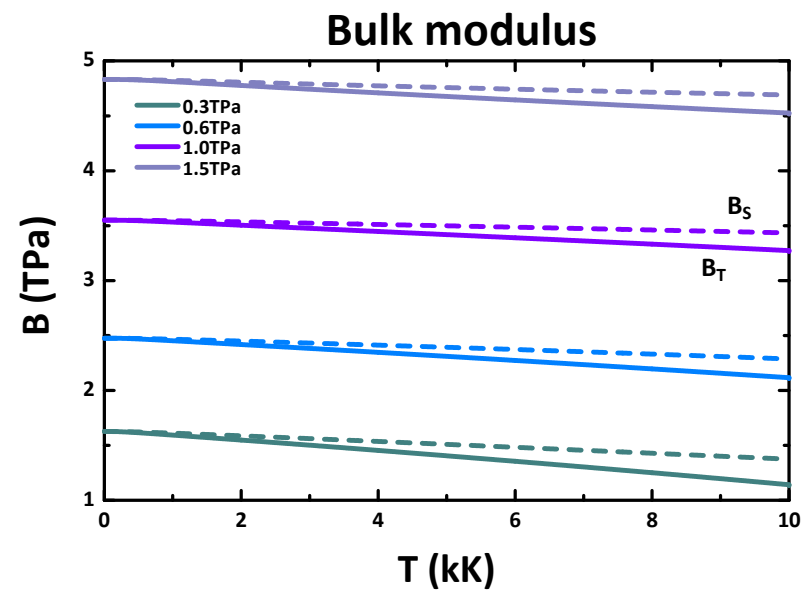
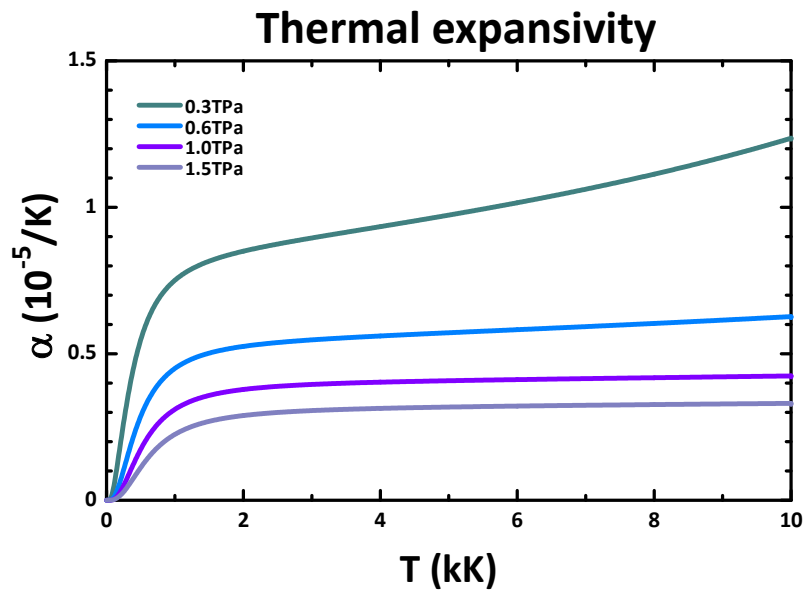


GEODYNAMICS RESEARCH CENTER
Hermann+ 2012 PNAS
J. Tsuchiya, unpub.

Ice also still remains insulating even at 2 TPa.

Metallization in solids only for compounds with heavy (*d*) metals

Thermodynamic properties of Fe₂P-type SiO₂



Tsuchiya & Tsuchiya (2011)

Modeling of the silica-rich planetary mantle

Density

Gravity

Mass

Pressure

$$\frac{d\rho}{dr} = \frac{\rho(r)g(r)}{\phi(r)}$$

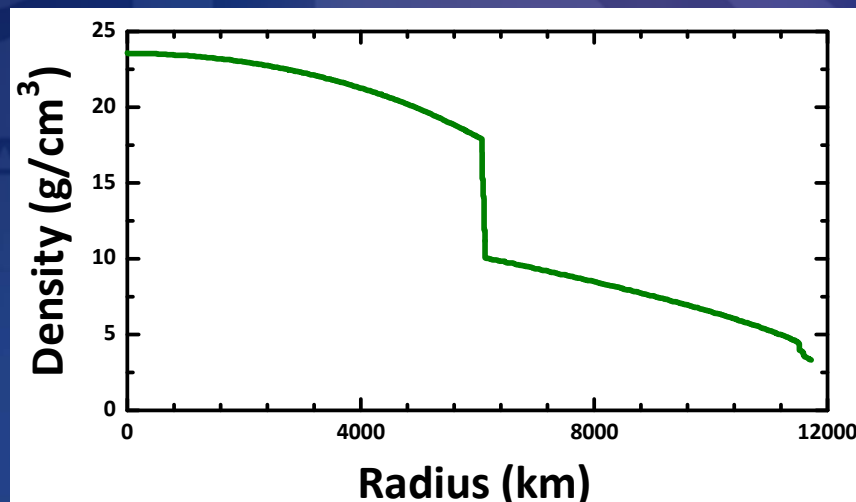
$$\frac{dg}{dr} = 4\pi G\rho(r) - \frac{2Gm(r)}{r^3}$$

$$\frac{dm}{dr} = 4\pi r^2 \rho(r)$$

$$\frac{dP}{dr} = -\rho(r)g(r)$$

$$\phi(r) = B_S(r)/\rho(r)$$

The $\rho - r$ relationship for a super-Earth with $10M_\oplus$ evaluated by *Valencia+ (2006)*

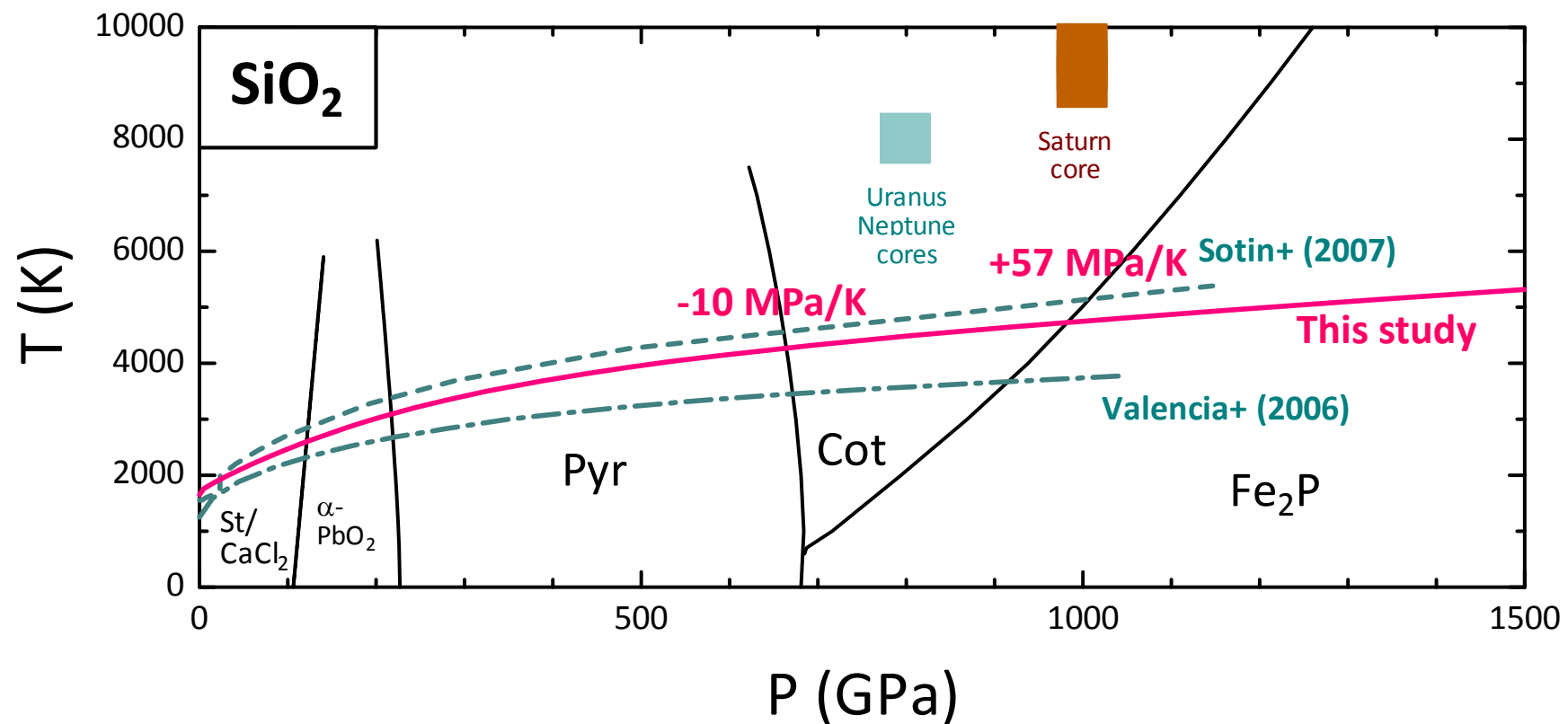


Thermal structure of SE

Adiabatic temperature gradient

$$\left(\frac{dT}{dP}\right)_S = \frac{\alpha(P)g(P)T}{C_P(P)}$$

Almost no difference by using MgSiO_3 parameters



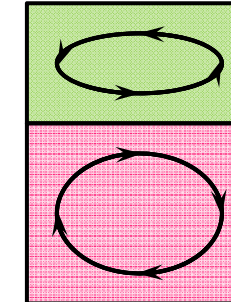
Phase transition buoyancy parameter

T Tsuchiya, 9th ISPS, 25 June 2012
Christensen and Yuen (1985)

$$P_h = \frac{\Gamma(\Delta\rho/\rho)}{\alpha\rho gh}$$

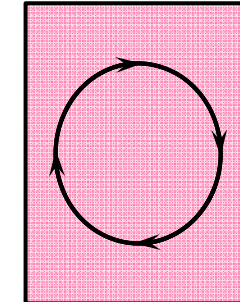
For 660-km discontinuity, $P_h \sim -0.2$

Negatively large P_h



Layered convection

Small or positive P_h



Whole convection

For the Pyr-Cot transition in a super-Earth with $10M_{\oplus}$:

$$\begin{aligned}\Gamma &= -10 \text{ MPa K}^{-1} \\ \frac{\Delta\rho}{\rho} &= 0.04 \\ \rho &= 8400 \text{ kg m}^{-3} \\ \alpha &= 0.53 \times 10^{-5} \text{ K}^{-1} \\ g &= 31 \text{ m s}^{-2} \\ h &= 4500 \text{ km}\end{aligned}$$

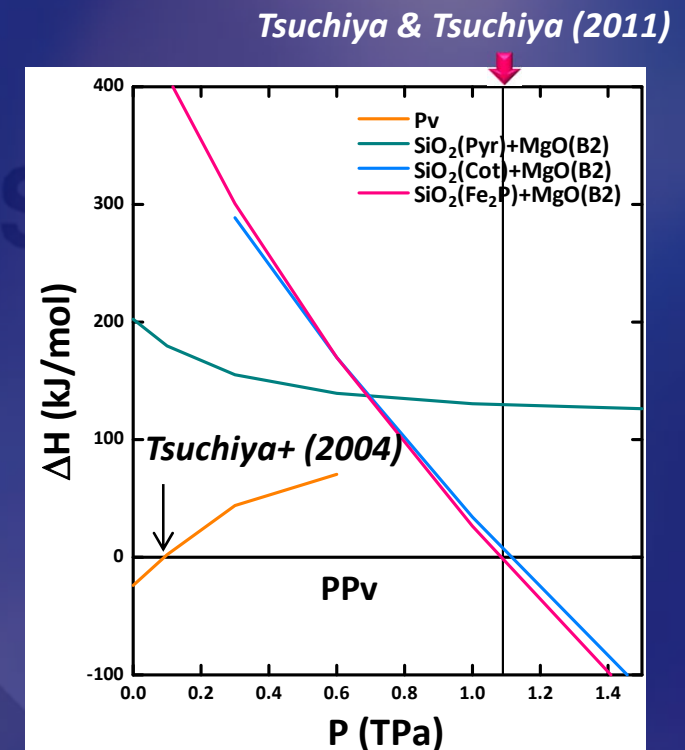
\Rightarrow

$$P_h \sim -0.064$$

The transition might have not so large effect even with a negative boundary.

Decomposition of MgSiO₃ post-perovskite

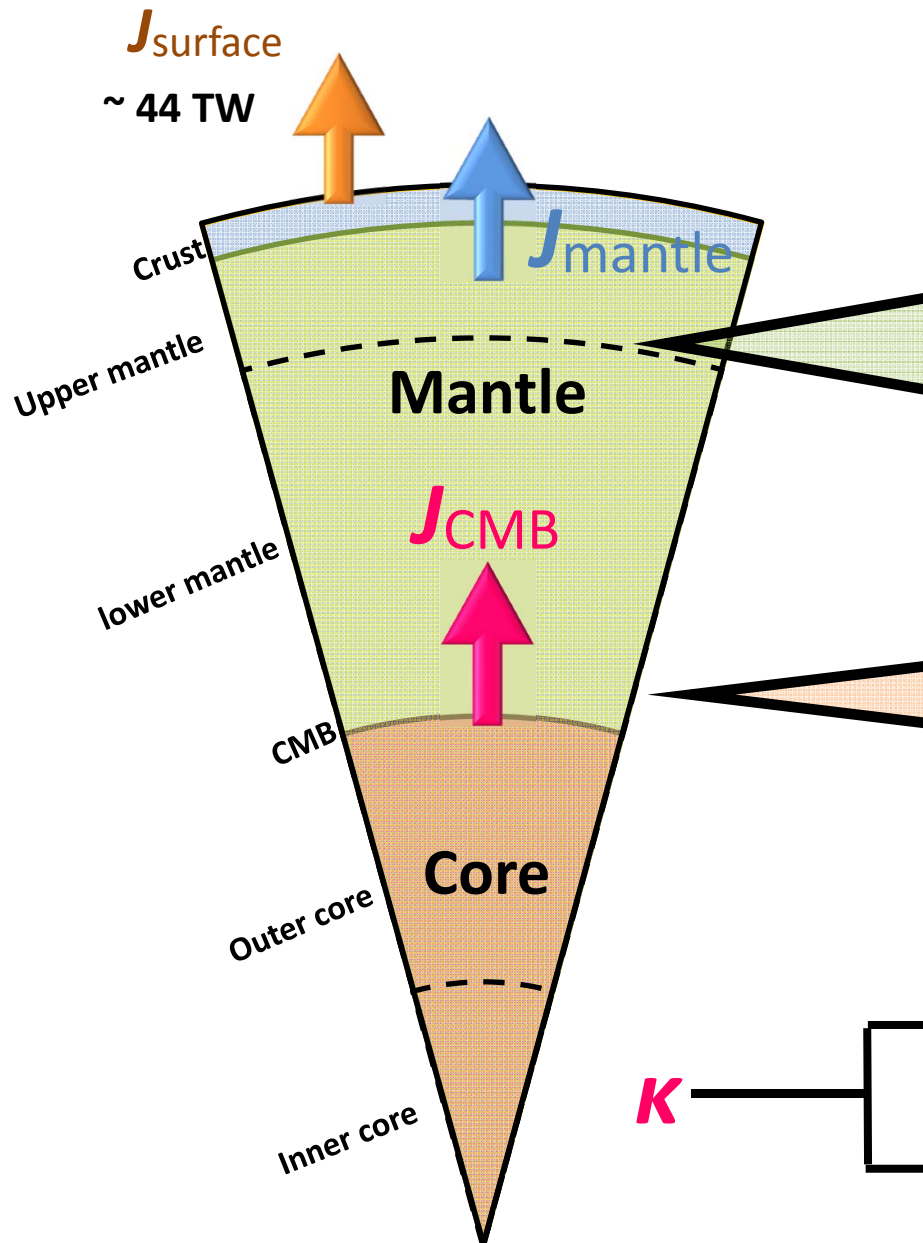
- ◆ MgSiO₃ (PPv) → MgO (B2) + SiO₂ (Cot or Fe₂P)
(Umemoto+ 2006;
Tsuchiya & Tsuchiya 2011)
- ◆ An intermediate state with MgSi₂O₅ + MgO
(Umemoto+ 2011)
- ◆ Disproportionation reaction in NaCoF₃
NaCoFe₃ (PPv) → Na₅Co₃F₁₁ + NaCo₃F₇
(Yusa+ 2012)



Further studies with careful structure search maybe needed

But no eccentric changes such as metallization seem likely.

Energy transportation in the Earth



Mantle convection

Rayleigh number

$$Ra = (\alpha g \Delta T C_p \rho^2 z^3) / (v K)$$

→ Convection style

CMB heat flux

$$q = -K \Delta T / \delta_{TBL}$$

$$J_{\text{CMB}} = \int q \, da$$

→ Geodynamo

→ Inner core growth

Lattice conductivity

Propagation of photon

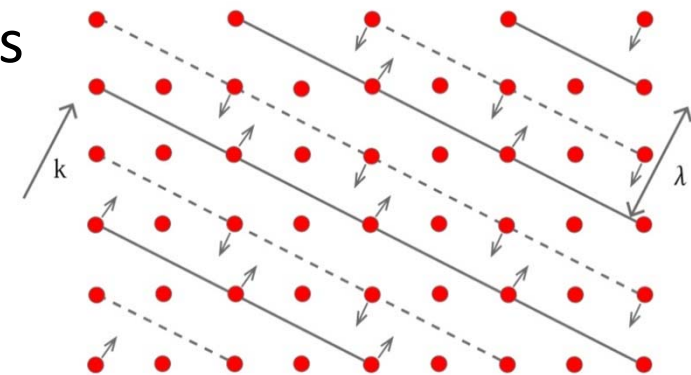
Radiative conductivity

Emission of photon

K

Lattice thermal conductivity

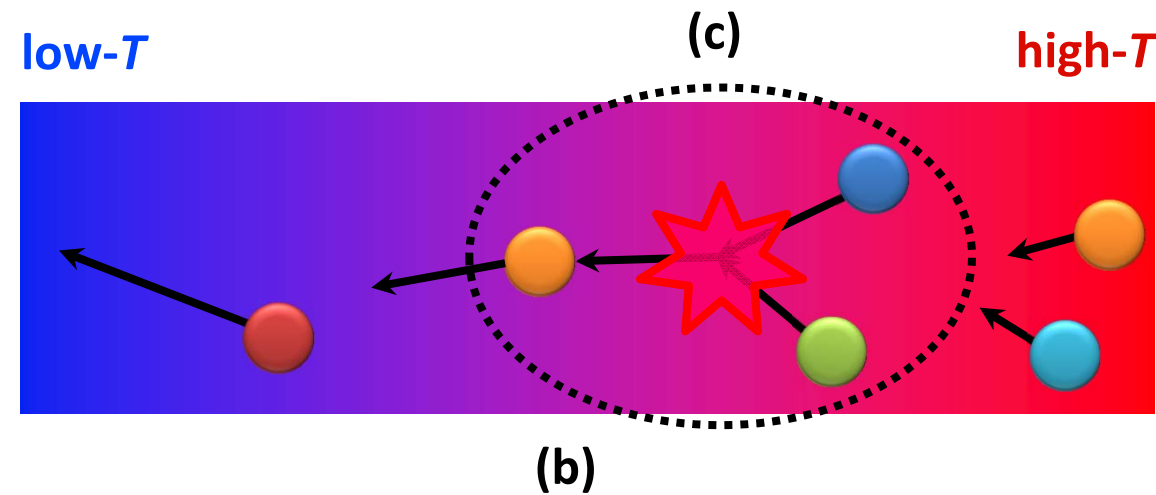
(a) Phonon = Quantized lattice vibrations



(b) Phonon-phonon scattering → Thermal resistivity

(c) Anharmonicity → Interaction of phonons

Density functional
perturbation theory
(DFPT)



Lattice thermal conductivity (Higher order anharmonic lattice dynamics)

$$\kappa = \frac{1}{3} \sum_s^{3n} \int v_{\mathbf{q},s}^2 c_{\mathbf{q},s} \tau_{\mathbf{q},s} d\mathbf{q}$$

Harmonic quantities

 $v_{\mathbf{q},s}$

Phonon group velocity

 $c_{\mathbf{q},s}$

Mode specific heat

Anharmonic phonon

Phonon lifetime

$$\tau_{\mathbf{q},s} = \frac{1}{2\Gamma(\omega_{\mathbf{q},s})}$$

Bose-Einstein function

$$n_{\mathbf{q}j} = \frac{1}{e^{\hbar\omega_{\mathbf{q}j}/k_B T} - 1}$$

Phonon damping function

$$\begin{aligned} \Gamma_{\mathbf{q}j}(\omega) = & \frac{\pi}{2} \sum_{\mathbf{q}', j', j''} [V_3(-\mathbf{q}j, \mathbf{q}'j', \mathbf{q}-\mathbf{q}'j'')] \times \\ & [1 + n_{\mathbf{q}'j'} + n_{\mathbf{q}-\mathbf{q}'j''}] \delta(\omega_{\mathbf{q}'j'} + \omega_{\mathbf{q}-\mathbf{q}'j''} - \omega) + 2[n_{\mathbf{q}-\mathbf{q}'j''} \\ & - n_{\mathbf{q}'j'}] \delta(\omega_{\mathbf{q}'j'} - \omega_{\mathbf{q}-\mathbf{q}'j''} - \omega) \}. \end{aligned}$$

 V_3 : anharmonic coupling coefficient

Previous works on K

Ab initio (non-equilibrium) molecular dynamics (MD), etc

- Large simulation cell size
- High computational cost

Limited to simple crystal structures like MgO

(de Koker 2009; Tang & Dong 2010; etc)

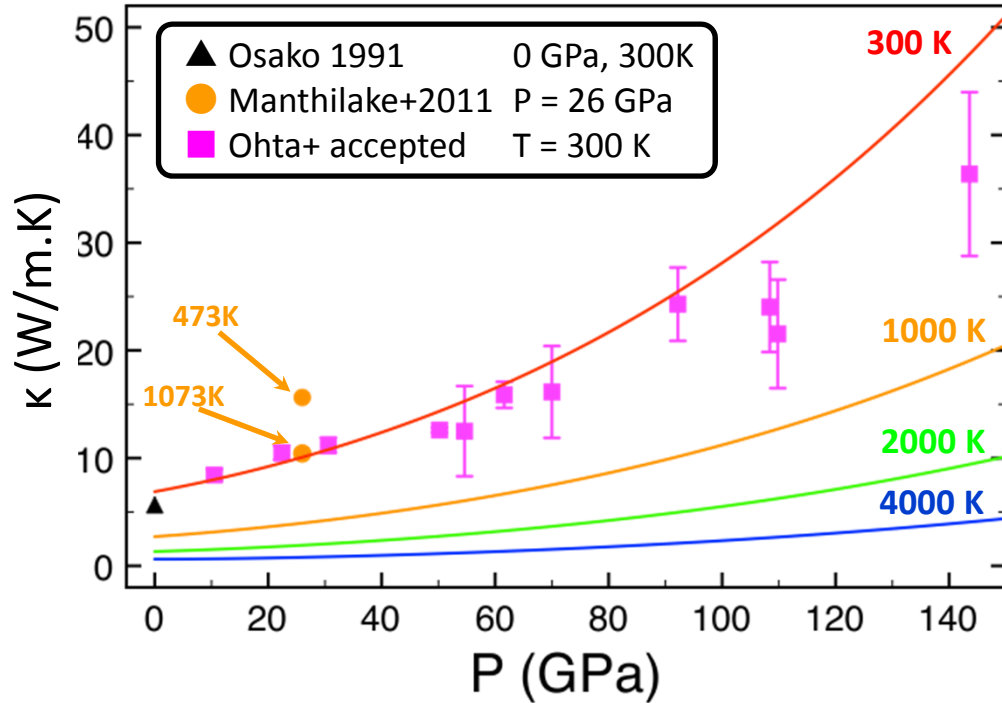
Our technique

DFPT approach

- Small (primitive) unit cell size
- High efficiency & low numerical error

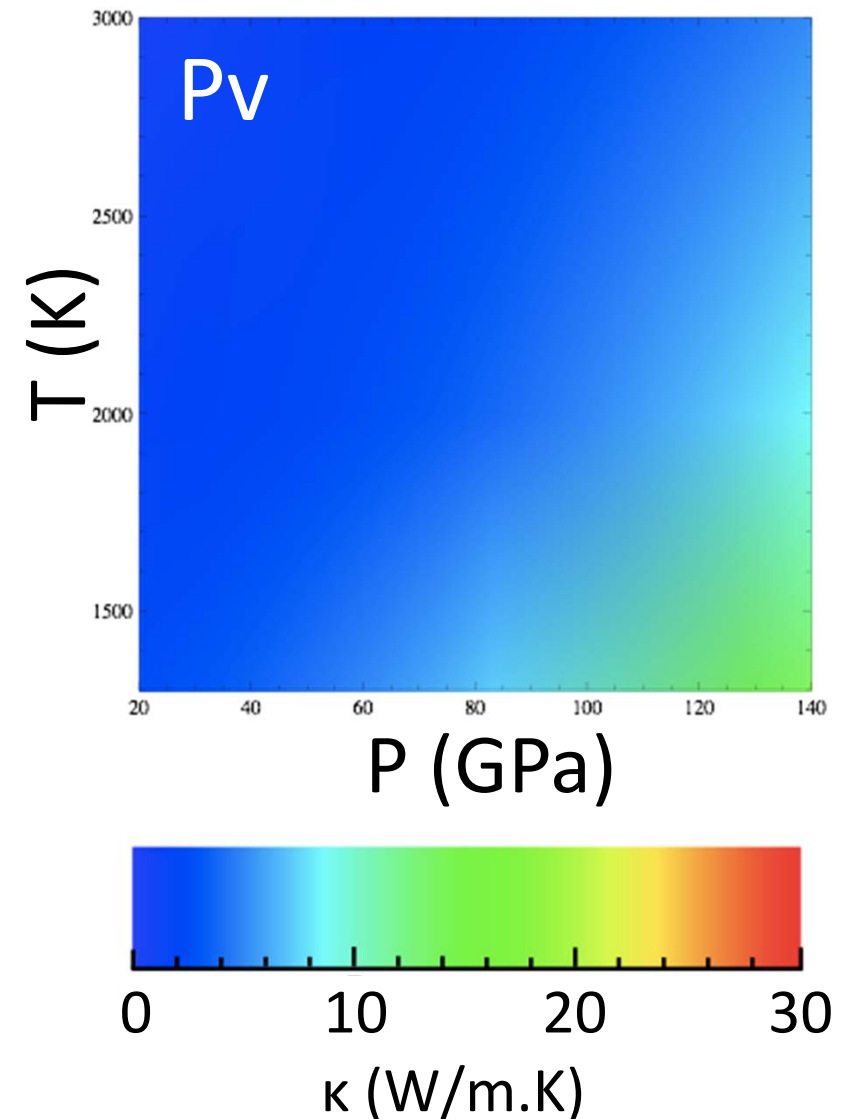
Applicable to complex structures like MgSiO₃

κ of MgSiO₃-Pv



Lattice thermal conductivity rapidly increase with increasing pressure.

$$\kappa_{\text{Pv}}(2900 \text{ km}) \sim 3 \kappa_{\text{Pv}}(660 \text{ km})$$



Rayleigh number of mantles

$$Ra = \alpha g \Delta T \rho^2 C_P Z^3 / (\nu \kappa)$$

Earth

$$\Delta T = 500 \text{ [K]}$$

$$\nu \sim 10^{21} - 10^{23} \text{ [Pa s]}$$

Mitrovica & Forte (2004)

$$\kappa \sim 2 - 7 \text{ [W m}^{-1}\text{K}^{-1}\text{]}$$

This study

Super-Earth with $10M_{\oplus}$

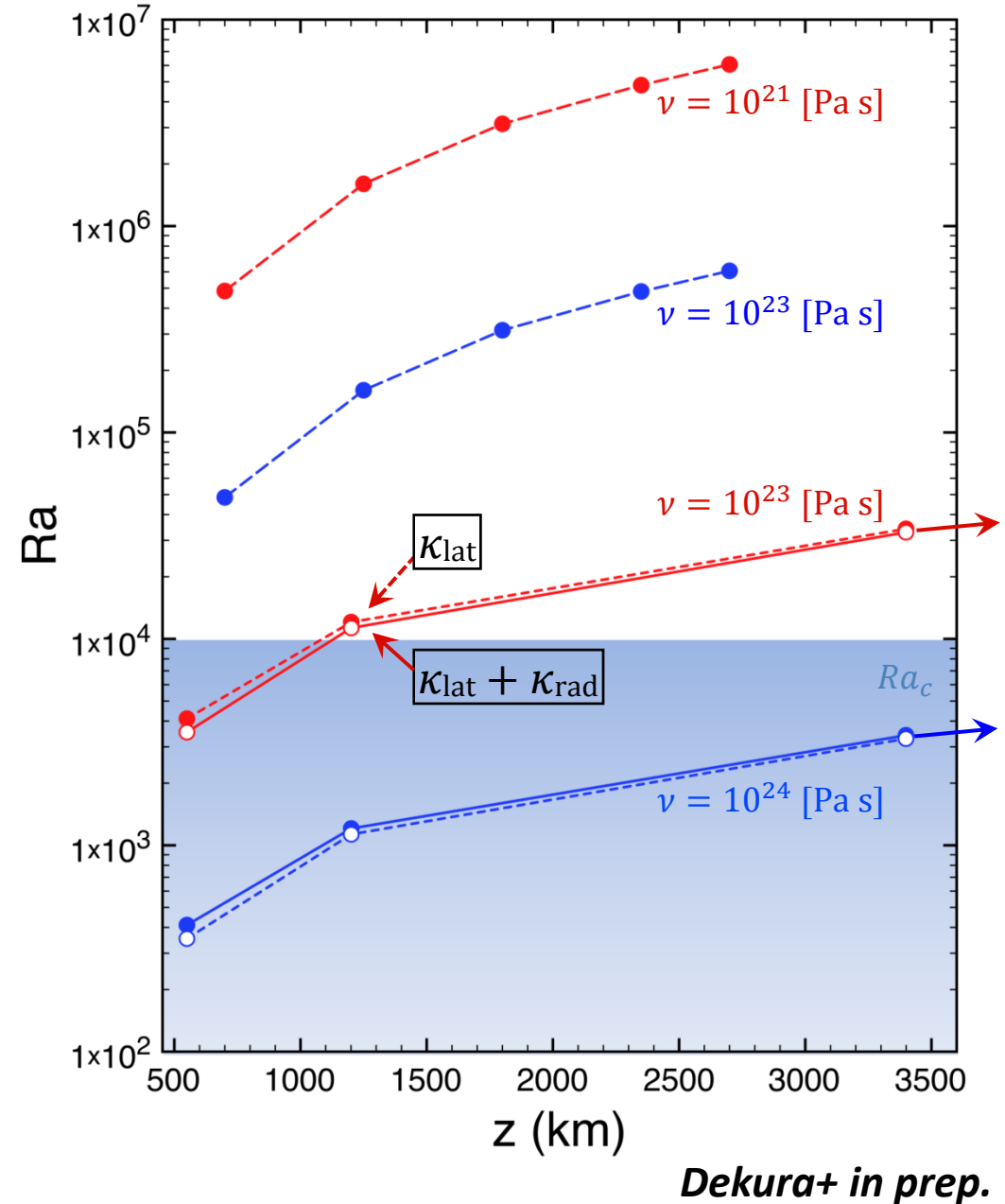
$$\Delta T = 500 \text{ [K]}$$

$$\nu \sim 10^{23} - 10^{24} \text{ [Pa s]}$$

$$\kappa \sim 4 - 200 \text{ [W m}^{-1}\text{K}^{-1}\text{]}$$

This study

⇒ Mantle convection maybe significantly suppressed
 (Consistent with a recent modeling by Stamenkovic+ 2011)



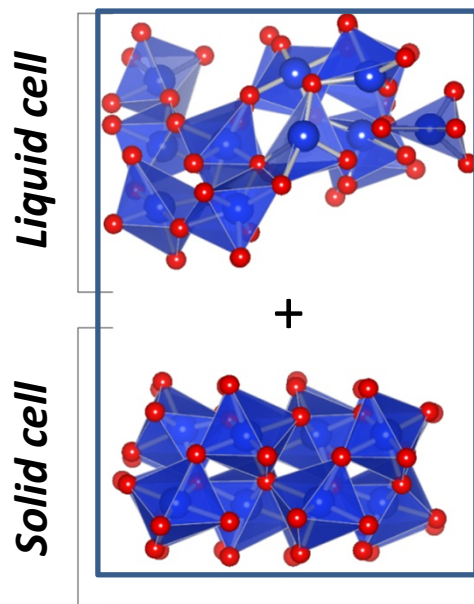
Melting temperature

Ab initio two-phase coexisting MD

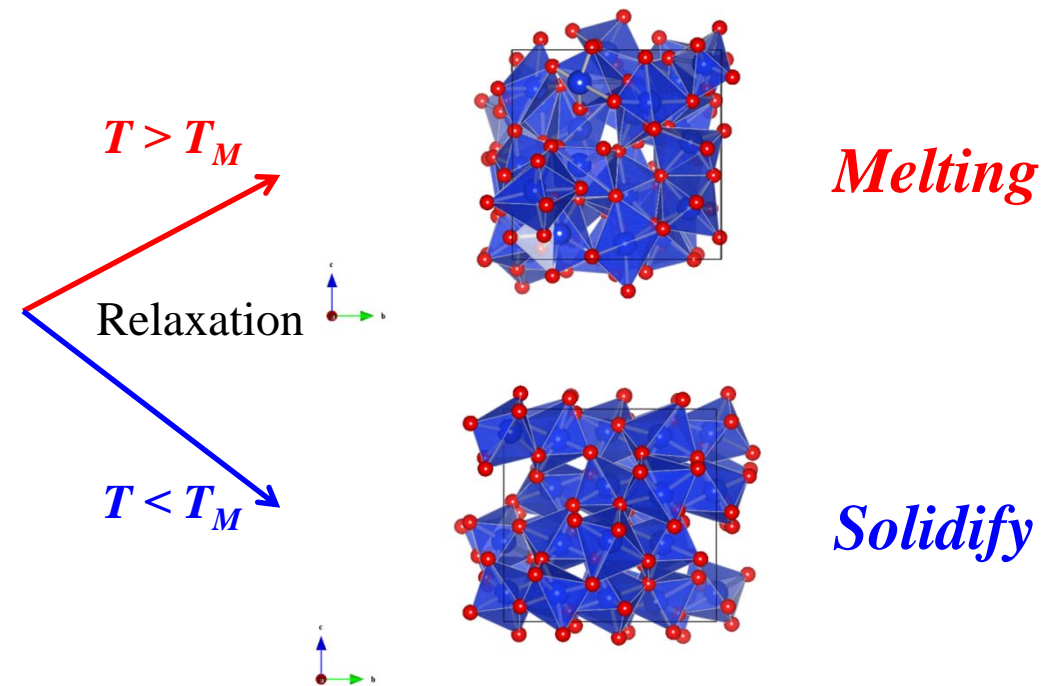
(Alfe 2009; Usui & Tsuchiya 2010; etc)

- Equilibrate a supercell with *Sol-Liq* interfaces at several P, T conditions
- A method to avoid the kinetic effects (super-cooling and -heating) across melting and freezing

Initial structure



Final structure



Ex) SiO_2 stishovite

a) $T > T_M$

Melt stable

$t = 1 \text{ fs}$
 $T = 5610 \text{ K}$
 $P = 79 \text{ GPa}$

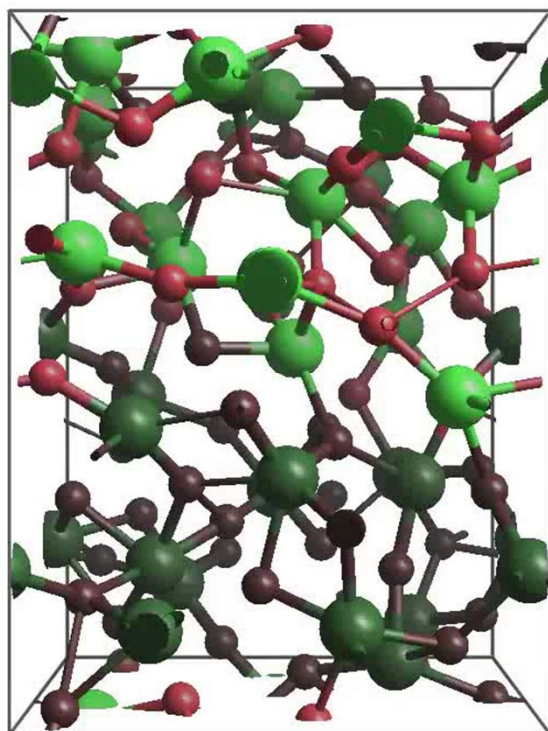
Si

O

Si

O

z
 x

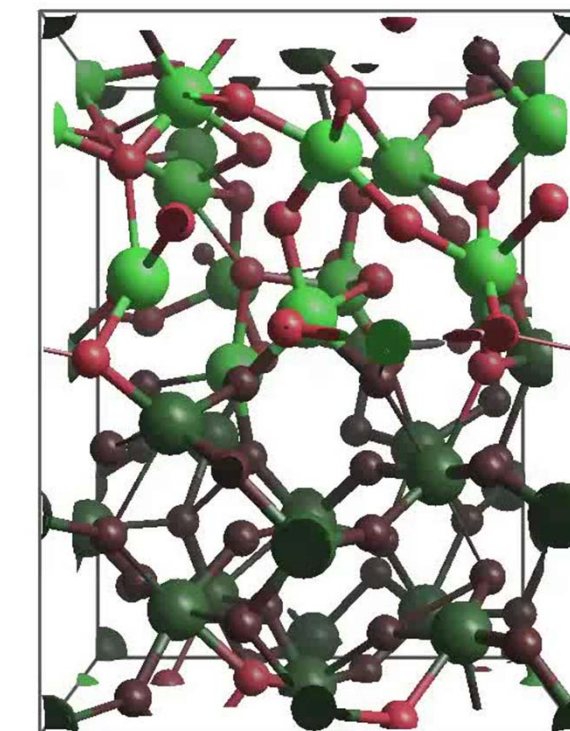


$P = 73 \text{ GPa}, T = 5,600 \text{ K}$

b) $T < T_M$

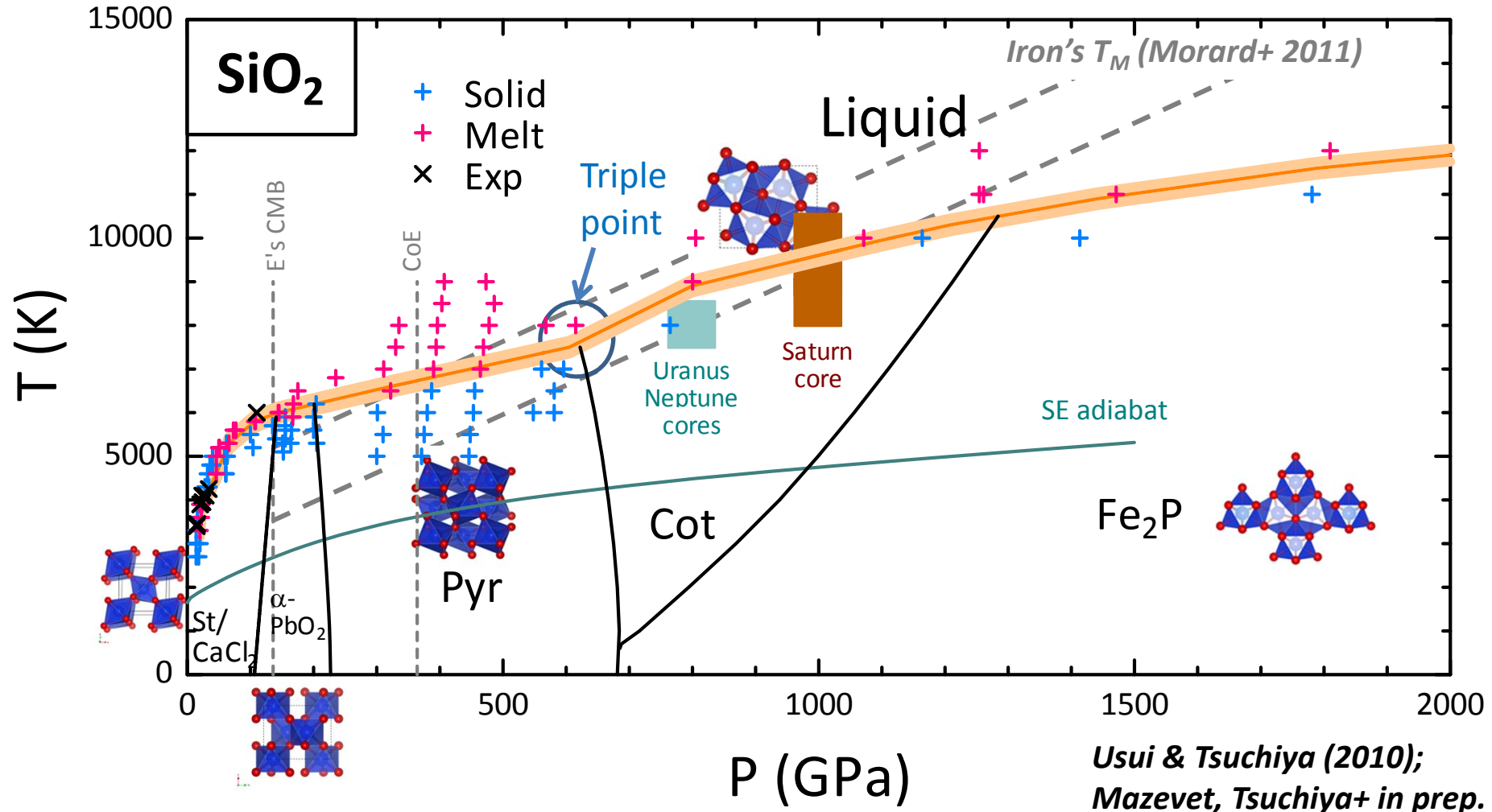
Solid stable

$t = 1 \text{ fs}$
 $T = 5306 \text{ K}$
 $P = 68 \text{ GPa}$



$P = 62 \text{ GPa}, T = 5,300 \text{ K}$

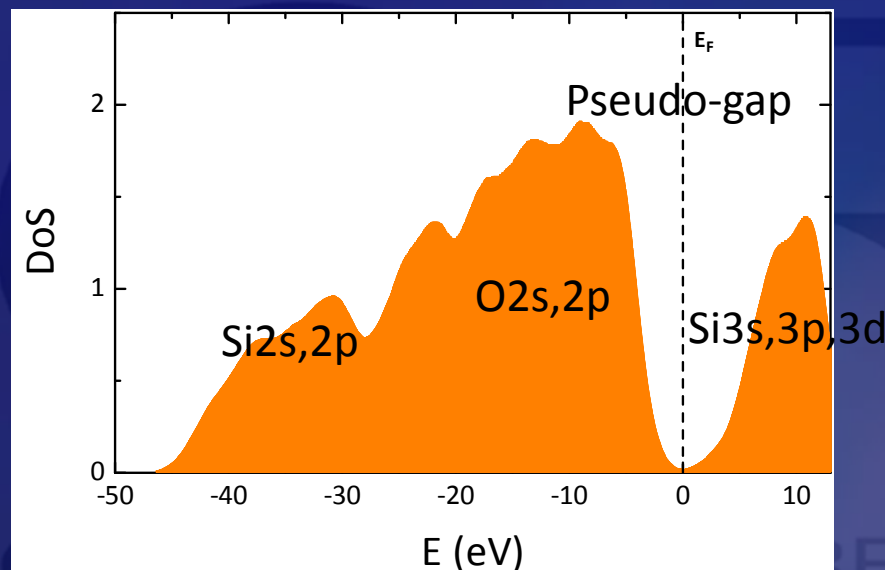
Melting curve of SiO_2



T_M quite comparable to the core conditions of some planets

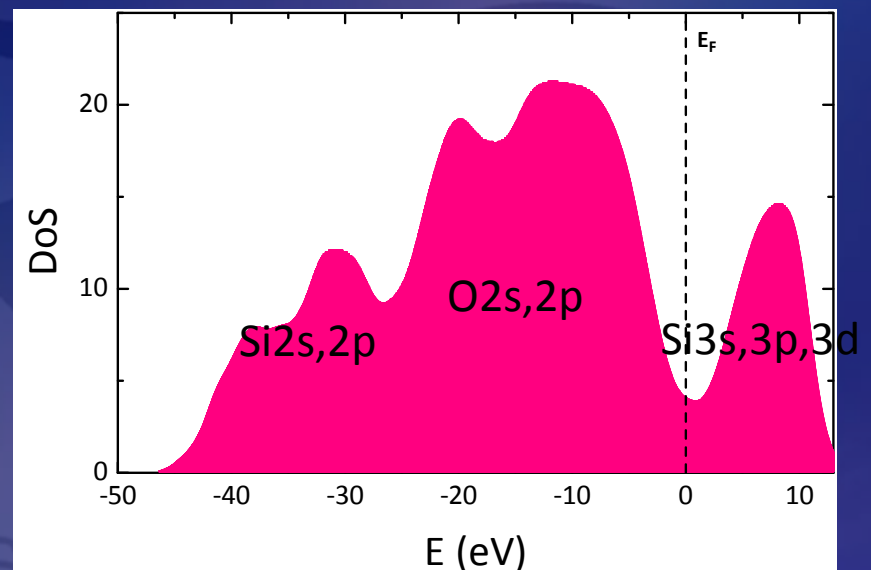
Electronic DoS of silicate melt

Subsolidus condition
(1800 GPa, 10000 K)
Fe₂P-type SiO₂



Semi-metallic

Supersolidus condition
(1800 GPa, 12000 K)
Liquid SiO₂

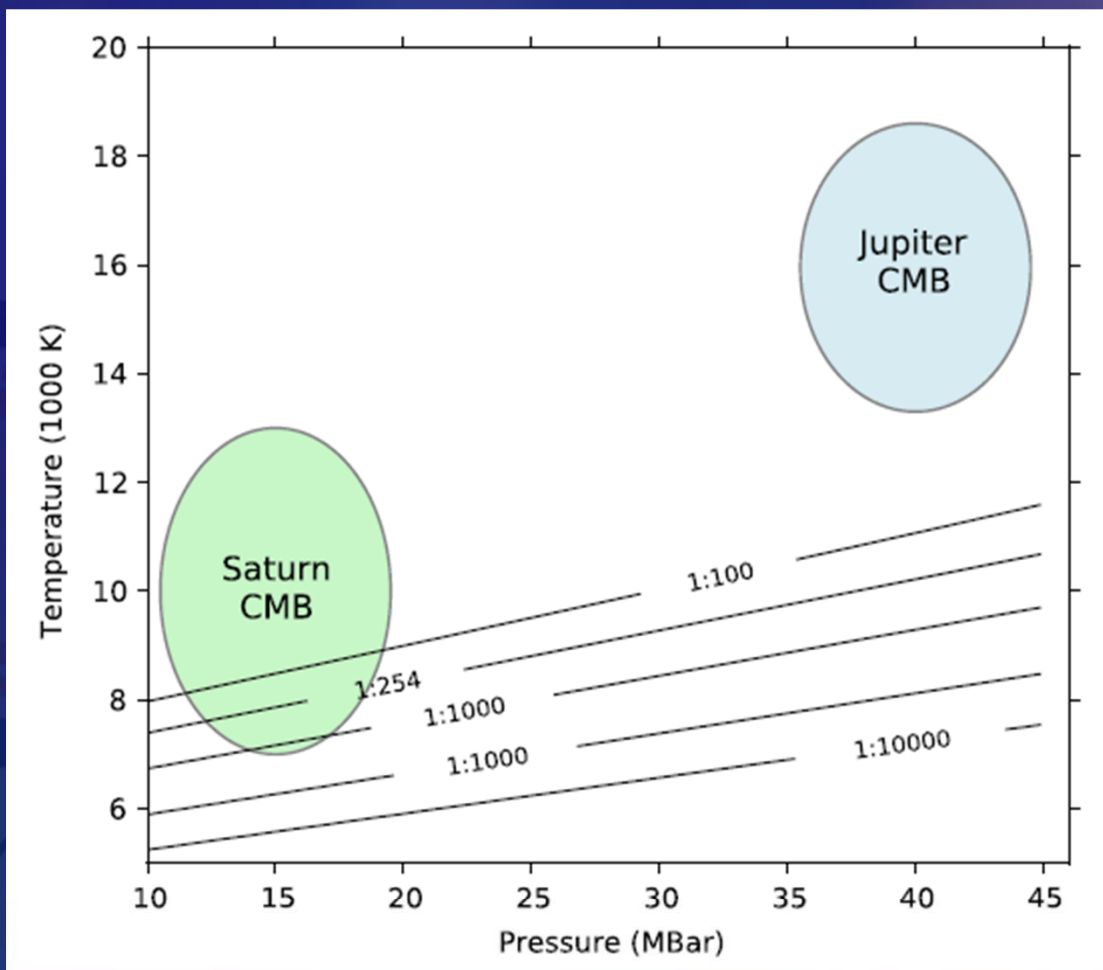


Metallic

Metallization (band gap closure) across melting (cf. Karki 2007 PRB)

Liquid silicate maybe easily mix with H or H₂O. → Core erosion (cf. Wilson+ 2012 PRL)

Solubility of oxide into liquid H

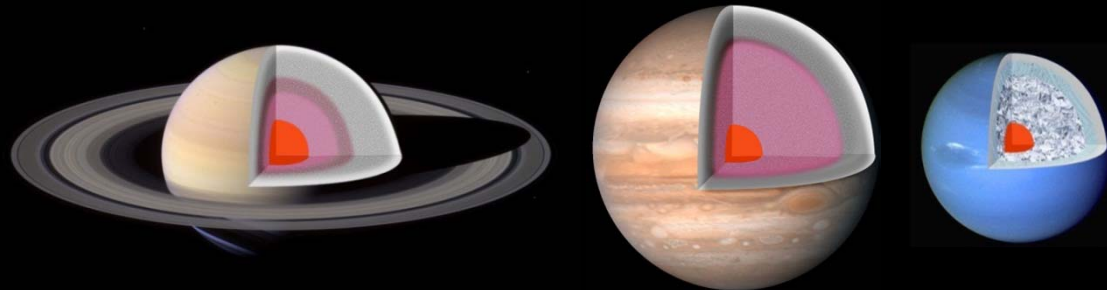


Wilson & Militzer (2012) PRL

Oxides soluble to liquid H at $T_{\text{gass giant}}$ but not at T_{SE}

Current views

Gas & ice planets



- Molten metallic rocky core
- Liquid iron core



Active interior
Core erosion

Super-Earths



- Solid insulating thermally well conductive rocky mantle
- Solid iron core



Less active interior

EHIME UNIVERSITY



GEODYNAMICS RESEARCH CENTER

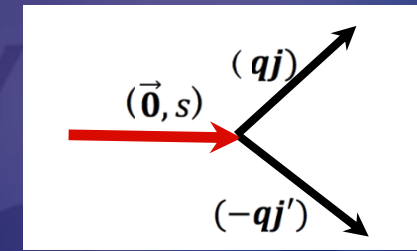
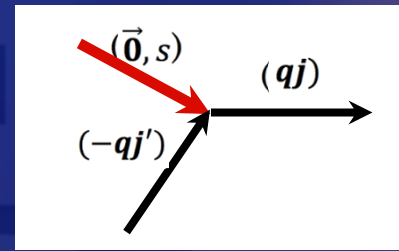
EHIME UNIVERSITY



GEODYNAMICS RESEARCH CENTER

Lattice thermal conductivity (Higher order anharmonic lattice dynamics)

$$\kappa = \frac{1}{3} \sum_s^{3n} \int v_{\mathbf{q},s}^2 c_{\mathbf{q},s} \tau_{\mathbf{q},s} d\mathbf{q}$$



Anharmonic phonon

Phonon lifetime

$$\tau_{\mathbf{q},s} = \frac{1}{2\Gamma(\omega_{\mathbf{q},s})}$$

Bose-Einstein function

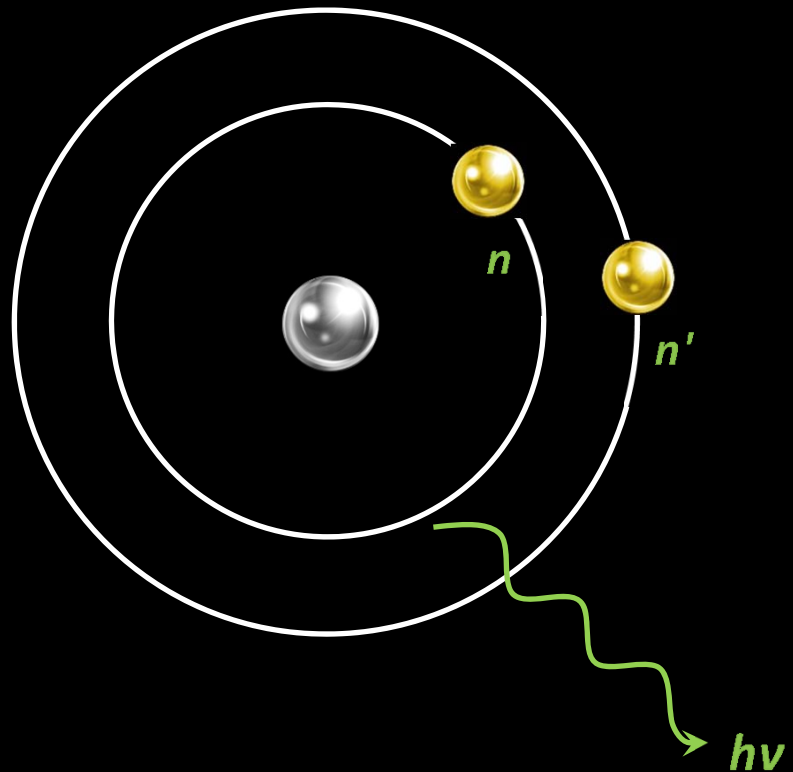
$$n_{\mathbf{q}j} = \frac{1}{e^{\hbar\omega_{\mathbf{q}j}/k_B T} - 1}$$

Phonon damping function

$$\begin{aligned} \Gamma_{\mathbf{q}j}(\omega) = & \frac{\pi}{2} \sum_{\mathbf{q}', j', j''} [V_3(-\mathbf{q}j, \mathbf{q}'j', \mathbf{q}-\mathbf{q}'j'')] \times \\ & [1 + n_{\mathbf{q}'j'} + n_{\mathbf{q}-\mathbf{q}'j''}] \delta(\omega_{\mathbf{q}'j'} + \omega_{\mathbf{q}-\mathbf{q}'j''} - \omega) + 2[n_{\mathbf{q}-\mathbf{q}'j''} \\ & - n_{\mathbf{q}'j'}] \delta(\omega_{\mathbf{q}'j'} - \omega_{\mathbf{q}-\mathbf{q}'j''} - \omega) \}. \end{aligned}$$

V₃: anharmonic coupling coefficient

Bohr-Sommerfeld quantization condition



$$\nu \propto \frac{1}{n^2} - \frac{1}{n'^2}$$

$$l = m_e v r = n \hbar$$

$$n = 1, 2, 3, \dots$$

\hbar : Plank constant

l is discrete, not constant.

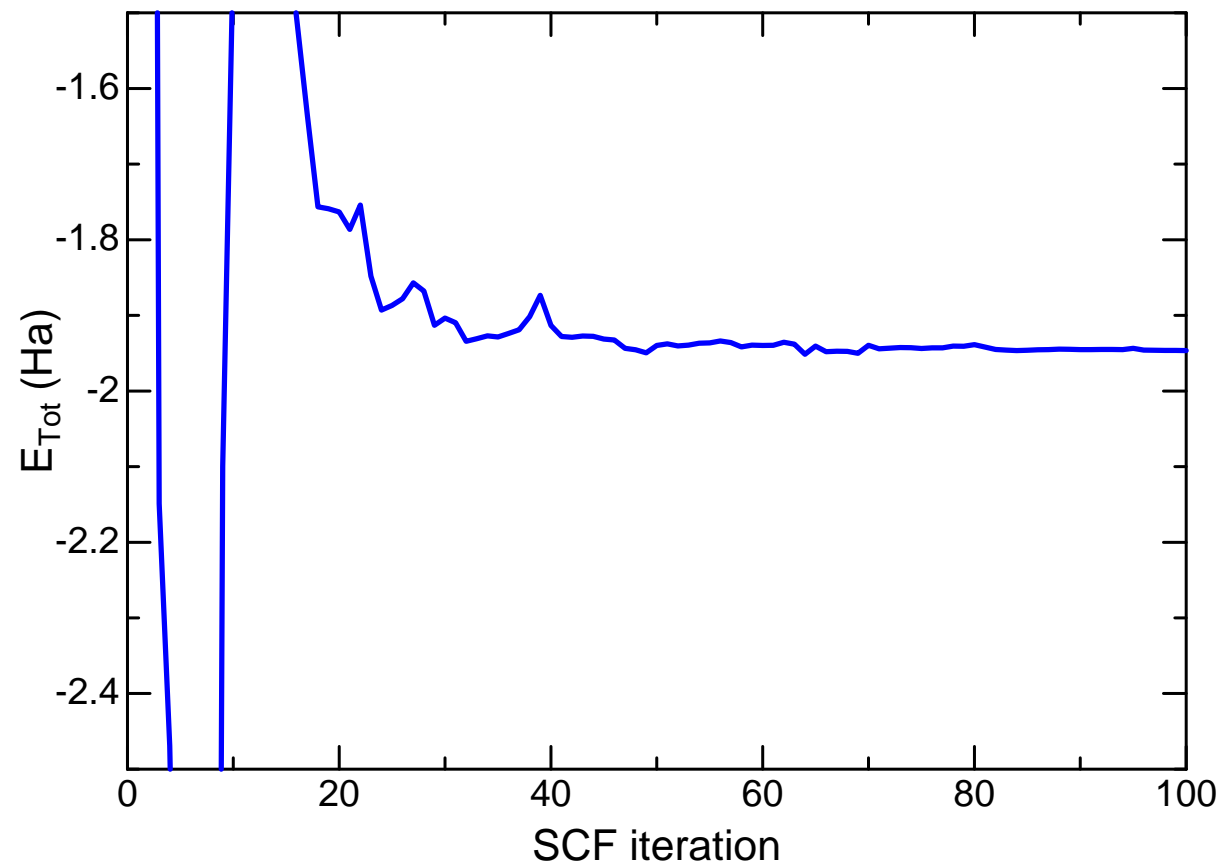


$$\oint p dq = n \hbar$$

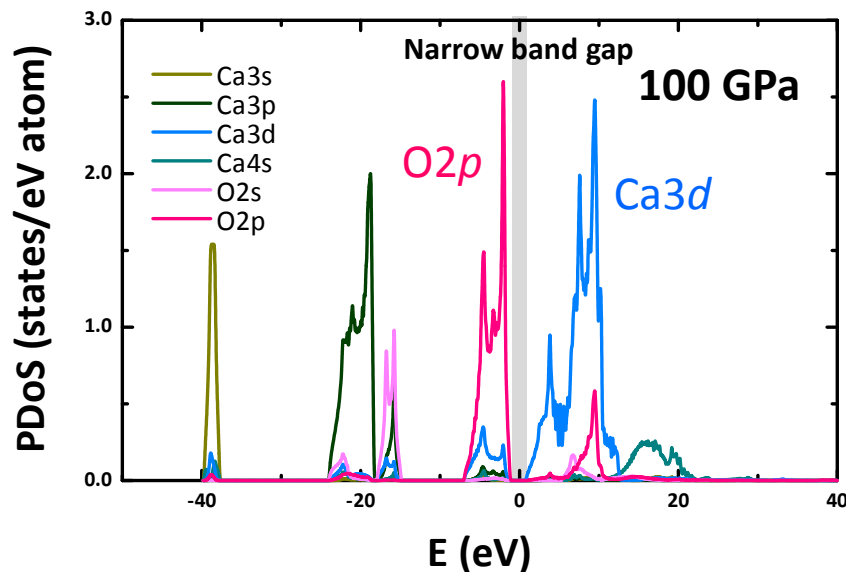
Quantization condition

SCF cycle vs total energy variation

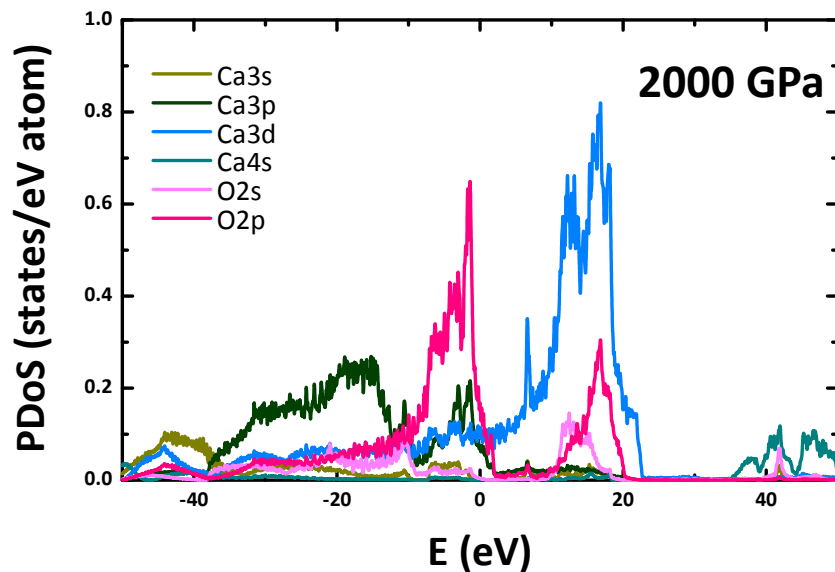
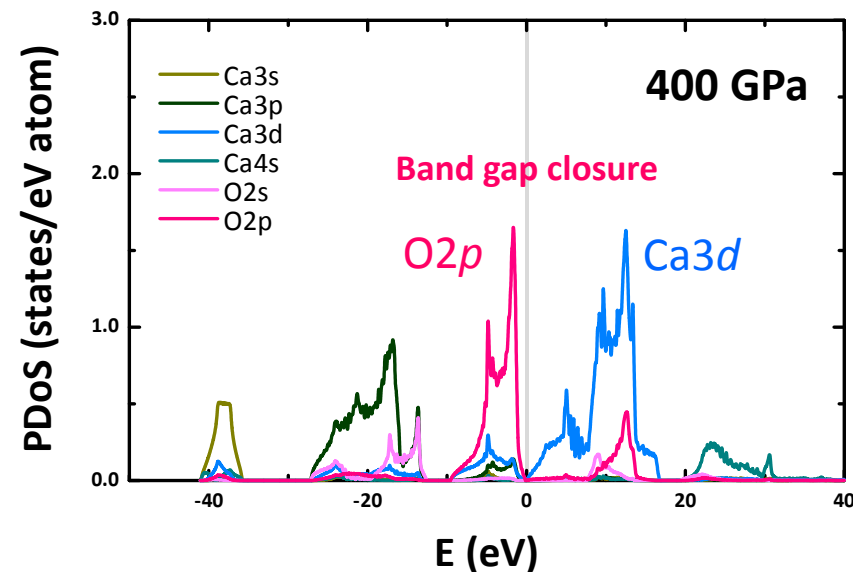
Au fcc structure



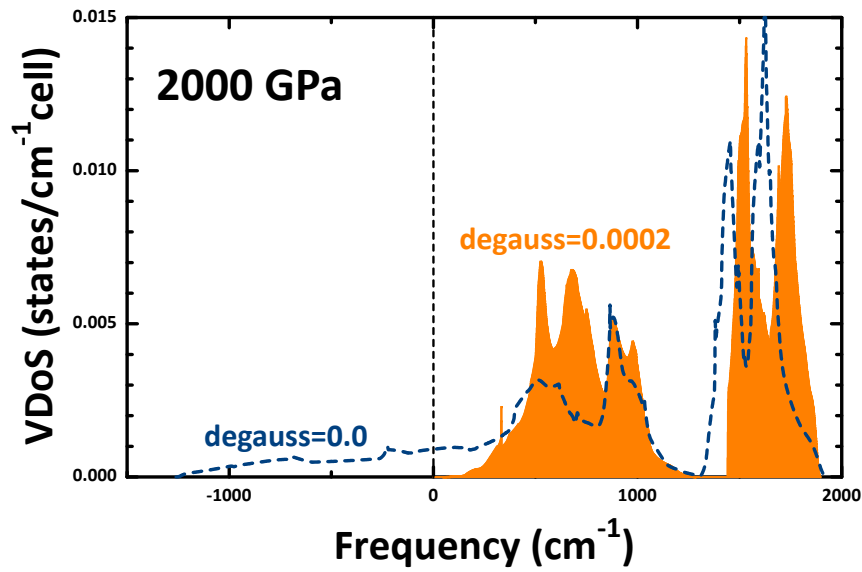
B2-CaO electronic DoS



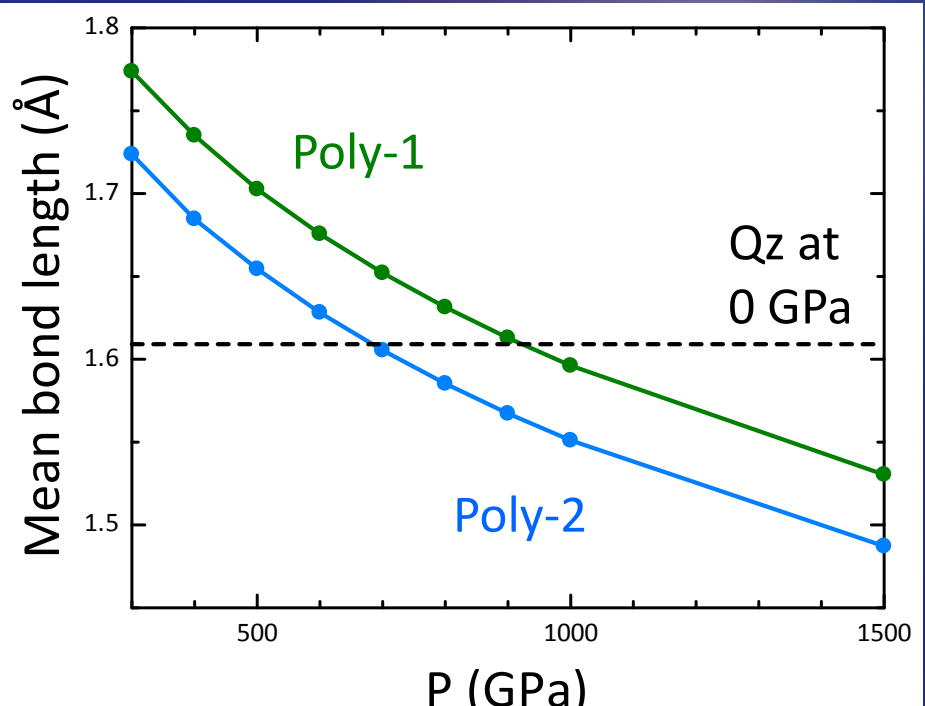
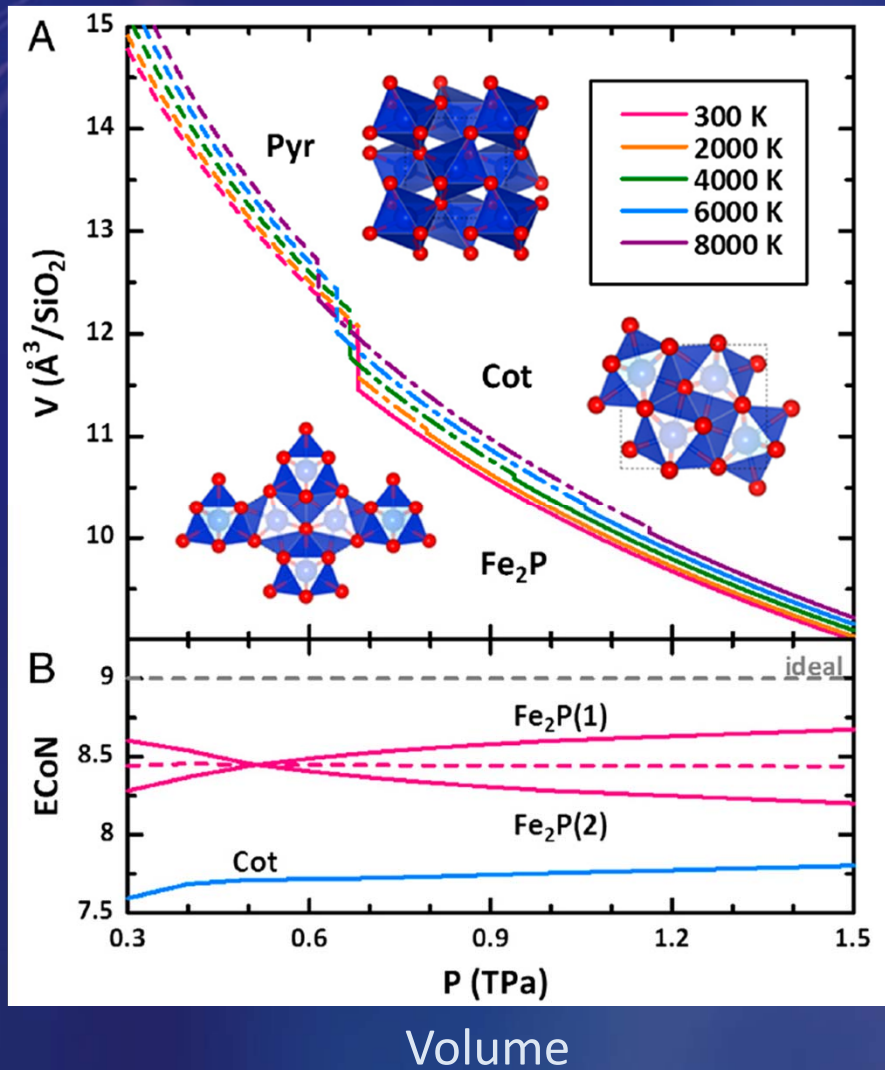
T Tsuchiya, 9th ISPS, 25 June 2012
Tsuchiya & Tsuchiya (2011)



B2-CaO Vibrational DoS



Compression behaviors

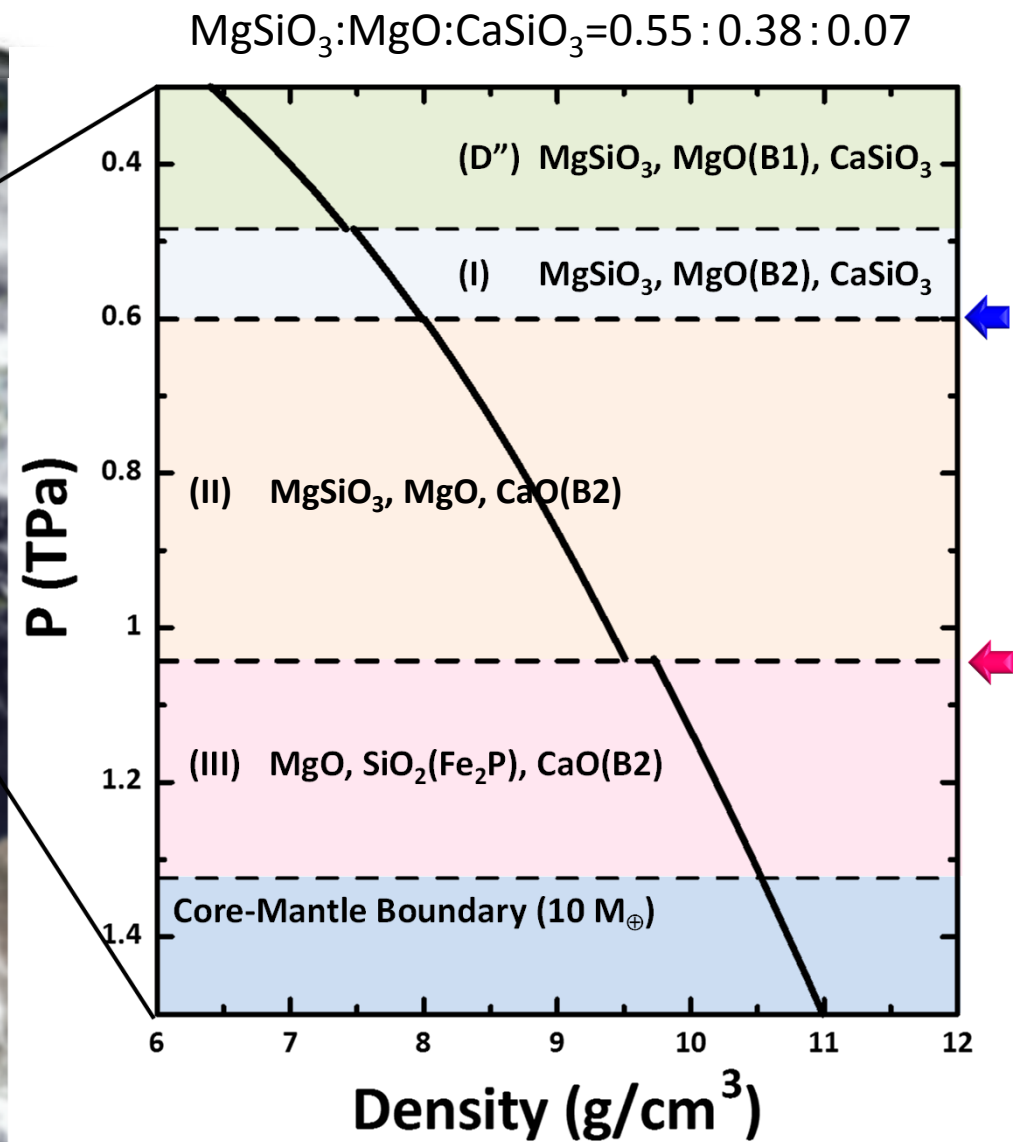
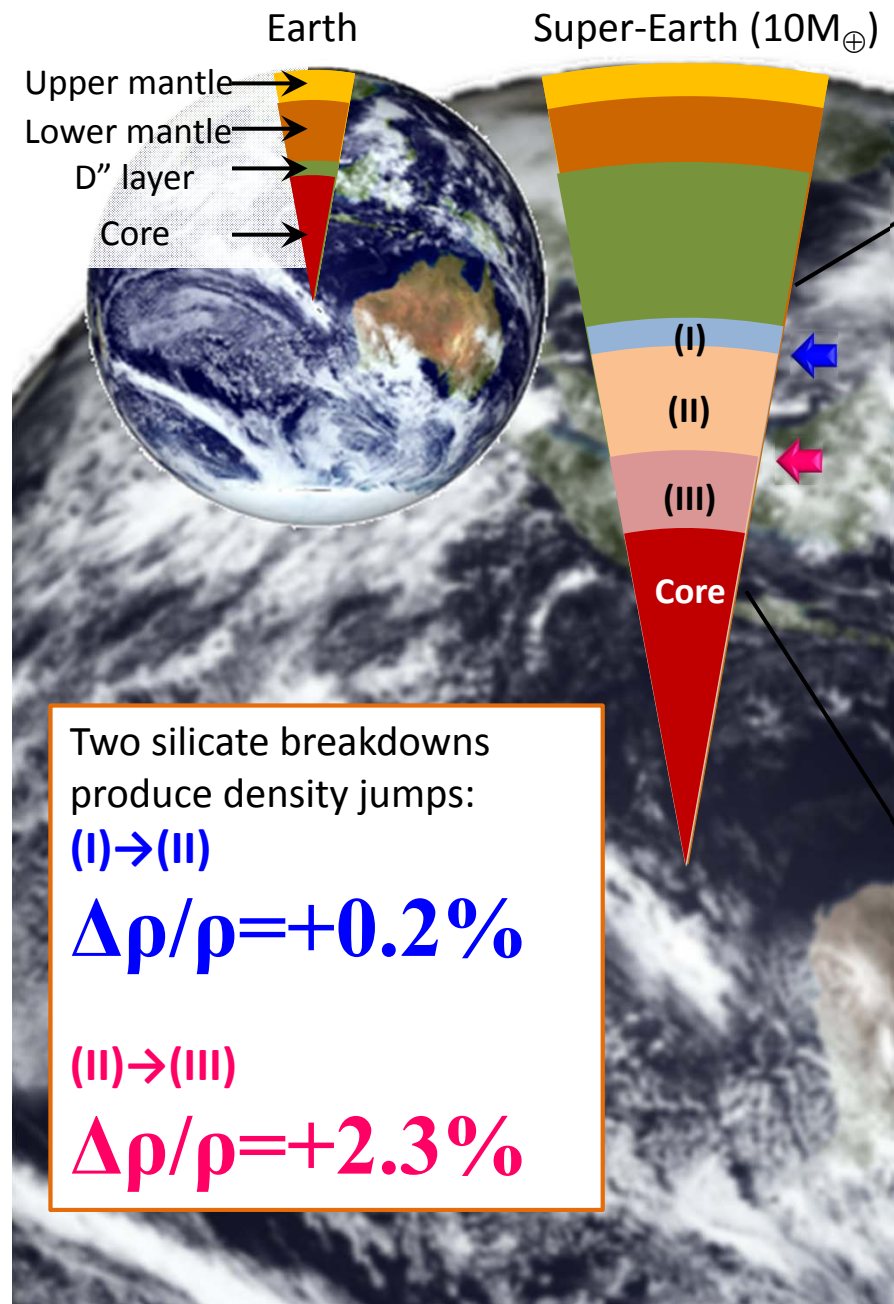


Mean bond lengths in Fe₂P

$$V_{\text{Fe}_2\text{P}}^{700 \text{ GPa}} \sim 0.33 V_{\text{Qz}}^0 \text{ GPa}$$

But the Si-O distance in Fe₂P comparable to
in Qz even at 1 TPa!!!

Density variation of super-Earth with assuming pyrolytic composition



Periodic boundary condition for a crystal

$$\phi(x + a) = \phi(x)$$

$$Ga = \pm 2n\pi \quad (n = 0, 1, 2, 3, \dots)$$

$$G = 0, \pm \frac{2\pi}{a}, \pm \frac{4\pi}{a}, \dots, \pm \frac{2n\pi}{a}$$

3-dimensional

$$\mathbf{G}_\alpha = \pm \frac{2n\pi}{\Omega} (\mathbf{a}_\beta \times \mathbf{a}_\gamma)$$

Reciprocal lattice vector

第一原理電子状態計算の限界

①バンドギャップ問題： バンドギャップを過小評価

$$E_{gap}^{LDA} \sim 0.5 E_{gap}^{\text{exp}}$$

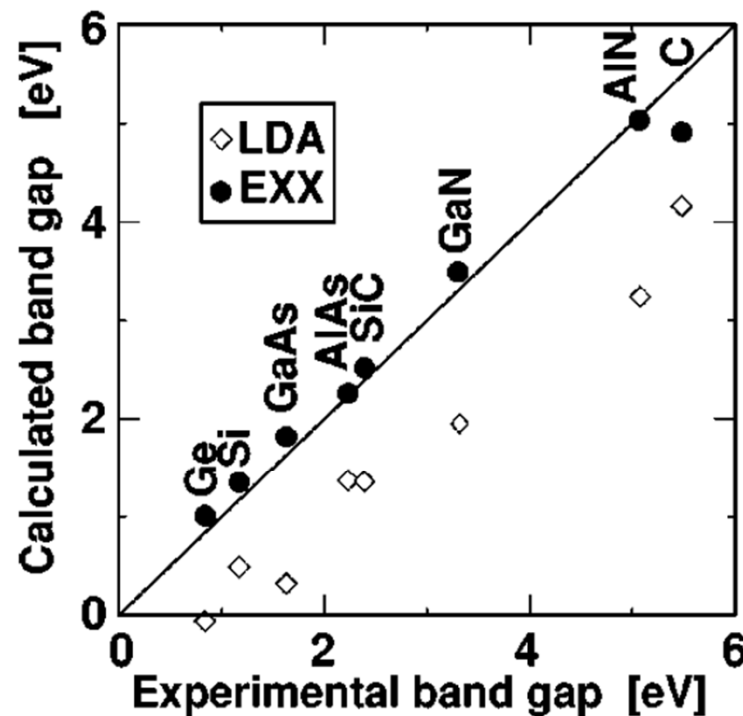


FIG. 3. Comparison of self-consistently calculated LDA and EXX band gaps (in eV) of various semiconductors with experimental data from Refs. 73 and 89–91.

Stadelo+ (1999) PRB

②弱い結合：例) LDA結合距離を過小評価(overbind)

TABLE I. Properties of Bernal-Fowler ice.

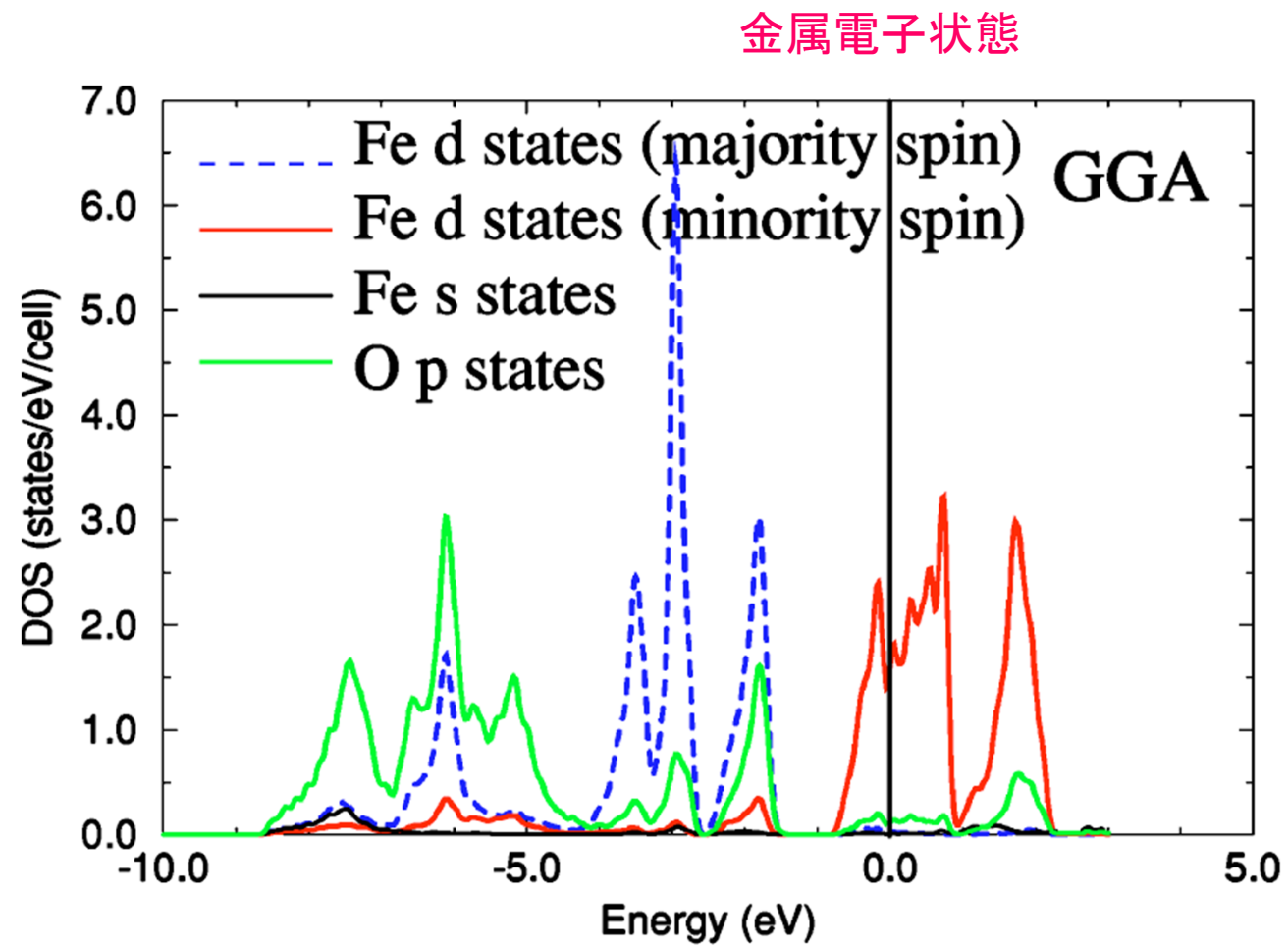
	Volume (Å ³)	Error (%)	Bulk		Sublimation	
			Modulus (GPa)	Error (%)	Energy (eV)	Error (%)
LDA	26.43	-18	25.3	+132	0.99	+71
勾配補正 (GGA)	BP86	30.85	-4	13.5	+24	0.68
	PW91	31.35	-2	13.5	+24	0.55
	PBE	31.82	-1	12.8	+17	0.53
	B-Loc.	39	+22	4	-63	0.24
	Exp.	32.05 ^a		10.9 ^b		0.58 ^c

Hamann+ (1997) PRB

GGAにより大きく改善

③遷移金属酸化物の基底状態(強相関電子状態)

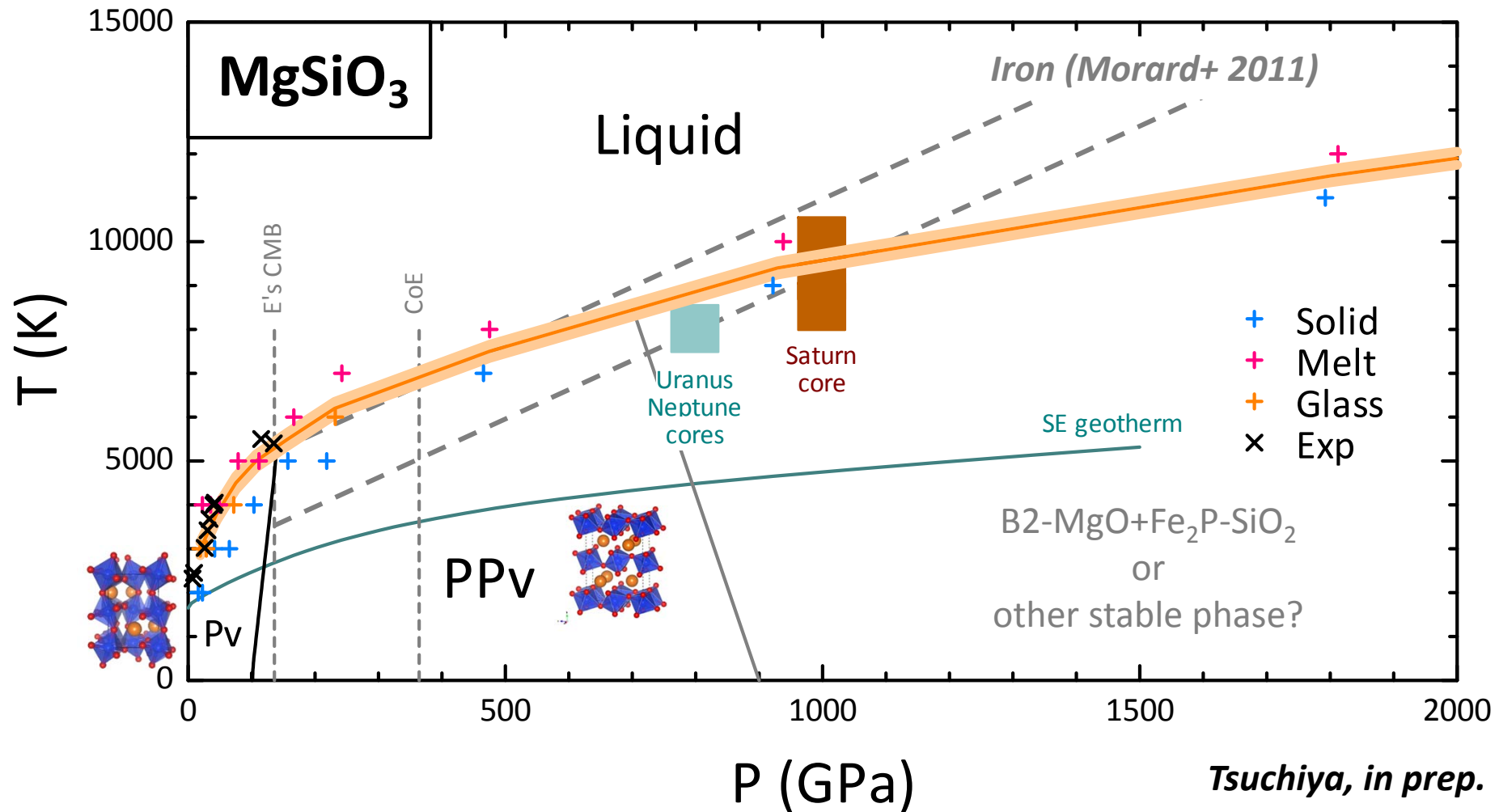
例) FeO



Cococcioni & de Gironcoli (2005) PRB

実際の絶縁基底状態($E_g \sim 2\text{eV}$)が再現されない！

Melting curve of MgSiO_3



Comparable to the SiO_2 's T_M and also Fe's T_M

Study on the ultrahigh-pressure phases of Earth and planetary materials

- Just started and now rapidly progressing
- Unexpected phases are continuously discovered.
There would still be many other unrevealed structures.
- Off-Hugoniot laser shock appears quite important to confirm calculations experimentally, maybe a unique technique from the experimental side.

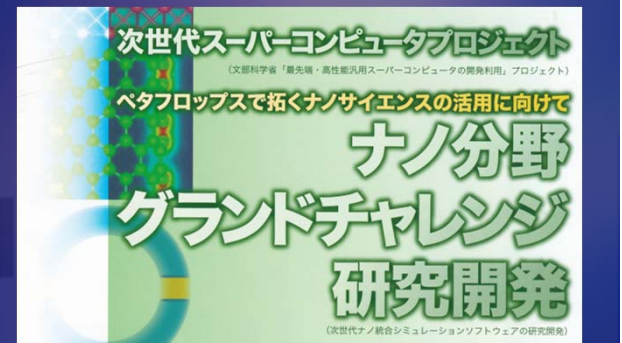
Large scale computation

GRC-SRFC parallel cluster systems

Pyrope



Knorringleite1,2



GEODYNAMICS



World fastest



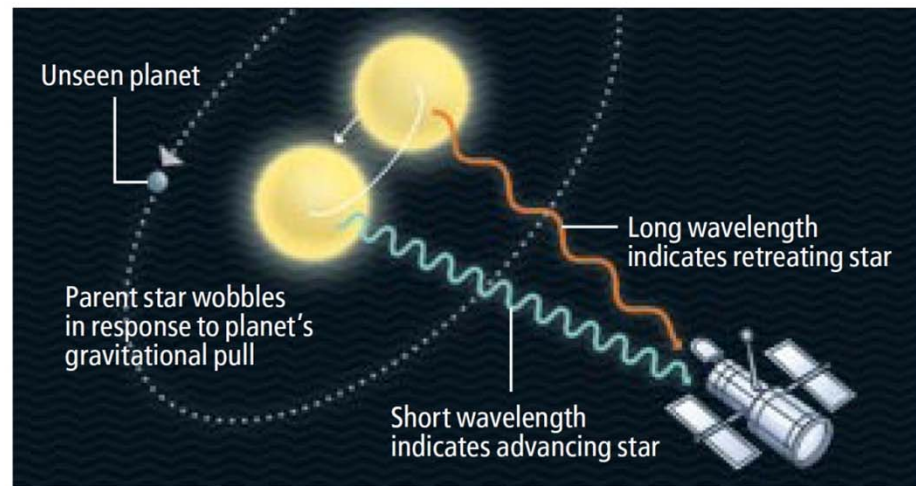
Observation of exoplanets

Doppler method

Gravitational interaction between a parent star and a planet



- Existence of a planet
 - **Mass** of a planet

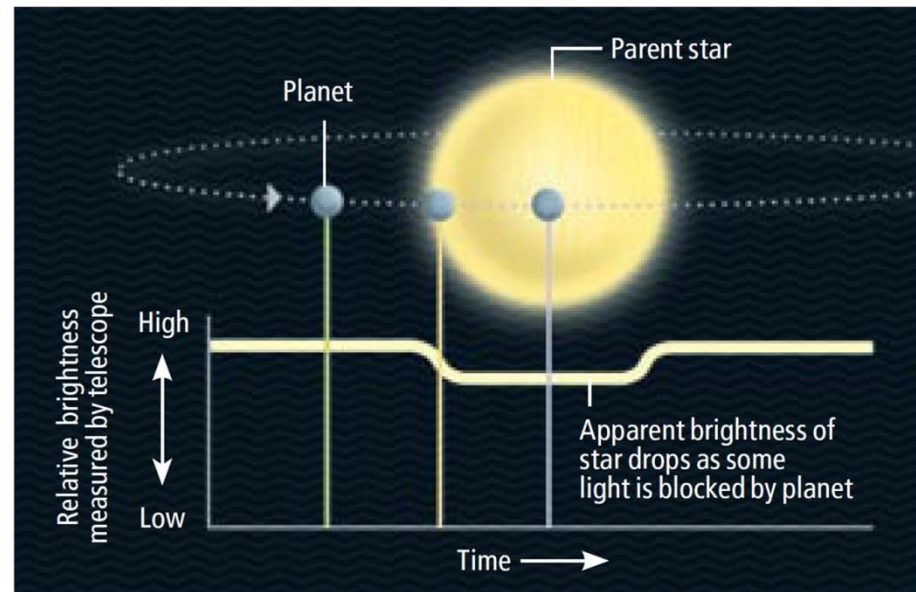


Transit method

Eclipse by a planet, i.e., the light of a parent star dimmed by a transiting planet



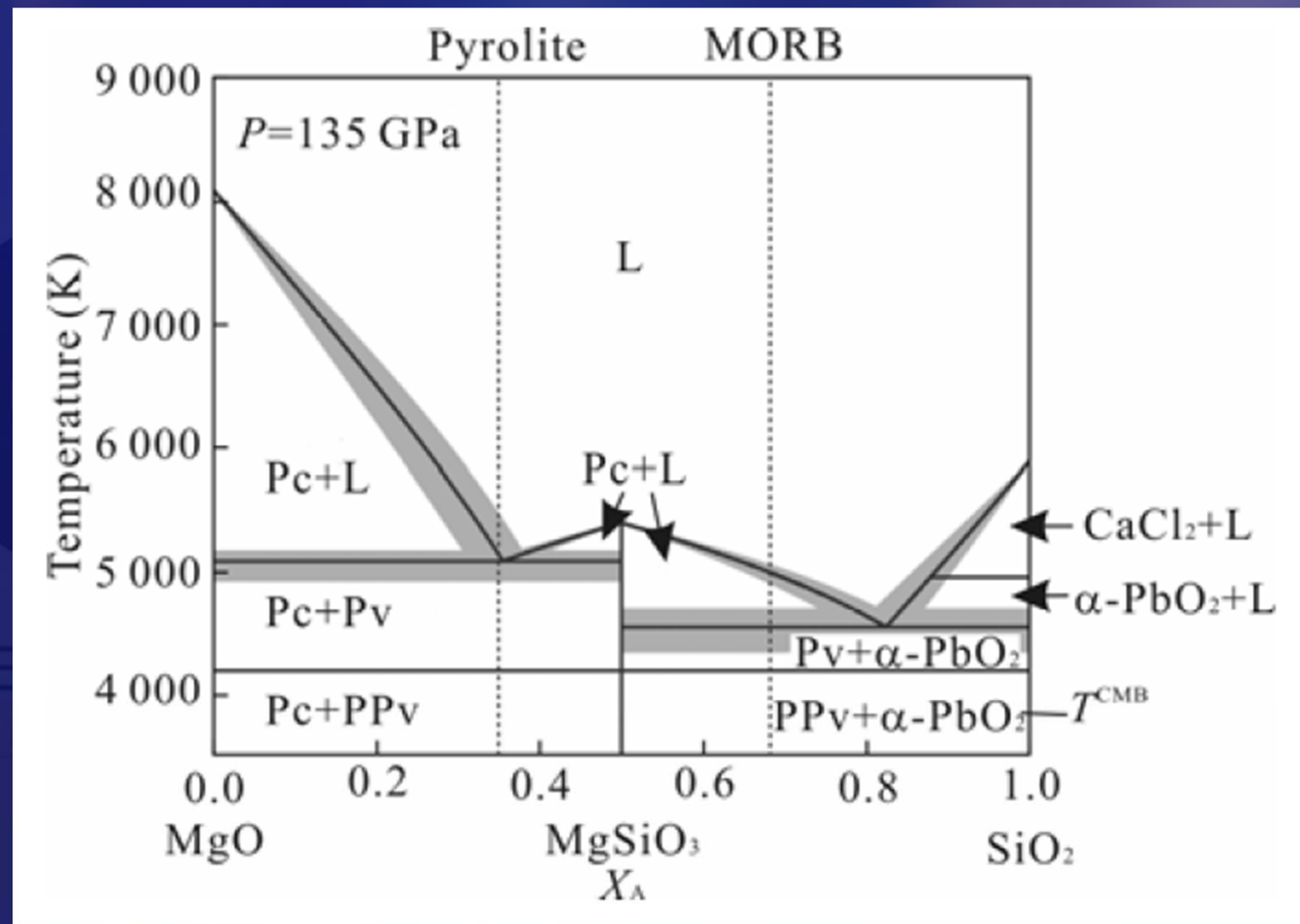
- Existence of a planet
 - **Size** of a planet



Mass + Size ⇒ Mean density

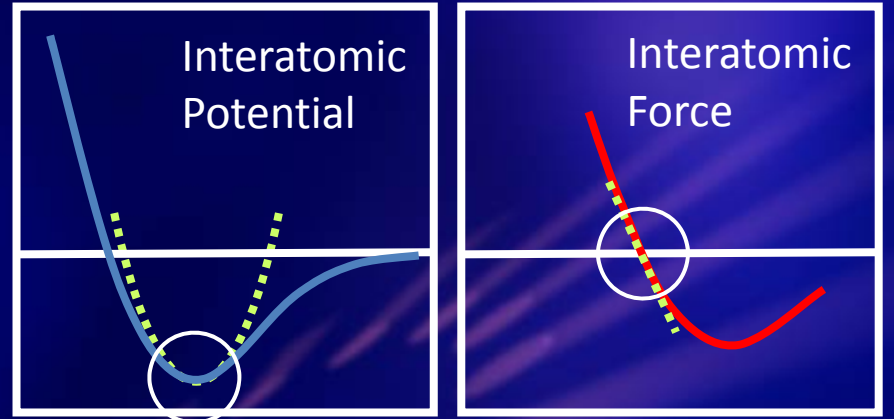
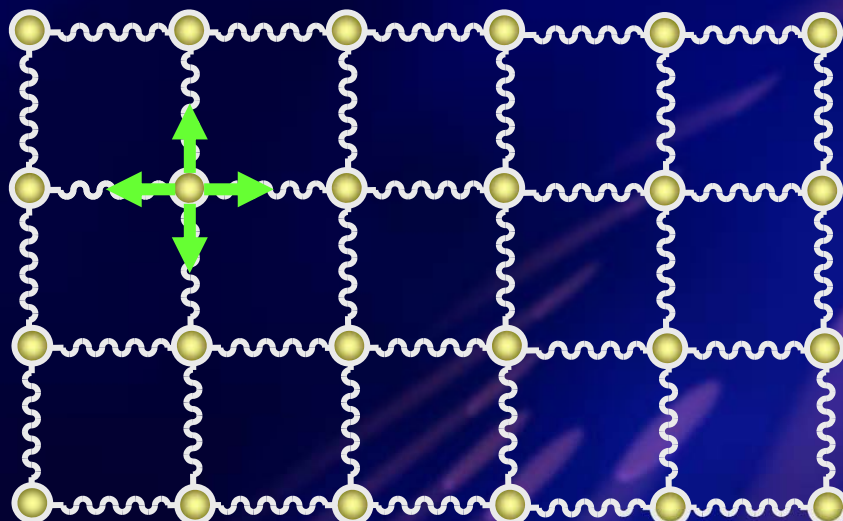
Sasselov (2008)

Eutectic melting relation in the MgO-SiO₂ system



Lattice Dynamics method

Atomic thermal vibration in solid
⇒ Collective motion of oscillators (phonon)



Harmonic
Approximation
 $\Delta E = (k/2)\Delta x^2$

Linear
Approximation
 $F = -k\Delta x$

Dynamical matrix

$$D_{\kappa\kappa'}^{\alpha\beta}(\mathbf{q}) = \frac{1}{\sqrt{m_\kappa m_{\kappa'}}} \sum_l \Phi_{\kappa\kappa'}^{\alpha\beta}(0l) \exp\{-i\mathbf{q} \cdot (\mathbf{x}_0 - \mathbf{x}_l)\}$$

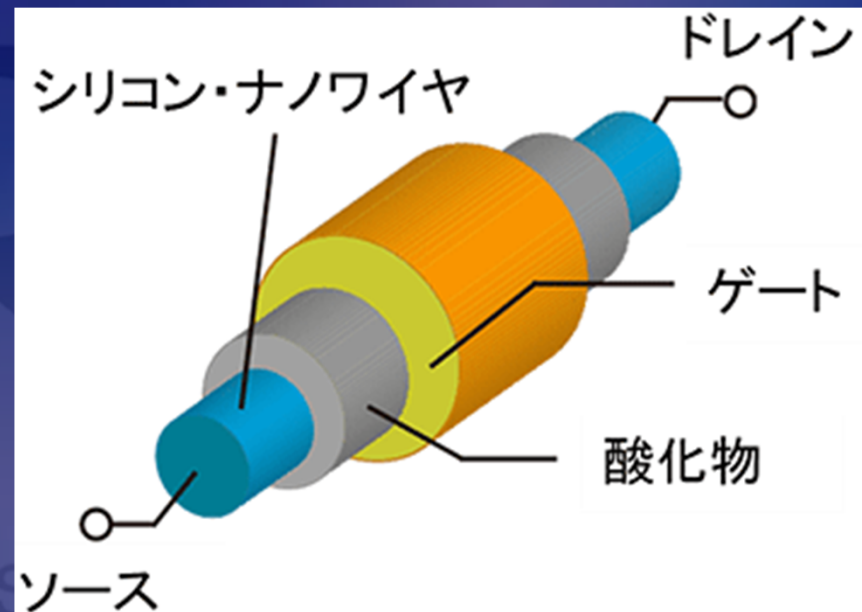


Phonon dispersion relation

A milestone from K (November/2011):
*First-principles calculations of electron states of a
silicon nanowire*

www.riken.jp

EHIME UNIVERSITY

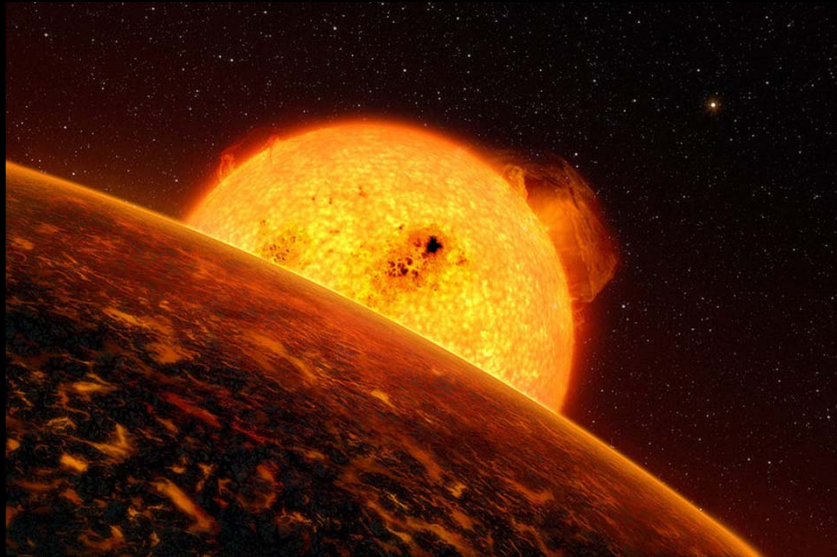


100,000 atoms!!!

Calculations with a few hundred atoms now not special

Examples of the transit planet

CoRoT-7b



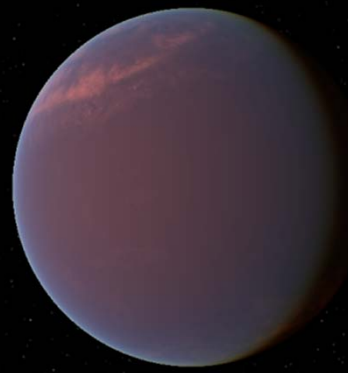
Discovery: 2009

$$M = \sim 4.8 M_{\oplus}$$

$$R = \sim 1.7 R_{\oplus}$$

$$\langle \rho \rangle = \sim 5.6 \text{ g/cm}^3 \sim \langle \rho_{\oplus} \rangle$$

GJ1214b



Discovery: 2009

$$M = \sim 6.55 M_{\oplus}$$

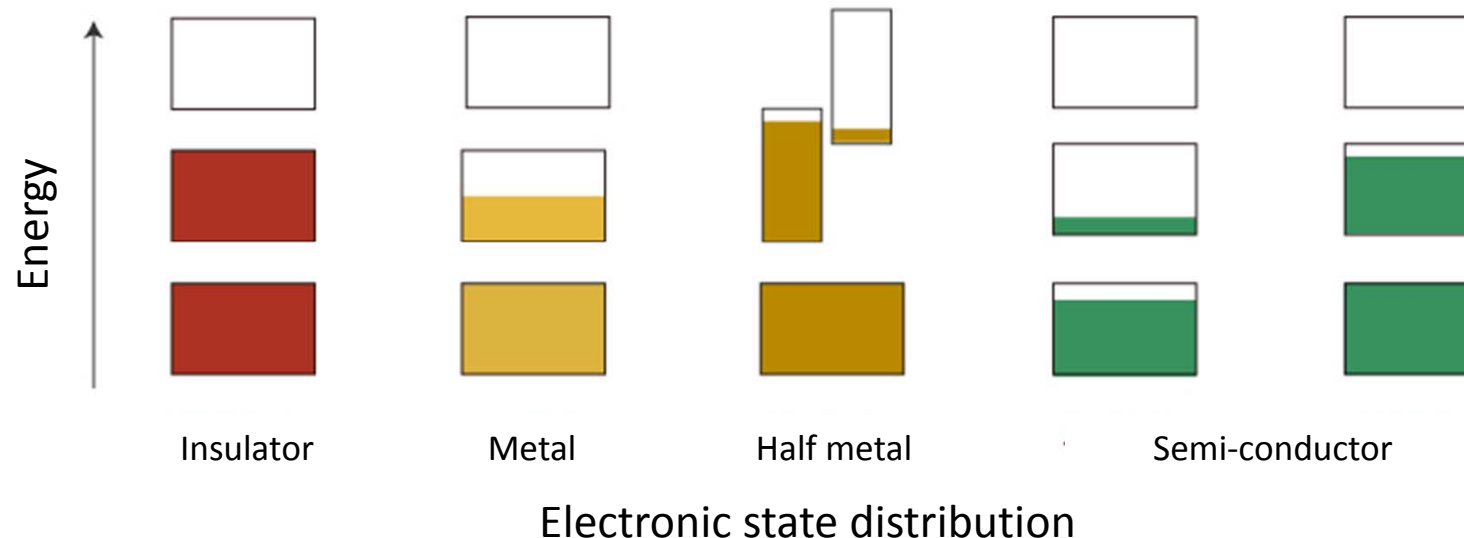
$$R = \sim 2.7 R_{\oplus}$$

$$\langle \rho \rangle = \sim 1.9 \text{ g/cm}^3 < \langle \rho_{\oplus} \rangle$$

Rocky

Icy

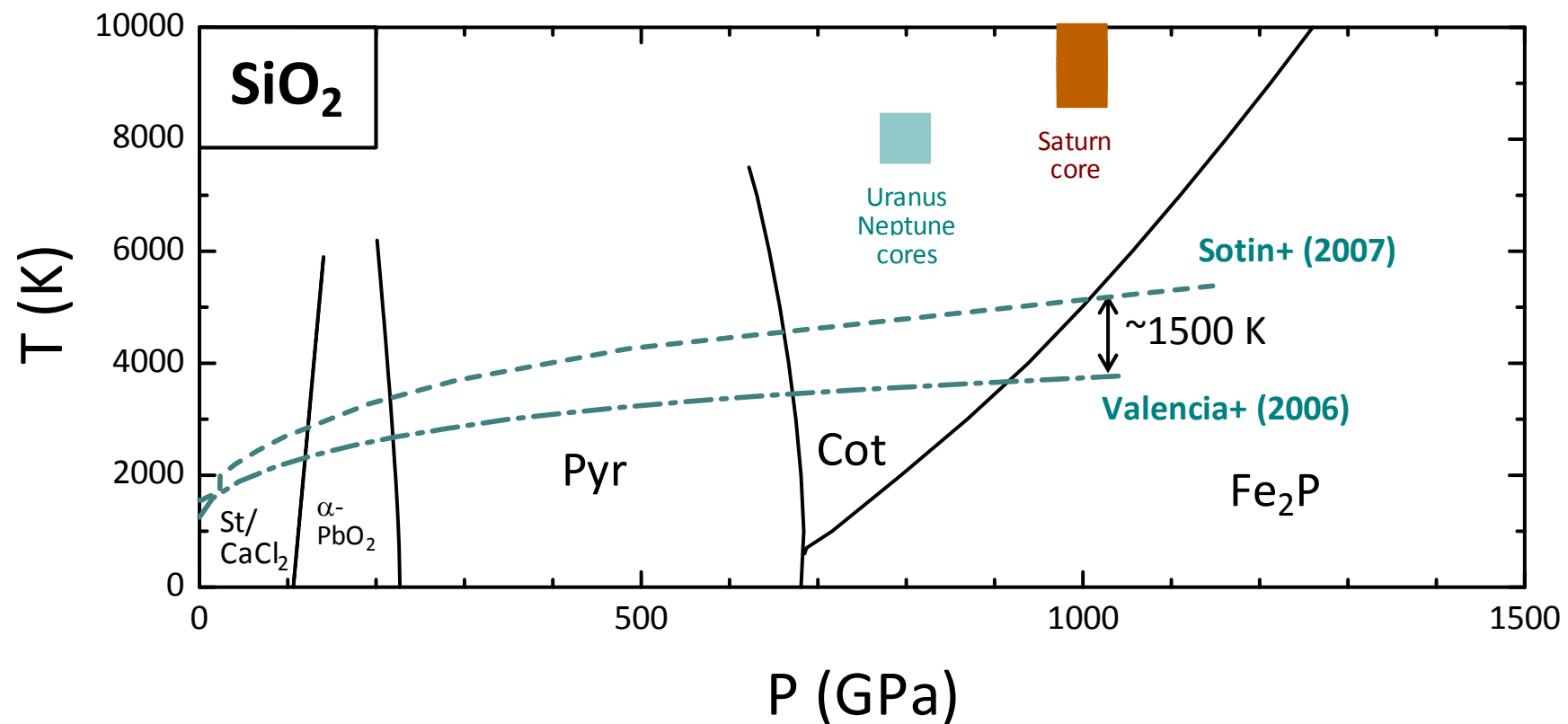
Electronic structure of solids

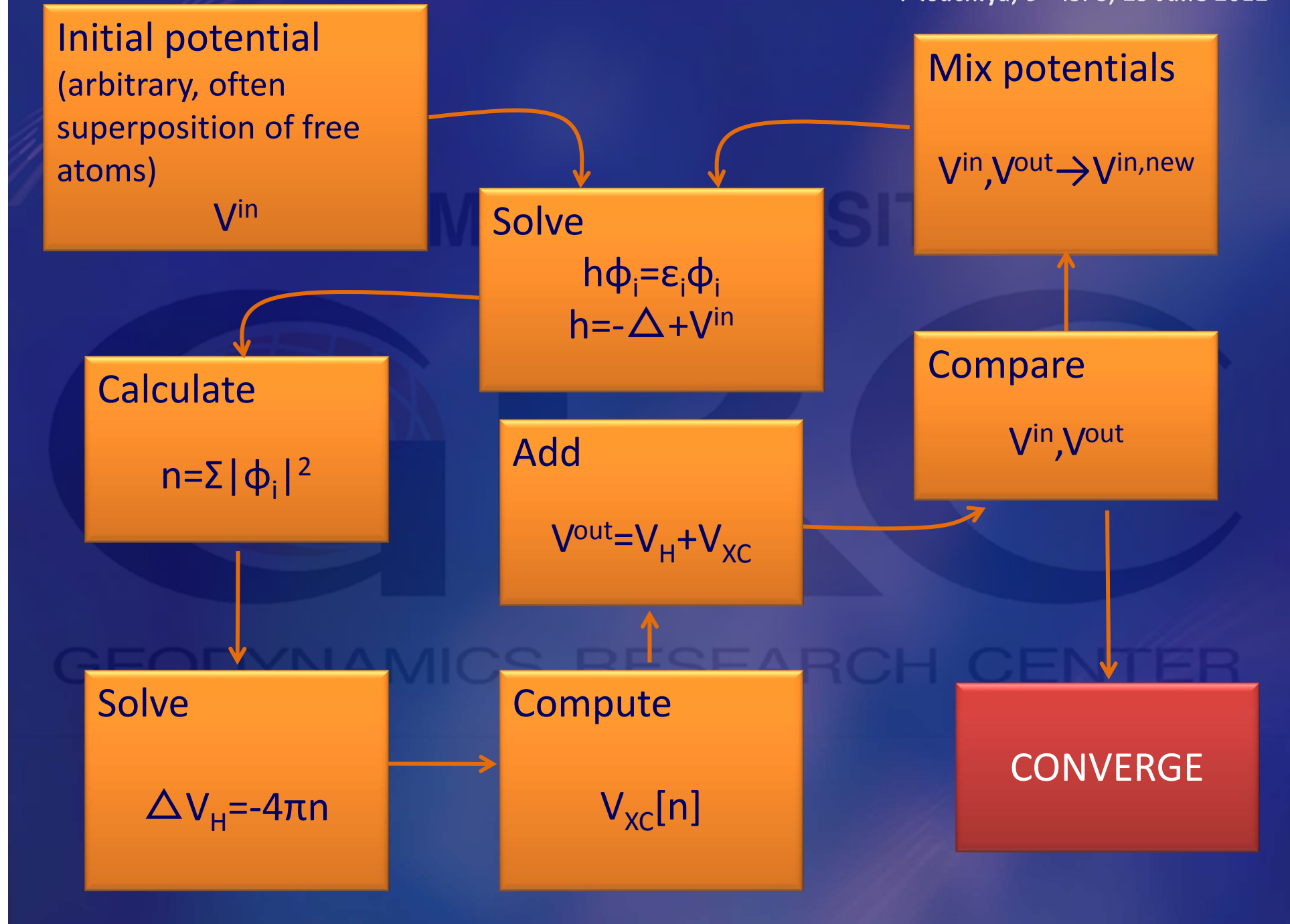


Thermal structure of SE

Adiabatic temperature gradient

$$\left(\frac{dT}{dP}\right)_S = \frac{\alpha(P)g(P)T}{C_P(P)}$$





References (1)

- Akaogi, M., Ito, E., 1993: Heat capacity of MgSiO_3 perovskite, GRL, 20, 105-108.
- Akaogi, M., Kojitani, H., Morita, T., Kawaji, H., Atake, T., 2008: Low-temperature heat capacities, entropies and high-pressure phase relations of MgSiO_3 ilmenite and perovskite, Phys. Chem. Mineral, 35, 287-297.
- Alfè,D., 2009: Temperature of the inner-core boundary of the Earth: Melting of iron at high pressure from first-principles coexistence simulations, Phys. Rev. B, 79, 060101.
- Baroni, S., Giannozzi, P., 1987: Pressure-induced structural instability of cesium halides from ab initio pseudopotential techniques, Phys. Rev. B, 35, 765-769.
- Baroni, S., de Gironcoli, S., dal Corso, A., Giannozzi, P., 2001: Phonons and related crystal properties from density-functional perturbation theory, Rev. Mod. Phys., 73, 515-562.
- Barnes, R., Raymond, S. N., Greenberg, R., Jackson, B., Kaib, N. A., 2010: CoRoT-7b: Super-Earth or Super-*Io*?, Astrophys. J. Lett., 709, L95-L98.
- Charbonneau, D., Berta, Z. K., Irwin, J., Burke, C. J., Nutzman, P., Buchhave, L. A., Lovis, C., Bonfils, X., Latham, D. W., Udry, S., Murra Clay, R. A., Holman, M. J., Falco, E., Winn, J. N., Queloz, D., Pepe, F., Mayor, M., Delfosse, X., Forveille, T., 2009: A super-Earth transiting a nearby low-mass star, Nature, 462, 891-894.
- Christensen, U. R., Yuen, D. A., 1985: Layered convection induced by phase transitions, 1985, JGR, 90, 10291-10300.
- Cococcioni, M., de Gironcoli, S., 2005: Linear response approach to the calculation of the effective interaction parameters in the LDA+U method, Phys. Rev. B, 71, 035105.
- Cordier, P., Ungár, T., Zsoldos, L., Tichy, G., 2004: Dislocation creep in MgSiO_3 perovskite at conditions of the Earth's uppermost lower mantle, Nature, 428, 837-840.
- Correa, A. A., Bonev, S. A., Galli, G., 2006: Carbon under extreme conditions: Phase boundaries and electronic properties from first-principles theory, PNAS, 103, 1204-1208.
- de Koker, N., 2009: Thermal Conductivity of MgO Periclase from Equilibrium First Principles Molecular Dynamics, Phys. Rev. Lett., 103, 125902.
- Dekura, H., Tsuchiya, T., Kuwayama, Y., Tsuchiya, J., 2011: Theoretical and Experimental Evidence for a New Post-Cotunnite Phase of Titanium Dioxide with Significant Optical Absorption, Phys. Rev. Lett., 107, 045701.
- Dziewonski, A. M., Anderson, D. L., 1981: Preliminary reference Earth model, PEPI, 25, 297-356.
- Fiquet, G., Andrault, D., Dewaele, A., Charpin, T., Kunz, M., Haüsermann, D., 1998: P-V-T equation of state of MgSiO_3 perovskite, PEPI, 105, 21-31.
- Guillot, T., 1999: Interior of Giant Planets Inside and Outside the Solar System, Science, 286, 72-77.
- Hamann, D. R., 1997: H_2O hydrogen bonding in density-functional theory, Phys. Rev. B, 55, R10157-R10160.

References(2)

- Hermann, A., Ashcroft, N. W., Hoffmann, R., 2012: High pressure ices, PNAS, 109, 745-750.
- Hicks, D. G., Boehly, T. R., Eggert, J. H., Miller, J. E., Celliers, P. M., Collins, G. W., 2006: Dissociation od Liquid Silica at High Pressure and Temperatures, Phys. Rev. Lett., 97, 025502.
- Hohenberg, P., Kohn, W., 1964: Inhomogeneous Electron Gas, Phys. Rev., 136, 864-871.
- Karki, B. B., Bhattacharai, D., Stixrude, L., 2007: First-principles simulations of liquid silica: Structural and dynamical behavior at high pressure, Phys. Rev. B, 76, 104205.
- Kawai, K., Tsuchiya, T., 2009: Temperature profile in the lowermost mantle from seismological and mineral physics joint modeling, PNAS, 106, 22119-22123.
- Knudson, M. D., Desjarlais, M. P., Dolan, D. H., 2008: Shock-Wave Exploration of the High-Pressure Phases of Carbon, Science, 322, 1822-1825.
- Knudson, M. D., Desjarlais, M. P., Lemke, R. W., Mattsson, T. R., French, M., Nettelmann, N., Redmer, R., 2012, Phys. Rev. Lett., 108, 091102.
- Kohn, W., Sham, L. J., 1965: Self-Consistent Equations Including Exchange and Correlation Effects, Phys. Rev., 140, 1133-1138.
- Kuwayama, Y., Hirose, K., Sata, N., Ohishi, Y., 2005: The Pyrite-Type High-Pressure Form of Silica, Science, 309, 923-925.
- Metsue, A., Tsuchiya, T., 2011: Lattice dynamics and thermodynamic properties of $(\text{Mg}, \text{Fe}^{2+})\text{SiO}_3$ postperovskite, JGR, 116, B08207.
- Metsue, A., Tsuchiya, T., 2012: Ab initio investigation into the elasticity of ultrahigh-pressure phase of SiO_2 , Phys. Chem. Min., 39, 177-187.
- Mitrovica, J. X., Forte, A. M., 2004: A new inference of mantle viscosity based upon joint inversion of convection and glacial isostatic adjustment data, EPSL, 225, 177-189.
- Morard, G., Bouchet, J., Valencia, D., Mazevert, S., Guyot, F., 2011: The melting curve of iron at extreme pressures: Implications for planetary cores, HEDP, 7, 141-144.
- Molales, M. A., Pierleoni, C., Schwegler, E., Ceperley, D. M., 2010: Evidence for a first-order liquid-liquid transition in high-pressure hydrogen from ab initio simulations, PNAS, 107, 12799-12803.
- Murakami, M., Hirose, K., Kawamura, K., Sata, N., Ohishi, Y., 2004: Post-Perovskite Phase Transition MgSiO_3 , Science, 304, 855-858.
- Murakami, M., Ohishi, Y., Hirao, N., Hirose, K., 2012: A perovskitic lower mantle inferred from high-pressure, high-temperature sound velocity data, Nature, 485, 90-94.
- Nielsen, O. H., Martin, R. M., 1985: Quantum-mechanical theory of stress and force, Phys. Rev. B, 32, 3780-3791.

References (3)

- Nielsen, O. H., Martin, R. M., 1985: Stresses in semiconductors: Ab initio calculations on Si, Ge, and GaAs, *Phys. Rev. B*, 32, 3792-3805.
- Nimmo, F., 2007: Treatise on Geophysics, Elsevier B. V., 9, 217-241.
- Rivera, E., Lissauer, J. J., Butler, R. P., Marcy, G. W., Vogt, S. S., Fischer, D. A., Brown, T. M., Laughlin G., Henry, G. W., 2005, *Astrophys. J.*, 634, 625-640.
- Sasselov, D. D., 2008: Astronomy: Extrasolar planets, *Nature*, 451, 29-31.
- Saxena, S. K., Dubrovinsky, L. S., Tutti, F., le Bihan, T., 1999: Equation of state of MgSiO_3 with the perovskite structure based on experimental measurement, *Amer. Mineral.*, 84, 226-232.
- Schwegler, E., Sharma, M., Gygi, F., Galli, G., 2008: Melting of ice under pressure, *PNAS*, 105, 14779-14783.
- Sotin, C., Grasset, O., Mocquet, A., 2007: Mass radius curve for extrasolar Earth-like planets and ocean planets, *Icarus*, 191, 337-351.
- Städle, M., Moukara, M., majewski, J. A., Vogl, P., Görling, A., 1999: Exact exchange Kohn-Sham formalism applied to semiconductors, *Phys. Rev. B*, 59, 10031-10043.
- Stamenković, V., Breuer, D., Spohn, T., 2011: Thermal and transport properties of mantle rock at high pressure: Applications to super-Earths, *Icarus*, 216, 572-596.
- Stixrude, L., 2012: Structure of Iron to 1 Gbar and 40 000 K, *Phys. Rev. Lett.*, 108, 055505.
- Tang, X., Dong, J., 2010: Lattice thermal conductivity of MgO at conditions of Earth's interior, *PNAS*, 107, 4539-4543.
- Tsuchiya, J., Tsuchiya, T., Wentzcovitch, R. M., 2005: Vibrational and thermodynamic properties of MgSiO_3 postperovskite, *JGR*, 110, B02204.
- Tsuchiya, J., Tsuchiya, T., 2008: Postperovskite phase equilibria in the $\text{MgSiO}_3\text{-Al}_2\text{O}_3$ system, *PNAS*, 105, 19160-19164.
- Tsuchiya, T., 2003: First-principles prediction of the P-V-T equation of state of gold and the 660-km discontinuity in Earth's mantle, *JGR*, 108, 2462.
- Tsuchiya, T., 2011: Elasticity of subducted basaltic crust at the lower mantle pressures: Insights on the nature of deep mantle heterogeneity, *PEPI*, 188, 142-149.
- Tsuchiya, T., Tsuchiya, J., 2006: Effect of impurity on the elasticity of perovskite and postperovskite : Velocity contrast across the postperovskite transition in $(\text{Mg}, \text{Fe}, \text{Al})(\text{Si}, \text{Al})\text{O}_3$, *GRL*, 33, L12S04.
- Tsuchiya, T., Tsuchiya, J., 2007: High-pressure-high-temperature phase relations of MgSiO_3 : First-principles calculations, *Phys. Rev. B*, 76, 092105.
- Tsuchiya, T., Tsuchiya, J., 2011: Prediction of a hexagonal SiO_2 phase affecting stabilities of MgSiO_3 and CaSiO_3 at multimegabar pressure, *PNAS*, 108, 1252-1255.

References (4)

- Tsuchiya, T., Tsuchiya, J., Umemoto, K., Wentzcovitch, R. M., 2004: Phase transition in MgSiO₃ perovskite in the earth's lower mantle, EPSL, 224, 241-248.
- Tsuchiya, T., Wentzcovitch, R. M., da Silva, Cesar R. S., de Gironcoli, S., 2006: Spin Transition in Magnesiowüstite in Earth's Lower Mantle, Phys. Rev. Lett., 96, 198501.
- Udry, S., Bonfils, X., Delfosse, X., Forveille, T., Mayor, M., Perrier, C., Bouchy, F., Lovis, C., Pepe, F., Queloz, D., Bertaux, J. L., 2007: The HARPS search for southern extra-solar planets. XI. Super-Earths (5 and 8 M[⊕]) in a 3-planet system, A&A, 469, L43-L47.
- Umemoto, K., Wetzcovitch, R. M., 2011: Two-stage dissociation in MgSiO₃ post-perovskite, EPSL, 311, 225-229.
- Umemoto, K., Wetzcovitch, R. M., Allen, P. B., 2006: Dissociation of MgSiO₃ in the Cores of Gas Giants and Terrestrial Exoplanets, Science, 311, 983-986.
- Usui, Y., Tsuchiya, T., 2010: Ab initio two-phase molecular dynamics on the melting curve of SiO₂, J. Earth Sci., 21, 801-810.
- Valencia, D., O'Connell, R. J., Sasselov, D., 2006: Internal structure of massive terrestrial planets, Icarus, 181, 545-554.
- Vítek, V., 1968: Intrinsic stacking faults in body-centred cubic crystals, Phil. Mag., 18, 773-786.
- Wentzcovitch, R. M., Tshuchiya, T., Tsuchiya, J., 2006: MgSiO₃ postperovskite at D'' conditions, PNAS, 103, 543-546.
- Wilson, H. F., Militzer, B., 2012: Rocky Core Solubility in Jupiter and Giant Exoplanets, Phys. Rev. Lett., 108, 111101.
- Yusa, H., Shirako, Y., Akaogi, M., Kojitani, H., Hirao, N., Ohishi, Y., Kikegawa, T., 2012: Perovskite-to-Postperovskite Transitions in NaNiF₃ and NaCoF₃ and Disproportionation of NaCoF₃ Postperovskite under High Pressure and High Temperature, Inorg. Chem., 51, 6559-6566.

GEODYNAMICS RESEARCH CENTER